PHAGE-BASED TECHNOLOGIES FOR NON-STERILE BIOLIPIDS PRODUCTION FROM LIGNOCELLULOSE

A Dissertation

by

MYUNG HWANGBO

Submitted to the Office of Graduate and Professional Studies of
Texas A&M University
in partial fulfillment of the requirements for the degree of

DOCTOR OF PHILOSOPHY

Chair of Committee,	Kung-Hui Chu
Committee Members,	Ry Young
	Jason J. Gill
	Xingmao Ma
Head of Department,	Robin L. Autenrieth

August 2020

Major Subject: Civil Engineering

ABSTRACT

Lipid-based biofuel is a clean and renewable energy source that has been recognized as a promising replacement for petroleum-based fuels. Lipid-based biofuel can be made from intracellular biolipids from lignocellulosic biomass using lipid-producing microorganisms. However, large scale production of lipid-based biofuel remains expensive due to several technical challenges such as inefficient pretreatment of lignocellulose, sterile cultivation of lipid-producing microorganisms, and costly biolipid extraction from the biolipid-filled microorganisms. This research explored several approaches to overcome these challenges in order to enable economical and sustainable production and release of biolipids for large scale lipid-based biofuel.

The first approach was to improve sugar release during enzymatic hydrolysis of pretreated lignocellulose while reducing the cost of enzymes for hydrolysis. Specifically, this study explores a one-step saccharification of pretreated lignocellulose using immobilized biocatalysts containing five different saccharifying enzymes (SEs) with a similar optimum operating condition. The five SEs were successfully produced from engineered *Escherichia coli* in quantity, worked synergistically to saccharify pretreated biomass to release more reduced sugars than those observed using two commercial enzymes. Additionally, when cross-linked in the absence or the presence of magnetic nanoparticles, the five SEs can be reused at least three times.

To overcome challenges related to sterile cultivation and biolipid extraction, this study successfully demonstrated non-sterile cultivation of an engineered *Rhodococcus opacus* PD631 and released its biolipids triacylglycerols (TAGs) using a solvent-free,

phage-based cell lysis approach. The newly developed salt-tolerant *R. opacus* PD631 carrying an inducible plasmid with a phage lytic gene cassette was able to grow in non-sterile saline growth medium while producing TAGs. The TAG-filled strain was able to release its TAGs into the culture medium on demand. This newly developed strain is a promising candidate to overcome the two major challenges of current biolipid-based biofuel production.

Lastly, this study explored the possibility of editing prophage Mushu4 DNA in the genome of *Rhodococcus opacus* strains to produce and release lignin peroxidase in quantity for effective depolymerization of lignin, as an efficient biological pretreatment of lignocellulose. Two homologous recombination approaches, i.e., using an inserted phage recombinase or own recombinases of prophage, were used but unsuccessful. Based on the results, new approaches were suggested for future study.

Overall, results of this study suggest that non-sterile biolipids can be produced and released from the engineered salt-tolerant lipid-producing bacteria using pretreated lignocellulose, prepared by an efficient one-step saccharification. Also, the trial of prophage genome editing provided knowledge to serve as the first step for the development of a *Rhodococcus*-based factory for production and release of needed enzymes for effective depolymerization of lignin. Results of the approaches explored in this study not addressed two major challenges and offered a new strategy to reduce the overall production cost of biolipid-based biofuel from lignocellulose.

ACKNOWLEDGEMENTS

I would like to thank my committee chair, Dr. Kung-Hui Chu, for her excellent assistance and guidance in my research, during my Ph.D. program. Mainly, I want to thank for making me think more for my research and keep standing in this academic field.

Also, I would like to thank my other committee members, Dr. Ry Young and Dr. Jason J. Gill for their scientific suggestions and constructive advice in my research idea, and Dr. Xingmao Ma, for his useful comments and suggestions in my proposal and final defense.

I also want to express my thanks to members from my lab and collaborating lab for their assistance and friendship. Thanks also go to my friends and colleagues and the department faculty and staff for making my time at Texas A&M University a great experience. Finally, thanks to my family for their encouragement and their patience and love.

CONTRIBUTORS AND FUNDING SOURCES

Contributors

This work was supervised by a dissertation committee consisting of Dr. Kung-Hui Chu [advisor] and Dr. Xingmao Ma of Department of Civil and Environmental Engineering, Dr. Ry Young of Department of Biochemistry and Biophysics, and Dr. Jason J. Gill of Department of Animal Science. All work described in this dissertation was conducted solely by the student independently, except for some experiments in Chapter 3 and Chapter 5. The analyses depicted in Chapter 3 was conducted in part by Janessa L. Tran of the Department of Civil and Environmental Engineering and Theodore E. G. Alivio of the Department of chemistry for helping the FE-SEM analysis. This Chapter 3 was published in 2019. The genome analysis of phage Mushu4 in Chapter 5 was conducted in part by Shih-Hung Yang of the Department of Civil and Environmental Engineering.

Funding Sources

This work was made possible in part by the National Science Foundation Funding under Grant Number 1134488. The contents of this dissertation are solely the responsibility of the author(s) and do not necessarily represent the official views of the National Science Foundation.

TABLE OF CONTENTS

Page

LIST OF FIGURES

Page

LIST OF TABLES

Page

1. INTRODUCTION AND OBJECTIVES

1.1. Introduction

Biofuel is a renewable and environmentally friendly energy source that can be produced from renewable feedstocks (Guo et al., 2015). Liquid biofuel such as bioethanol and biodiesel has been recognized as eco-friendly alternative fuels to petroleum-based energy (Guo et al., 2015), and they can be produced from lignocellulosic biomass (lignocellulose) (Singhvi et al., 2014; Wang et al., 2014). Lignocellulose is a promising feedstock because it is the most abundant renewable resource on the Earth (Billion-Ton, 2016). However, the current price for biofuel production remains high, and biofuel production from lignocellulose faces a number of challenges, making the production of lignocellulose-based biofuel not economical nor competitive against petroleum-based energy.

Lignocellulose consists of sugar polymers (cellulose and hemicellulose) and non-sugar, phenolic alcohol-based polymers (lignin) (Limayem and Ricke, 2012) and thus requires physical/chemical pretreatment to remove lignin, followed by enzyme hydrolysis to extract sugars for biofuel-producing bacteria (Nlewem and Thrash, 2010; Wang et al., 2014). Current physical/chemical pretreatment processes are costly, require toxic chemicals, and commonly lead to production of inhibitory compounds affecting downstream biofuel production (Sun et al., 2016). Additionally, current enzymatic hydrolysis is inefficient in releasing sugars from the pretreated biomass because of the limited selection of commercial enzymes due to a different operating condition of them

(Agbor et al., 2011; Khare et al., 2015). Mostly, the enzymatic hydrolysis cost is high, for example, it accounts for 36% of the total bioethanol production cost (Hwangbo et al., 2019). Sterilization of hydrolysates to prevent bacterial contamination is another challenge of liquid biofuel production because it needs another energy and costs input (Junker et al., 2006).

Lipid-based biofuel, known-as biodiesel, is an ideal diesel replacement, as it is a renewable, clean-burning liquid fuel that can be produced from animal fats, waste oils, vegetable oils, or biolipids through a well-known transesterification process (Guo et al., 2015). One major limitation of biodiesel production is the sustainable supply of the feedstock. Biolipids such as triacylglycerols (TAGs) can be produced by microorganisms from lignocellulose (Sharma et al., 2018; Wang et al., 2014). Among several TAGs-accumulating microorganisms, *Rhodococcus* strains have shown a great potential for TAGs production as they have abilities to metabolize organic compounds quickly and produce lipid storage compounds (Davila Costa et al., 2017). Especially, *R. opacus* PD630 (referred as PD630) can accumulate TAGs up to 76% of its cell dry weight under nitrogen starvation (Alvarez et al., 2000; Garay et al., 2014). A recent study reported that PD630 can accumulate high TAGs from lignocellulosic biomass and grow on lignin-derived compounds (Gill et al., 2018; Wang et al., 2014).

Biolipid extraction is another costly process during biodiesel production. To extract biolipids from lipids-producing organisms (including algae, yeast or bacteria), solvent extraction method is commonly used and it is another challenge of biodiesel production because current extraction is the energy-intensive and costly (Brennan and

Owende, 2010). New extraction methods such as bacteriophage-based technology have been successfully applied to release granules of polyhydroxybutyrate (PHB) from PHB-accumulating bacterium without additional energy and solvent input by lysing *Pseudomonas oleovorans* (Hand et al., 2016), suggesting that similar approach can be applied to extract granule biolipid. Bacteriophage (phage) is a bacterial virus and replicates inside bacteria as a host. Phages have received great interest because of not only their rapid replication but also the ability to break down the cell envelope by expression of lysis proteins to release intracellular contents of hosts (Cahill and Young, 2019; Pires et al., 2016; Young, 2014). Thus, if phage lysis proteins are applied to *R. opacus*, the cell envelope can be degraded, and TAGs can be released spontaneously. Recently, a novel phage Toil has been isolated and shown to lyse *R. opacus* PD631, a domesticated derivative of PD630, directly resulting in 30% of intracellular TAGs released from phage Toil-infected PD631 (Gill et al., 2018).

The goal of this research is to explore several methods to overcome challenges associated with lipid-based biofuel production from lignocellulose biomass as mentioned above. This research explores new approaches and technologies to increase depolymerization efficacy of lignocellulose, to seek for non-sterile production of biolipids, and to effectively extract biolipids from TAGs-producing bacteria. Firstly, to increase the efficiency of saccharification of pretreated biomass, one-step saccharification using five different saccharifying enzymes (SEs) with a similar optimum pH and temperature and reusability of SEs are demonstrated. To reduce the overall TAGs production and extraction costs, this study investigates non-sterile TAGs production and cell lysis by

induction of phage lytic gene cassette. To this end, this study explores the possibility of prophage genome editing on the bacterial genome to overexpress lignin peroxidase which degrades lignin of lignocellulose to reduce the costs of pretreatment. The results of this study are expected to lead to more efficient and cheaper ways for producing lipid-based biofuels.

1.2. Goal, objectives, and hypotheses

The overall goal of this research is to develop phage-based technologies to enable economical non-sterile biolipid production from lignocellulose. Especially, this research examines the ability to increase the efficiency of pretreatment of biomass and reduce the costs of TAGs production by TAGs-accumulating bacteria. Also, bacteriophage-based methods are explored to lyse the cells for TAGs extraction and produce lignin-degrading enzymes in quantity for pretreatment. To achieve this goal, experiments are conducted to complete three specific objectives as shown in Figure 1.1 and described below.

Objective 1: Develop an effective one-step saccharification of lignocellulosic biomass using reusable saccharifying enzymes (SEs) that are active under similar optimal pH and temperature

Hypothesis: Saccharifying enzymes (SEs) with similar optimum pH and temperature can be produced from engineered *E. coli* in large quantities as crude enzymes. The crude enzymes can be immobilized as magnetic-cross-linked enzyme aggregates and reused to enable effective scarification of lignocellulosic biomass.

Task 1a: Construct the plasmids for each SEs by cloning and examine over expression of SEs from *E. coli*

Task 1b: Prepare immobilized SEs for easy recover and reuse

Task 1c: Compare effectiveness of free crude SEs and immobilized SEs on saccharification of pretreated biomass

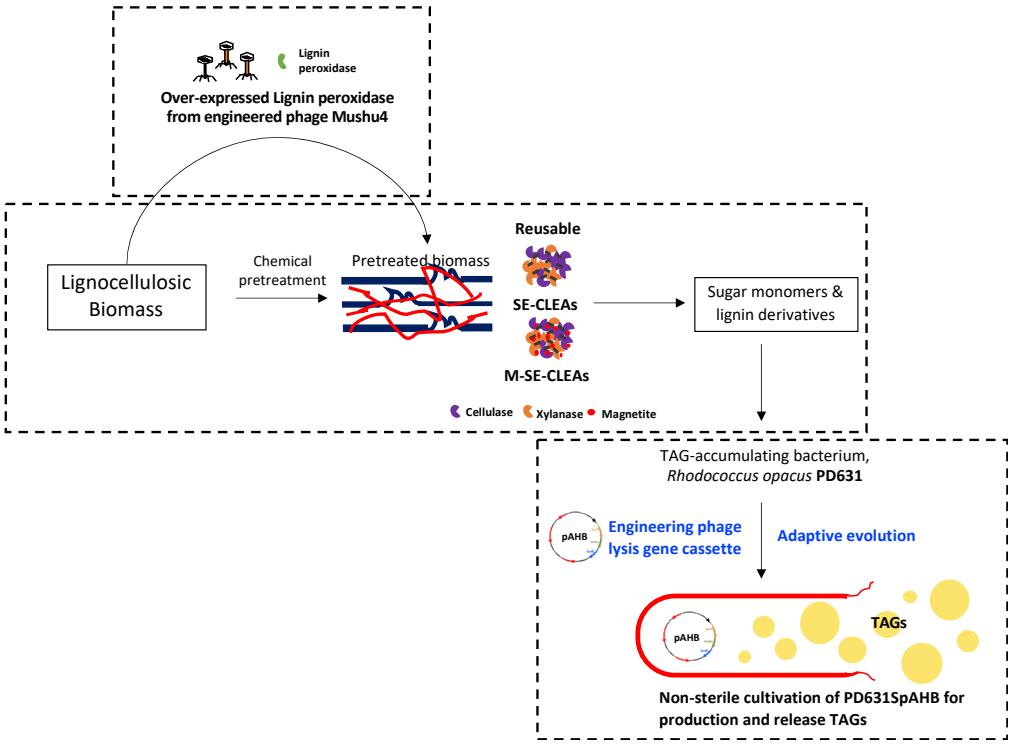

Figure 1.1. Overview of proposed technical objectives in this research.

Objective 2: Develop a salt-tolerant *Rhodococcus opacus* PD631 with phage lytic cassette for non-sterile biolipid production and extraction

Hypothesis: The engineered salt-tolerant PD631 with a plasmid carrying an inducible phage lysis gene cassette can outcompete the growth of non-TAGs-producing

microorganisms in non-sterile saline growth medium and can release TAGs to supernatant by induction of phage lytic genes.

Task 2a: Clone phage lytic genes into a *Rhodococcus* plasmid and electroporate into PD631 and examine the cell lysis of engineered PD631 by controlled lytic gene expressions at desired timeframe

Task 2b: Develop a salt-tolerant PD631 and examine the non-sterile TAGs production

Task 2c: Develop salt-tolerant PD631 containing phage lytic genes and investigate non-sterile production and release of TAGs from this strain

Objective 3: Engineer a prophage element in *Rhodococcus* to express high levels of lignin peroxidase for effective depolymerization of lignin

Hypothesis: Lignin peroxidase can be produced in quantity from engineered prophage by substituting a major capsid proteins (MCPs) gene which is highly expressed by the host cell during lytic cycle. The hypothesis is based on the following rationale. The prophage, integrated into the bacterial chromosome, can be induced to the lytic cycle under constitutively at high frequency. During viral self-assembly, the capsid, which is an icosahedral protein shell, is generated, and a main component of the capsid is MCPs. For an icosahedral shell, normally 415 copies of MCPs are generated per phage containing 30-60 kb genome.

Task 3a: Clone lignin peroxidase and selective marker into *Rhodococcus* plasmid

Task 3b: Engineer the phage Mushu4 DNA to replace a MCPs gene with lignin peroxidase gene by exogenous recombination system

Task 3c: Engineer the phage Mushu4 DNA to replace a MCPs gene with lignin peroxidase gene by homologous recombination during spontaneous induction of Mushu4

1.3. Dissertation overview

This dissertation is organized into six chapters. In Chapter 1, overview of this dissertation, research goals, hypothesis, and specific objectives are outlined. Chapter 2 is literature review focused on recent advances in production and extraction of bacterial lipids for biofuel production. This chapter has been published as a literature review paper in *Science of the Total Environment* (Hwangbo and Chu, 2020). Chapter 3 describes effective one-step saccharification of lignocellulosic biomass using magnetite-biocatalysts containing saccharifying enzymes. Experiments described in Chapter 3 were designed to validate Hypothesis 1, and the results have been published in *Science of the Total Environment* (Hwangbo et al., 2019). Development of non-sterile cultivation and solvent-free biolipid bioextraction to reduce production cost of biolipid-based biofuel is presented in Chapter 4. Experimental results were designed to address Hypothesis 2. Development of novel prophage-based microbial factory for production and release of high titers of lignin peroxidase for lignocellulose depolymerization is present in Chapter 5. Experiments were designed to validate Hypothesis 3. Finally, the conclusion of this research and future works are summarized in Chapter 6.

1.4. References

Agbor, V.B., Cicek, N., Sparling, R., Berlin, A. and Levin, D.B. 2011. Biomass pretreatment: Fundamentals toward application. Biotechnol Adv 29(6), 675-685.

Alvarez, H.M., Kalscheuer, R. and Steinbüchel, A. 2000. Accumulation and mobilization of storage lipids by *Rhodococcus opacus* PD630 and *Rhodococcus ruber* NCIMB 40126. Appl Microbiol Biotechnol 54, 218-223.

Billion-Ton. 2016. Advancing domestic resources for a thriving bioeconomy, U.S. Department of Energy.

Brennan, L. and Owende, P. 2010. Biofuels from microalgae—A review of technologies for production, processing, and extractions of biofuels and co-products. Renewable and Sustainable Energy Reviews 14(2), 557-577.

Cahill, J. and Young, R. 2019. Phage lysis: Multiple genes for multiple barriers. Adv Virus Res 103, 33-70.

Davila Costa, J.S., Silva, R.A., Leichert, L. and Alvarez, H.M. 2017. Proteome analysis reveals differential expression of proteins involved in triacylglycerol accumulation by *Rhodococcus jostii* RHA1 after addition of methyl viologen. Microbiology 163(3), 343-354.

Garay, L.A., Boundy-Mills, K.L. and German, J.B. 2014. Accumulation of high-value lipids in single-cell microorganisms: A mechanistic approach and future perspectives. J Agric Food Chem 62(13), 2709-2727.

Gill, J.J., Wang, B., Sestak, E., Young, R. and Chu, K.H. 2018. Characterization of a novel *tectivirus* phage Toil and its potential as an agent for biolipid extraction. Scientific Reports 8(1), 1062.

Guo, M., Song, W. and Buhain, J. 2015. Bioenergy and biofuels: History, status, and perspective. Renewable and Sustainable Energy Reviews 42, 712-725.

Hand, S., Gill, J. and Chu, K.H. 2016. Phage-based extraction of polyhydroxybutyrate (PHB) produced from synthetic crude glycerol. Science of the Total Environment 557-558, 317-321.

Hwangbo, M. and Chu, K.H. 2020. Recent advances in production and extraction of bacterial lipids for biofuel production. Science of the Total Environment 734, 139420.

Hwangbo, M., Tran, J.L. and Chu, K.H. 2019. Effective one-step saccharification of lignocellulosic biomass using magnetite-biocatalysts containing saccharifying enzymes. Science of the Total Environment 647, 806-813.

Junker, B., Lester, M., Brix, T., Wong, D. and Nuechterlein, J. 2006. A next generation, pilot-scale continuous sterilization system for fermentation media. Bioprocess and Biosystems Engineering 28(6), 351-378.

Khare, S.K., Pandey, A. and Larroche, C. 2015. Current perspectives in enzymatic saccharification of lignocellulosic biomass. Biochemical Engineering Journal 102, 38-44.

Limayem, A. and Ricke, S.C. 2012. Lignocellulosic biomass for bioethanol production: Current perspectives, potential issues and future prospects. Progress in Energy and Combustion Science 38(4), 449-467.

Nlewem, K.C. and Thrash, M.E.J. 2010. Comparison of different pretreatment methods based on residual lignin effect on the enzymatic hydrolysis of switchgrass. Bioresour Technol 101(14), 5426-5430.

Pires, D.P., Cleto, S., Sillankorva, S., Azeredo, J. and Lu, T.K. 2016. Genetically engineered phages: A review of advances over the last decade. Microbiology and Molecular Biology Reviews 80(3), 523-543.

Sharma, P.K., Saharia, M., Srivstava, R., Kumar, S. and Sahoo, L. 2018. Tailoring microalgae for efficient biofuel production. Frontiers in Marine Science 5, 382.

Singhvi, M.S., Chaudhari, S. and Gokhale, D.V. 2014. Lignocellulose processing: A current challenge. RSC Advances 4(16), 8271-8277.

Sun, S., Sun, S., Cao, X. and Sun, R. 2016. The role of pretreatment in improving the enzymatic hydrolysis of lignocellulosic materials. Bioresource Technology 199, 49-58.

Wang, B., Rezenom, Y.H., Cho, K.C., Tran, J.L., Lee, D.G., Russell, D.H., Gill, J.J., Young, R. and Chu, K.H. 2014. Cultivation of lipid-producing bacteria with lignocellulosic biomass: effects of inhibitory compounds of lignocellulosic hydrolysates. Bioresour Technol 161, 162-170.

Young, R. 2014. Phage lysis: three steps, three choices, one outcome. J Microbiol 52(3), 243-258.

2. RECENT ADVANCES IN PRODUCTION AND EXTRACTION OF BACTERIAL LIPIDS FOR BIOFUEL PRODUCTION[*]

2.1. Summary

Lipid-based biofuel is a clean and renewable energy that has been recognized as a promising replacement for petroleum-based fuels. Lipid-based biofuel can be made from three different types of intracellular biolipids; triacylglycerols (TAGs), wax esters (WEs), and polyhydroxybutyrate (PHB). Among many lipid-producing prokaryotes and eukaryotes, biolipids from prokaryotes have been recently highlighted due to simple cultivation of lipid-producing prokaryotes and their ability to accumulate high biolipid contents. However, the cost of lipid-based biofuel production remains high, in part, because of high cost of lipid extraction processes. This review summarizes the production mechanisms of these different types of biolipids from prokaryotes and extraction methods for these biolipids. Traditional and improved physical/chemical approaches for biolipid extraction remain costly, and these methods are summarized and compared in this review. Recent advances in biological lipid extraction including phage-based cell lysis or secretion of biolipids are also discussed. These new techniques are promising for bacterial biolipids extraction. Challenges and future research needs for cost-effective lipid extraction are identified in this review.

---

[*] Reprinted from "Recent advances in production and extraction of bacterial lipids for biofuel production" by Hwangbo, M. and Chu, K.H., 2020, *Science of the Total Environment*, Vol. 734, 139420, Copyright 2020, with permission by Elsevier.

Graphical Summary

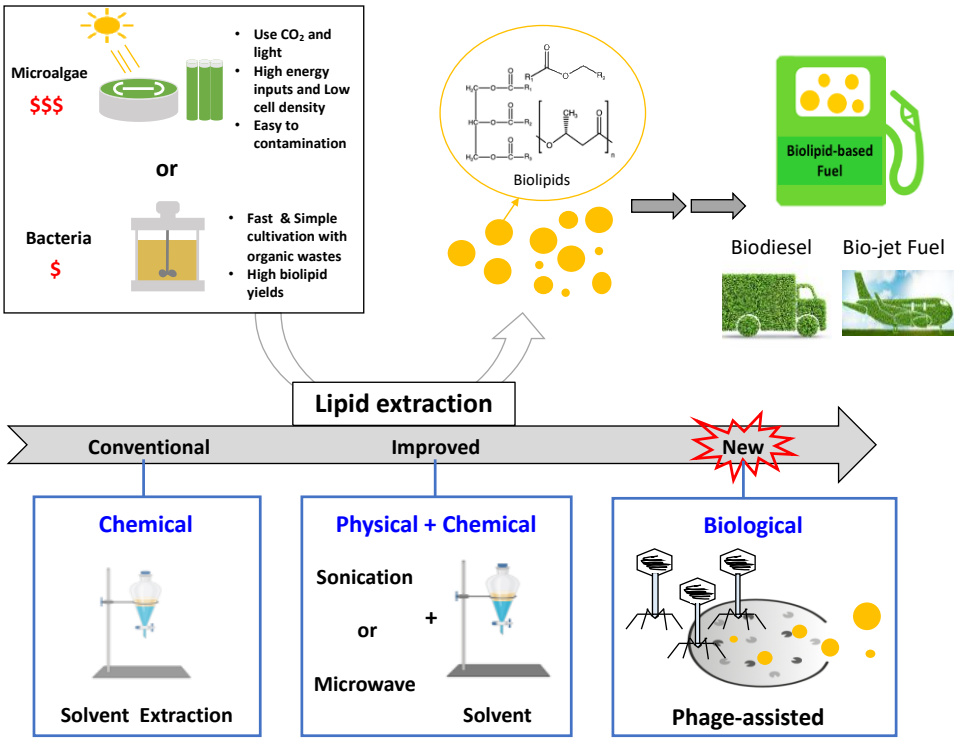

Figure 2.0. Graphical summary of Chapter 2.

Highlights

- Biolipids from prokaryotes are cost-effective feedstocks for biofuel production.
- Conventional chemical and physical biolipid extractions are inefficient and costly.
- Modified chemical and physical approaches require high energy inputs.
- Phage-based and advanced biological techniques are promising bioextraction methods.

2.2. Introduction

Lipid-based biofuel is a liquid fuel that not only is compatible to existing transportation infrastructure but also is nontoxic and renewable energy source than petroleum-based fuel (Guo et al., 2015; Yellapu et al., 2018). Biolipids are starting materials for lipid-based biofuels. As biolipids can be produced from renewable non-food sources without compromising the food resources, lipid-based biofuel is thus considered as one of the favorable biofuel types (Singhvi et al., 2014).

Lipid-based biofuels can be manufactured using three types of bacterial lipids: triacylglycerols (TAGs), wax esters (WEs), and polyhydroxyalkanoates (PHAs) such as polyhydroxybutyrate (PHB) (Figure 2.1). TAGs are simple neutral lipids, consisting of three long-chain fatty acids and one glycerol via ester linkages. TAGs have been used as the primary feedstock to manufacture biodiesel in the form of fatty acid methyl esters (FAMEs) or fatty acid ethyl esters (FAEEs) via transesterification (Ruhul et al., 2015) (Figure 2.2a). WEs are esters formed by combining long-chain fatty acids and long-chain alcohols. WEs have a wide range of industrial applications, including cosmetics, coating stuff, printing inks, lubricants, and biodiesel production (Santala et al., 2014). Similar to TAGs, WEs can be transesterified into FAMEs (as biodiesel) (Budge and Iverson, 2003). In addition, through fast deoxygenation under H_2-free conditions, WEs can be converted into high-heat value and stable fuels like gaseous hydrocarbons, gasoline, jet fuels, or light cycle oil (Figure 2.2b) (Shimada et al., 2018). PHAs are intracellular polymeric lipids. The most common type of PHAs is PHB. PHB consists of a short-chain fatty acid and has been considered as a promising substitute for petroleum-based plastics (Muller et al.,

2014). Similar to the production of biodiesel from TAGs and WEs, PHB can be also used as a feedstock to react with methanol to produce lipid-based biofuel in the form of hydroxybutyrate methyl esters (HBMEs) (Figure 2.2c) (Choonut et al., 2017).

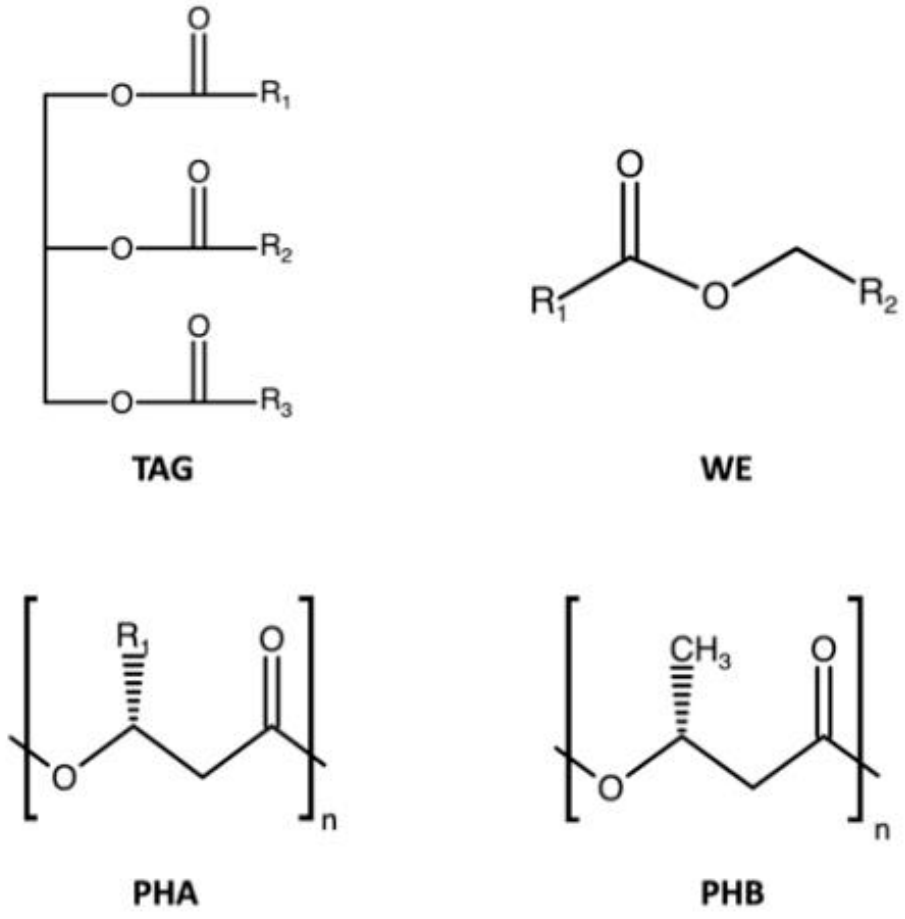

Figure 2.1. Structure of common intracellular lipids from prokaryotes. TAG: Triacylglycerol, WE: Wax Ester, PHA: Polyhydroxyalkanoate, and PHB: Polyhydroxybutyrate. PHB is a common type of PHAs. Other types of PHAs: Polyhydroxypropionate (PHP, R_1=H), Polyhydroxyvalerate (PHV, R_1=C_2H_5), Polyhydroxyhexanoate (PHX, R_1=C_3H_7).

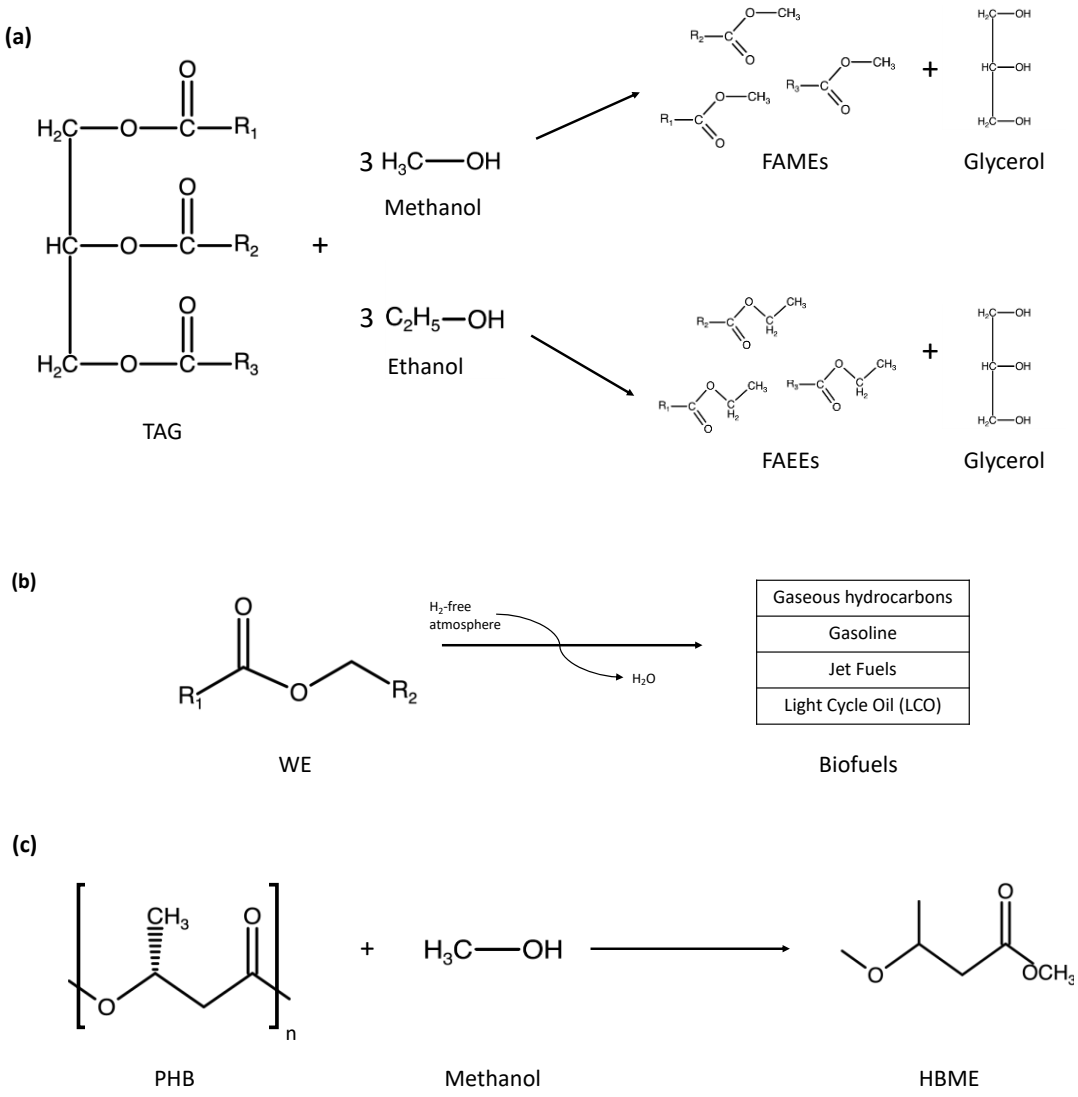

Figure 2.2. Production of lipid-based biofuels from different intracellular lipids. (a) Biodiesel production from TAGs by transesterification. TAGs: Triacylglycerols, FAMEs: Fatty acid methyl esters, FAEEs: Fatty acid ethyl esters. (b) Biofuels production from WEs by fast deoxygenation (revised from graphical abstract of (Shimada et al., 2018)). (c) Biofuel production from PHB by methyl esterification. PHB: Polyhydroxybutyrate, HBME: Hydroxybutyrate methyl ester.

Many microorganisms, including fungal-, algal-, archaeal- and bacterial-species, can accumulate different types of biolipids (Qadeer et al., 2018). Some fungi can produce TAGs and WEs, and only engineered *Yarrowia lipolytica* and *Saccharomyces cerevisiae*

strains can produce PHA/PHB (Du et al., 2018; Ji et al., 2018). Several archaeal strains are known to produce PHA/PHB (Han et al., 2007; Wang et al., 2019). Many microalgae and bacteria have been reported to accumulate TAGs, WEs, or PHA/PHB (Garay et al., 2014; Qadeer et al., 2018; Sharma et al., 2018; Tan et al., 2020).

Green or red algae, the most studied algae for TAG production, have TAG contents ranging from 20 to 50% of dry cell weight when cultured under nitrogen-limited conditions (Brennan and Owende, 2010; Sharma et al., 2018). Recent studies have reported that microalgae, *Chlorella vulgaris*, accumulated 25 to 42% TAGs from nutrient-rich sources such as domestic wastewater, seafood wastewater, or chicken compost (Leong et al., 2018; Nguyen et al., 2019; Tan et al., 2018b). The ability to produce WEs or PHB is much less common in algal species. For example, *Euglena gracilis* can produce WEs anaerobically (Abdo and Ali, 2019; Nakazawa et al., 2018) and *Haematococcus pluvialis* can accumulate PHB (Abdo and Ali, 2019). While the ability to accumulate TAGs and/or WEs by bacterial strains are only found in several species belonging *Mycobacterium*, *Rhodococcus*, and *Acinetobacter* (Alvarez, 2003; Garay et al., 2014; Lenneman et al., 2013), numerous bacterial strains are known to accumulate PHB (Murphy, 2012). Compared to algae, some bacterial strains showed a similar or even better TAG accumulating ability, i.e., accumulating 55 to 76% TAGs of their dry cell weight (Alvarez and Steinbüchel, 2002; Amara et al., 2016).

Algal TAGs have been recently considered as a sustainable feedstock for biodiesel production, because algae use CO_2 as a carbon source and can be cultivated with marginal water quality (Brennan and Owende, 2010). Yet, many limitations and challenges - such

as continuous light input, low cell density, and inefficient and costly cell harvesting and lipid extraction - have limited the sustainable supply of algal TAGs for biodiesel production (Benvenuti et al., 2016). These challenges and limitations might be overcome by cultivating TAG-accumulating bacterial strains, because they can grow rapidly on inexpensive carbon and/or nutrient sources such as organic wastes and can achieve high cell densities while producing higher TAG contents (up to 76% of its dry cell weight) (Alvarez and Steinbüchel, 2002; Amara et al., 2016). The high bacterial TAG contents are comparable to those of algal strains. Additionally, using organic wastes for TAG production will allow for carbon neutral. Due to easy cultivation and fast growth of high lipid-accumulating bacteria, high yields of bacterial lipids are feasible. Accordingly, bacterial lipids can be considered as an ideal feedstock material to reduce lipid-based biofuel production costs.

Despite the promise of lipid-based biofuel, the production cost of the biofuel is high, in part, due to expensive downstream processes such as cell harvesting and lipid extraction. The extraction of lipids from microorganisms is a main challenge, as the process accounts for 50% of the total energy consumption of biodiesel production (Dassey et al., 2014). Thus, technologies that can reduce extraction cost is critical to realization of industrial production of lipid-based biofuel. Solvent extraction is a common chemical method used for algal and bacterial lipids extraction (Brennan and Owende, 2010). However, the traditional extraction method poses several limitations for large-scale biodiesel production. These limitations are (i) chlorinated solvent - used in extraction is toxic; (ii) spent solvent becomes a secondary wastestream; and (iii) more energy is

required to separate solvent from lipids (Ren et al., 2017). These drawbacks have been partially addressed by improved methods by integrating solvent extraction with chemical and/or mechanical processes to achieve better lipid recovery (Harris et al., 2018). However, these improved techniques require high energy inputs and remain high costs. On the other hand, biological methods such as applications of enzymes to disrupt cell wall (Patel et al., 2018) and bacteriophages (viruses that lyse bacteria) as bioextractants to release TAGs or PHB from bacteria have been recently demonstrated (Gill et al., 2018; Hand et al., 2016).

To this end, this review summarizes recent progress in lipid extraction technologies from prokaryotes that are capable of producing TAGs, WEs, and PHAs/PHB. To understand the type of biolipids from prokaryotes, the production mechanism of three biolipids from prokaryotes are discussed in this review. Reviews on TAG extractions from microalgae are recently available elsewhere (Harris et al., 2018; Kumar et al., 2015a; Wang et al., 2020). In this review, conventional and improved chemical/physical methods for biolipid extraction methods are discussed, and their extraction efficiency is also compared. Mostly, new biological extraction methods for bacterial lipid extraction are summarized. Current knowledge gaps and future research needs for cost-effective biolipid extraction are also discussed and identified.

2.3. Intracellular lipids produced from prokaryotes

2.3.1. Production of triacylglycerols (TAGs) / wax esters (WEs)

Triacylglycerols (TAGs) are neutral lipids consisting of three medium-chain (C16-C20) fatty acids and one glycerol via ester linkage. Wax esters (WEs), formed by combining long-chain (C12-C24) fatty acids and long-chain alcohols, are another neutral lipid. Because neutral lipids can be used for biofuel production, TAGs/WEs are recently recognized as promising feedstocks (Klok et al., 2014). Eukaryotic microorganisms such as yeast and fungi are also able to accumulate TAGs or WEs under stressed conditions (Alvarez and Steinbüchel, 2002), and microalgal TAGs/WEs have been used for biodiesel production (Benvenuti et al., 2016; Sharma et al., 2018).

Unlike eukaryotic microorganisms, the accumulation of TAGs and/or WEs is less common in most prokaryotes. No archaeal strains have been reported to accumulate TAGs or WEs, and only a few bacteria can accumulate TAGs and/or WEs. These TAG- and/or WE-accumulating bacteria include Gram-positive actinomycete like *Dietzia*, *Mycobacterium*, *Nocardia*, *Rhodococcus*, and *Streptomyces*, and gram-negative bacteria like *Acinetobacter*, *Marinobacter*, and *Pseudomonas* (Table 2.1) (Alvarez, 2003; Alvarez et al., 1997; De Andres et al., 1991; Fixter et al., 1986; Garay et al., 2014; Ishige et al., 2003; Kosa and Ragauskas, 2012; Lenneman et al., 2013; McCarthy, 1971; Olukoshi and Packter, 1994). Bacteria generally synthesize TAGs/WEs under stressed conditions such as nitrogen deficiency with excess carbon. Various carbon sources including sugars, organic acids, alcohols, and lignocellulosic biomass, can be used to synthesize TAGs (Alvarez and Steinbüchel, 2002; Wang et al., 2014). *Acinetobacter baylyi* ADP1 is a

Gram-negative bacterium known for its ability to accumulate WEs (Santala et al., 2014). Among many *Rhodococcus* strains that are known to accumulate TAGs, *R. opacus* PD630 (referred as PD630 hereafter) has been considered as a model TAG-accumulating strain due to its ability to accumulate TAGs up to 76% of cell dry weight when grown on gluconate as a carbon source under nitrogen limited conditions (Alvarez, 2003; Garay et al., 2014). Strain PD630 and its domesticated strain PD631 can also metabolize a wide range of organic compounds in hydrolysate of lignocellulose while accumulate high levels of TAGs (Gill et al., 2018; Wang et al., 2014).

Table 2.1. Accumulation of intracellular lipids by prokaryotes.

Bacterium	Carbon source	Type of lipids	Extraction method	Lipid contents	References
Gram-negative bacteria					
Acinetobacter sp.	Olive oil	TAG	Solvent extraction	25%	Alvarez et al., 1997
Acinetobacter sp. M-1	n-hexadecane	WE	Solvent extraction	17%	Ishige et al., 2003
Marinobacter aquaeolei VT8	Citrate/ succinate	WE	Ultrasound-assisted solvent extraction	3.5%	Lenneman et al., 2013
Pseudomonas aeruginosa 44T1	Olive oil	TAG	Solvent extraction	38%	de Andres et al., 1991
Alcaligenes latus ATCC 29714	Sugarbeet juice	PHB	Solvent extraction	39%	Wang et al., 2013
Burkholderia cepacian ATCC 17759	Glycerol	PHB	Solvent extraction	82%	Zhu et al., 2010
Burkholderia sacchari IPT 101	Sugarcane bagasse hydrolysate	PHB	Chemical-assisted conversion	62%	Silva et al., 2004
Cupriavidus necator H16	Jatropha oil	PHB	Chemical-assisted conversion	87%	Ng et al., 2010
Cupriavidus necator H16	Sodium gluconate	PHB	Chemical-assisted conversion	66%	Heinrich et al., 2012
Halomonas halophila CCM 3662	Glucose	PHB	Solvent extraction	82%	Kucera et al., 2018
Halomonas halophila CCM 3662	Cellobiose	PHB	Solvent extraction	91%	Kucera et al., 2018
Methylobacterium sp. ZP24	Lactose	PHB	Solvent extraction	66%	Nath et al., 2008
Pseudomonas extremaustralis DSM 25547	Octanoate	PHB	Solvent extraction	36%	Catone et al., 2014
Pseudomonas oleovorans ATCC 29347	Glycerol	PHB	Phage-based extraction	32%	Hand et al., 2016
Pseudomonas pseudoflava ATCC 33668	Xylose	PHB	Chemical-assisted conversion	28%	Bertrand et al., 1990
Vibrio spp. M20	Glycerol	PHB	Solvent extraction	43%	Chien et al., 2007
Zobellella denitrificans MW1	Glycerol	PHB	Solvent extraction	67%	Ibrahim and Steinbuchel, 2009
Zobellella denitrificans ZD1	Glycerol	PHB	Chemical-assisted conversion	85%	Asiri et al., 2020
Gram-positive bacteria					
Dietzia maris 53	Hexaecane	Total Fatty Acids	Solvent extraction	19%	Alvarez, 2003
Mycobacterium avium B2900	Palmitic acid	TAG	Solvent extraction	5%	McCarthy, 1971
Nocardia resricta 560	Gluconate	Total Fatty Acids	Solvent extraction	19%	Alvarez, 2003
Nocardia globerula 432	Gluconate	Total Fatty Acids	Solvent extraction	19%	Alvarez, 2003
Rhodococcus jostii RHA1	Benzoate	TAG	Solvent extraction	55%	Amara et al., 2016
Rhodococcus opacus PD630	4-hydroxy benzoic acid	TAG	Solvent extraction	20%	Kosa and Ragauskas, 2012
Rhodococcus opacus PD630	Gluconate	Total Fatty Acids	Solvent extraction	76%	Alvarez, 2003
Rhodococcus opacus PD631	Gluconate	TAG	Phage Toil	-[a]	Gill et al., 2018
Rhodococcus erythropolis 17	Pentadecane	Total Fatty Acids	Solvent extraction	57%	Alvarez, 2003
Streptomyces lividans JI 1126	Glucose	TAG	Solvent extraction	9%	Olukoshi and Packter, 1994
Bacillus megaterium	Sugar cane	PHB	Chemical-assisted conversion	46%	Gouda et al., 2001

[a] The information is not available.

Table 2.1. Continued.

Archaea	Carbon source	Type of lipids	Extraction method	Lipid contents	References
Haloarcula sp. IRU1	Glucose	PHB	Solvent extraction	63%	Taran and Amirkhani, 2010
Haloarcula marismortui ATCC 43049	Glucose	PHB	Chemical-assisted conversion	21%	Han et al., 2007
Haloferax mediterranei	Glucose	PHB	Solvent extraction	17%	Fernandez-Castillo et al., 1986
Haloferax volcanii	Glucose	PHB	Solvent extraction	7%	Fernandez-Castillo et al., 1986

Fatty acids are common starting compounds for TAGs and WEs biosynthesis in bacteria (Figure 2.3). As shown in Figure 2.3a, bacterial TAGs are biosynthesized via several enzymes (Amara et al., 2016). With an expense of CoA and ATP, fatty acid-CoA synthase converts fatty acid into fatty acyl-CoA. Fatty acyl-CoA is subjected to sequential acylation of sn-glycerol-3-phosphate by glycerol-3-phosphate acyl transferase (GPAT) and acylglycerol-3-phophate acyl transferase (AGPAT) to form phosphatidic acid. Phosphatidic acid is then dephosphorylated by phosphatidic acid phosphatase (PAP) to yield diacylglycerol, of which is finally catalyzed by wax ester synthase/ acyl-CoA: diacylglycerol acyl transferase (WS/DGAT) to form TAG. In WEs synthesis pathway (Figure 2.3b), fatty acyl-CoA can be converted to fatty alcohol via two possible routes: one route is catalyzed by fatty acyl-CoA reductase (FAR) or the other route is sequentially catalyzed by acyl-CoA reductase (ACR) and fatty aldehyde reductase (FALDR). Similar to the last step of TAG synthesis, fatty alcohol is finally catalyzed by WS/DGAT to form WEs (Figure 2.3b).

There are several potential advantages of using bacterial TAGs/WEs for lipid-based biofuel production. In view of carbon footprint, bacterial TAGs/WEs derived from renewable organic sources like lignocellulosic biomass and organic wastes can be carbon neutral (Wältermann et al., 2005). Oils derived from plant seeds require more water and land usage, and the production of plant seeds can be highly affected by season and climate changes. For bacterial lipids, less water usage and land space are needed for cultivation of TAGs/WEs- producing bacteria and the production of bacterial TAGs/WEs can be all-year-round (Brennan and Owende, 2010; Cea et al., 2015).

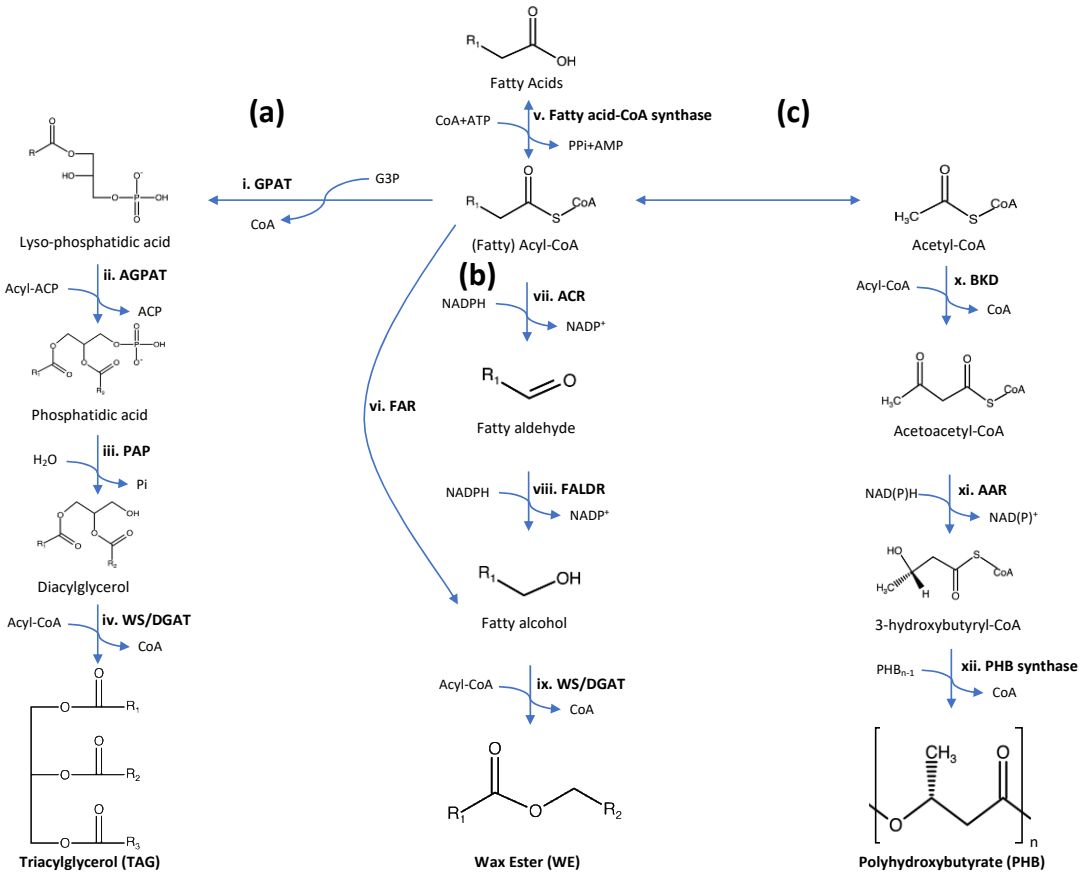

Figure 2.3. Synthesis pathways of intracellular lipids from prokaryotes. (a) Biosynthesis of triacylglycerol (TAG) from Acyl-CoA. GPAT: Glycerol-3-phosphate acyl transferase, AGPAT: Acylglycerol-3-phosphate acyl transferase, PAP: Phosphatidic acid phosphatase, and WS/DGAT: Wax ester synthetase/diacylglycerol acyltransferase. (b) Biosynthesis of wax ester (WE) from fatty acids. FAR: Fatty acyl-CoA reductase, ACR: Acyl-CoA reductase, and FALDR: Fatty aldehyde reductase. (c) Biosynthesis of polyhydroxybutyrate (PHB) granule from Acetyl-CoA. BKD: β-Ketothiolase and AAR: Acetoacetyl-CoA Reductase (revised from Fig. 1 of (Muller et al., 2014)).

Additionally, cultivation of bacteria is considered much easier and cheaper than microalgae cultivation in open ponds or photobioreactors which are commonly limited by availability of light and low solubility of CO_2 (Brennan and Owende, 2010; Cea et al., 2015). Fast bacterial growth rates and high bacterial cell density are advantageous in

terms of biolipid yield. For examples, the doubling-time of bacterium *Rhodococcus* is 3 to 4 h normally (Swain et al., 2012) compared to the doubling time of microalgae *Nannochloropsis* is 2 to 4 days (Kawaroe et al., 2015). Cell density of bacteria is generally higher (5.4 g/L) (Thanapimmetha et al., 2017) compared to that of microalgae (1 g/L) (Perin et al., 2015). Mostly, TAG-accumulating bacteria show higher TAG contents of cell dry weight than that of most of microalgae (Amara et al., 2016). Considering those advantages described above, bacterial lipids are a promising feedstock for lipid-based fuel production.

2.3.2. Production of polyhydroxybutyrate (PHB)

Polyhydroxybutyrate (PHB), a short-chain-length polyhydroxyalkanoate (PHA), has been recognized as a promising alternative to petroleum-based plastics, because PHB has similar properties of petroleum-based plastics and is biodegradable (Zhu et al., 2010). Some archaea and most bacteria can synthesize PHB as internal carbon and energy storage under non-growth conditions (i.e., during stationary phase) (Murphy, 2012). Recently, some bacteria with an ability to accumulate PHB via growth-associated mechanisms have been reported (Asiri et al., 2020; Ibrahim and Steinbüchel, 2009).

Archaeal species such as *Haloarcula* sp., *Haloarcula marismortui*, *Haloferax mediterranei,* and *Haloferax volcanii* have been reported to accumulate PHB (Table 2.1) (Fernandez-Castillo et al., 1986; Han et al., 2007; Hezayen et al., 2000; Taran and Amirkhani, 2010). Among these archaeal species, *Haloarcula* sp. showed the highest PHB accumulation content up to 63% of its dry cell weight when grown with excess

glucose (Taran and Amirkhani, 2010). PHB-accumulating bacteria including *Bacillus, Alcaligenes, Burkholderia, Cupriavidus, Halomonas, Methylobacterium, Pseudomonas, Vibrio,* and *Zobellella* are also listed in Table 2.1 (Asiri et al., 2020; Bertrand et al., 1990; Bormann and Roth, 1999; Catone et al., 2014; Chien et al., 2007; Gouda et al., 2001; Hand et al., 2016; Kucera et al., 2018; Madkour et al., 2013; Nath et al., 2008; Ng et al., 2010; Salakkam and Webb, 2015; Silva et al., 2004; Wang et al., 2013; Zhu et al., 2010).

Cupriavidus necator is a well-studied model strain to study PHB production from expensive carbon sources such as glucose and pure oils (Franz et al., 2012; Ng et al., 2010). To reduce overall PHB production cost, crude glycerol, a by-product of biodiesel production, has explored as a potential cheap carbon source for cultivation of PHB-accumulating bacteria. However, crude glycerol contains impurities such as methanol, fatty acids, and salts, and the growth of this strain has found to be inhibited by methanol (Salakkam and Webb, 2015). Interestingly, other PHB-accumulating strains such as *Bacillus, Pseudomonas oleovorans,* and *Zobellella denitrificans* ZD1 were able to tolerant methanol, fatty acids, and high salts while producing PHB from synthetic crude glycerol (Asiri et al., 2020; Hand et al., 2016). *Zobellella denitrificans* MW1 and ZD1 can grow with glycerol while accumulating high PHB content to 81% and 85%, respectively (Asiri et al., 2020; Ibrahim and Steinbüchel, 2009). Unlike most of archaea and bacteria accumulate PHB during non-growth phase, *Zobellella denitrificans* MW1 and ZD1 can accumulate PHB during active growth phase, and then achieve their maximum PHB contents during stationary phase. The growth-associated PHB production is a favorable characteristic of *Zobellella denitrificans* since production of PHB would be possible by

simply increasing the biomass of *Zobellella denitrificans* without using an additional nutrient limitation step.

Biosynthesis of PHB requires three key enzymes, as shown in Figure 2.3c. In this pathway, acetyl-CoA is firstly converted to acetoacetyl-CoA and then 3-hydroxybutyryl-CoA by β-ketothiolase (BKD) and acetoacetyl CoA reductase (AAR), encoded by the *phaA* and *phaB* genes respectively, and PHB is synthesized from 3-hydroxybutyryl-CoA by PHB synthase, which encoded by *phaC* gene (Muller et al., 2014; Murphy, 2012). These three essential genes are generally placed in a single operon in most PHB accumulating bacteria (Legat et al., 2010). After that, PHB spherical granules are formed by PHB granule-associated proteins (PhaM) and phasins, which encoded by *phaP* (Pfeiffer and Jendrossek, 2014).

To maximize PHB accumulation, this polymeric lipid synthesis pathway has been successfully engineered into non-oleaginous bacterial strains such as *Escherichia coli* (Madkour et al., 2013; Rahman et al., 2013; Xu et al., 2018). High PHB or TAGs production has been demonstrated using engineered *E. coli* carrying a plasmid containing a complete synthesis pathway of PHB or TAGs (Chen et al., 2018; Wu et al., 2016). While cultivation of PHB accumulators is easier and cheaper (Xu et al., 2018; Zhu et al., 2010), the price of PHB remains high due to high PHB granule extraction cost (Murphy, 2012).

2.4. Cultivation and harvest of lipid-producing microorganisms

Over the past few decades, a substantial knowledge on cultivation and harvest of TAG-producing microalgae/cyanobacteria has been accumulated, and recent reviews on

this topic are available in the literature (Markou and Georgakakis, 2011; Mata et al., 2010; Tan et al., 2020; Tan et al., 2018a). Similarly, cultivation and harvest of PHB-producing microorganisms (bacteria and archaeal species) have been intensively studied and reviewed (Ibrahim and Steinbüchel, 2009; Koller, 2018; Koller et al., 2012; Murphy, 2012; Peña et al., 2014). However, there are limited studies on TAG-producing bacteria (Castro et al., 2016; Wältermann et al., 2005). As cyanobacteria are bacteria not algae and cultivation of cyanobacteria has not been differentiated from that of microalgae (Pathak et al., 2018), a brief overview of methods for cultivation and harvest of TAG-producing microalgae/cyanobacteria and bacteria is described below.

Open raceway ponds and closed photobioreactors are two most commonly used microalgae/cyanobacteria cultivation systems. The open raceway pond system, typically equipped with paddle wheels and supplied with nutrients and pure CO_2, is widely used in industrial settings for microalgae/cyanobacteria cultivation, due to its low construction cost, easy operation and maintenance (Pathak et al., 2018; Tan et al., 2020). In recent years, to minimize the requirement of nutrient input, wastewater has been used as nutrient sources, but inhibition of microalgae/cyanobacteria growth has been reported due to high copper contents or toxic compounds in wastewater (Tan et al., 2018a). This open cultivation process is also subjected to many drawbacks such as contamination and competition with other microorganisms, difficulties in maintaining high-TGA-producing strains, and production of low total biomass that pose challenges in downstream harvesting process (Balat, 2011; Tan et al., 2018a). Different from the open system, photobioreactors are closed systems, allowing both indoor and outdoor cultivation and minimizing the

contamination problems (Mata et al., 2010). Yet, the closed system is not cost-effective for scale-up due to its difficulties in maintenance and high operation cost, particularly when an indoor light source is required (Tan et al., 2018a).

Industrial-scale production of TAG-producing prokaryotes has not been realized, as research interest on TAG-producing prokaryotes has sparked during high crude oil price and then subsided as crude oil price plunged recently. Laboratory-scale bioreactors are generally used for cultivation of TAG-producing prokaryotes (Kumar et al., 2015b). Several factors, such as bacterial species, carbon sources, carbon to nitrogen ratios, and cultivation time, have been found to affect the growth of TAG-producing prokaryotes and their TAG contents (Alvarez et al., 1997; Castro et al., 2016; Wältermann et al., 2005). As TAG-accumulating prokaryotes are heterotrophs, they can be cultivated with various carbon sources, including sugars, hydrocarbons, or organic acids, with different TAG accumulation efficiencies (Table 1). To reduce cultivation cost and offset carbon footprint, many inexpensive and renewable carbon and nutrient sources such as lignocellulosic biomass, glycerol and crude glycerol (biodiesel production by-product), wastewater, and agro-industrial organic wastes have been shown to support the growth of TAG-accumulating bacteria with TAG content ranging from 14% to 51% (Kumar et al., 2015b; Kurosawa et al., 2015; Muller et al., 2014; Wang et al., 2014). Compared to microalgae/cyanobacteria, the cultivation of prokaryotes is much simpler and faster based on their cultivation methods, shorter doubling times, higher cell densities, and high yields of biolipid accumulation (Alvarez and Steinbüchel, 2002; Amara et al., 2016; Kawaroe et al., 2015; Swain et al., 2012).

Different cultivation methods affect not only the biomass concentration and lipid content (Koller, 2018; Kumar et al., 2015b; Tan et al., 2018a) but also the effectiveness of biomass harvesting, the first step in downstream processes of lipid-based biofuels (Dickinson et al., 2017). Factors such as cell sizes, biomass concentrations, or surface characteristics of microorganisms determine the selection of harvest method to be used. Various harvesting approaches such as centrifugation, flocculation, and filtration from oleaginous microorganisms were reviewed recently (Dickinson et al., 2017; Tan et al., 2020; Yellapu et al., 2018). These approaches can also apply to harvest of oleaginous bacterial cultures, although there are limited studies on harvesting of TAG-producing bacteria. New approaches such as co-cultivation of microalgae and bacteria as a new way to increase algal TAG and facilitate the TAG extraction have been studied and recently reviewed (Wang et al., 2020; Zhang et al., 2020). Using osmotic challenge of thermophilic bacteria for PHA production was recently introduced (Pernicova et al., 2020).

2.5. Extraction of biolipids from prokaryotes

In this section, various extraction methods, ranging from conventional chemical-based methods to recent novel biological approaches, are introduced and compared.

2.5.1. Chemical and physical extraction methods

2.5.1.1. Solvent extraction of biolipids from whole cells

Biolipids are extracted by organic solvent mixture containing a polar solvent and a low-polarity solvent. The polar and low-polarity solvents in the mixture is essential to

separate neutral lipids (such as TAGs and WEs) and non-neutral lipids (such as PHAs and PHB) from non-granule lipid substances (such as phospholipids and glycolipids) (Patel et al., 2018). Applications of low-polarity solvents alone cannot extract neutral lipids successfully, because the low-polarity solvents were unable to access the strong hydrogen bonds of polar lipids of the cell wall and neutral lipids (Harris et al., 2018) (Figure 2.4). Generally, polar solvents such as methanol, ethanol, and acetone can disrupt the complex structure of neutral-polar lipids, and then low-polarity solvents like chloroform, diethyl ether, hexane, and benzene can solubilize the neutral lipids for easy separation from aqueous phase.

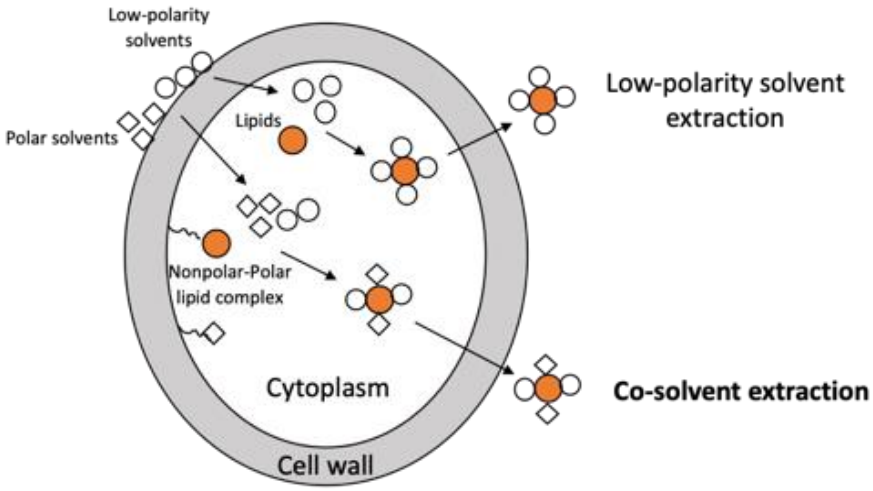

Figure 2.4. Conventional organic solvent extraction mechanism by low-polarity solvent or co-solvent extraction (revised from Fig. 6 of (Halim et al., 2012)).

Two common solvent methods for lipid extraction are (1) Folch method and (2) Bligh and Dyer method (Patel et al., 2018). In 1959, Folch used a mixture of

chloroform/methanol (2:1, v/v) to extract lipids from animal tissues, and this method was later called Folch method (Patel et al., 2018). In this method, methanol acts as a polar solvent, and chloroform acts as a low-polarity solvent to achieve a better extraction efficiency of neutral lipids. Three years later, Bligh and Dyer used chloroform/methanol/water (2:1:0.8, v/v/v) for lipid purification and extraction. The addition of water in the extraction mixture allows generating a distinct biphasic system, which is particularly effective for wet tissue samples. This method became known as Bligh and Dyer method (Harris et al., 2018).

Folch method is the most commonly used method for TAGs extraction from bacteria. This method can extract 49% of TAGs from *Rhodococcus* sp. 602 (Alvarez, 2003; Silva et al., 2010). Recent research showed that Folch method could extract 43% of TAGs from lyophilized *Rhodococcus rhodochrous* ATCC 21198 or 55% of TAGs from bead-beated *Rhodococcus jostii* RHA1 (Amara et al., 2016; Shields-Menard et al., 2015). Chloroform is also common solvent used for polymeric lipids extraction from bacteria (Madkour et al., 2013). Due to the concern of the toxicity of chloroform, nonhalogenated organic solvents such as ethylene carbonate and butyl acetate has been recently explored and demonstrated to recover 98% or 96% of PHB produced from *Cupriavidus necator* (Aramvash et al., 2015; Aramvash et al., 2018). Still, concerns about the solvent extraction methods are many including toxicity of the solvent, difficulties in solvent handling due to its flammability and volatility, and the high energy costs (Harris et al., 2018). The types and concentrations of extraction solvents and incubation times can affect the extraction efficiency (Kumar et al., 2015a). Moreover, recent studies suggested the

efficiency of biolipid extraction is strongly affected by cell disrupting pretreatment, which needs additional energy input and costs (Lee et al., 2017). These drawbacks of solvent extraction methods, particularly the high cost, prevent the large-scale lipid-based biofuel production.

2.5.1.2. Cell disruption-assisted solvent extraction

To release biolipids in the cytoplasm of bacteria, it is necessary to disrupt both cell membrane and cell wall. According to Gram staining, Gram-negative and Gram positive are two types of bacterial cell walls (1) Gram-negative cell wall contains a thin peptidoglycan layer, or (2) Gram-positive cell wall contains a thick peptidoglycan layer. Peptidoglycan is a polymer of sugars and amino acids and provides structural strength to bacteria. Most of TAG-accumulating bacteria are Gram-positive actinomycete. Some actinomycete such as *Mycobacterium* and *Rhodococcus* have a complex cell wall composition (Mitani et al., 2005). On the top of the thick peptidoglycan layer, there are two additional layers, an arabinogalactan layer and a mycolic acid layer (Figure 2.5a). Thus, to extract TAGs from actinomycete, one has to disrupt not only the peptidoglycan layer but also the mycolic acid layer.

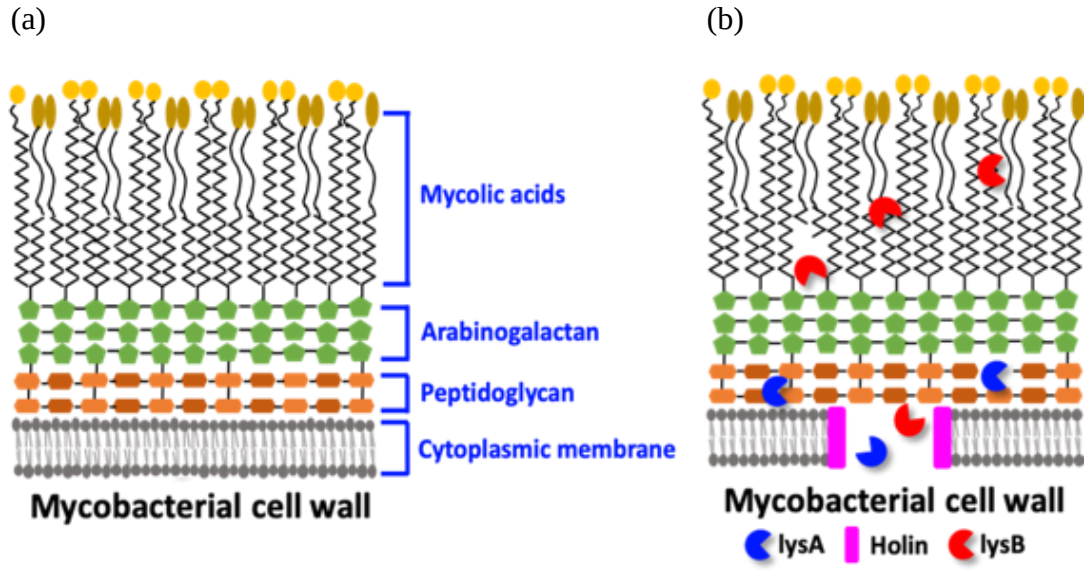

Figure 2.5. Cell wall structure and phage lytic proteins. (a) Structure of mycobacterial cell wall. (b) Phage lytic proteins needed for degrading mycobacterial cell walls. Holin disrupts the cytoplasmic membrane to allow release of lytic proteins, endolysin A and mycolate esterase. Endolysin A (lysA) hydrolyzes the peptidoglycan and mycolate esterase (lysB) hydrolyzes the ester bond between arabionogalactan and mycolic acids.

Breaking the structure of the cell wall (referred as cell disruption) has been shown to enhance extraction or purification of intracellular components like biolipids (Lee et al., 2017; Patel et al., 2018). Mechanical processes (such as bead beating, ultrasonication, microwave, and freeze-thaw processes) and non-mechanical approaches (such as chemical treatments and enzymatic lysis) have been used to disrupt cell wall structure (Lee et al., 2017). Below is a brief description of mechanical processes and chemical treatments for cell disruption. Enzymatic lysis is described in section 2.4.2.1.

(i) Bead beating, first used in cosmetic industry, creates a solid shear force to disrupt cells to extract intracellular components from microorganisms (Patel et al., 2018). Several factors such as speeds, bead sizes, or the load of beads can affect the efficiencies of cell disruption (Wang et al., 2020). Advantages of using bead beating for cell disruption are many including continuous operation, various applicability, and high efficiency (Patel et al., 2018).

(ii) Ultrasonication is the most common and useful cell disrupting method. Cell disruption by ultrasonication is achieved via two phenomena, cavitation and shock-wave propagation (Lee et al., 2017; Mubarak et al., 2016). During the ultrasonication, cavitation and shock-wave propagation create a pressure and a jet stream on cells, respectively, and then cell disruption occurs by shear forces from the pressure and jet stream (Lee et al., 2017; Patel et al., 2018). Ultrasonication has been generally used not only for cell lysis but also for a better biolipid extraction from microorganisms.

To prevent excessive heating, samples were incubated on the ice after each sonication cycle. Sonication number of cycles and intensity are important factors in cell lysis (Patel et al., 2018). Cell lysis of *Mycobacterium* or *Rhodococcus* is challenging due to their complex cell wall structure. Ultrasonication has showed higher effectiveness of protein extraction from *Rhodococcus* sp. than those using bead beating (Norazah et al., 2015; Rabodoarivelo et al., 2016).

(iii) Microwave is another effective way to disrupt cell for a better biolipid extraction. Cell disruption is caused by a high temperature and pressure from the thermal energy by a

microwave radiation, and then components inside cells can be released more easily (Harris et al., 2018; Hattab et al., 2015). The process has several advantages like simple method, short processing time, and less energy consumption than conventional heating process (Kapoore et al., 2018; Patel et al., 2018). Due to these advantages, microwave is generally used for bacterial and microalgal cell lysis to extract intracellular components including genome, proteins, and biolipids. Operation conditions based on the cell type are an important factor for microwave-assisted cell disruption (Woo et al., 2000). Cell lysis using microwave is well known to accelerate DNA extraction of several Gram-positive bacteria including *Mycobacterium*, *Rhodococcus*, and *Peptococcus* (Moore et al., 2004). It also can make significantly bigger pores on the cell wall of microalgal *Chlorella* sp., leading to effective cell disruption (Lee et al., 2017).

(iv) Freeze-thaw is a physical and thermal method to disrupt cell envelope. By repeating several cycles of rapid freezing in a freezer or dry ice bath and thawing at 37 °C, ice that formed inside the cell can lead to disrupt of cell membrane. Although this method is simple, freeze-thaw is time-consuming, energy intensive, and not suitable for release of temperature sensitive intracellular components (Islam et al., 2017). Also, several factors like number of cycles, temperature, and incubation time can affect the cell disruption efficiencies (Tang et al., 2003).

(v) Chemical assisted-cell lysis is a non-mechanical treatment. Cell disruption can be accomplished by adding chemicals such as acids, bases, solvents, or surfactants.

Sulfuric acid (H_2SO_4) is commonly used in chemical industry to hydrolyze sugar polymers due to the low price of the acid (Lee et al., 2017). For alkaline lysis, sodium hydroxide (NaOH) is used to generate OH^- ions for cell lysis (Brown and Audet, 2008). Solvents such as methanol, toluene, or dimethyl sulfoxide can detach lipid components from cell wall structure, and thus cell lysis occurs effectively (Harris et al., 2018). By using sodium hypochlorite (bleach), approximately 92% of poly(3-hydroxybutyrate) (P(3HB)), one type of PHB, was recovered from *Cupriavidus necator* H16 cells (Heinrich et al., 2012). However, application of solvents is difficult in an industrial process mainly due to toxicity, flammability, and volatility of solvents (Patel et al., 2018).

Surfactants can disassemble lipids and proteins of the cell membrane and create pores on the membrane to cause cell lysis (Brown and Audet, 2008). Among different zwitterionic, ionic, and non-ionic surfactants, studies have showed that Gram-negative and Gram-positive bacterial cells were lysed successfully by Triton X-100 (non-ionic surfactant) or sodium dodechyl sulphate (SDS) (ionic surfactant) (Brown and Audet, 2008; Danilevich et al., 2008). For example, about 90% of P(3HB) from *R. eutropha* cells was released following cell lysis by SDS, and more than 97% of P(3HB) was recovered by using a mixture of SDS and hypochlorite (Jacquel et al., 2008; Kim et al., 2003). However, the high cost of surfactants is the main disadvantage for its application to the industrial scale (Madkour et al., 2013).

Improved lipid extraction has been recently demonstrated by ultrasound-assisted extraction, a process using ultrasonication and solvent extraction simultaneously (Harris et al., 2018). As shown in Figure 2.6, the ultrasonication pretreatment allows to release lipids into medium, and thus only a short extraction time and small amount of solvents are needed for effective lipid extraction. For example, 100% of TAGs were extracted from *Trichosporon oleaginosus* within 15 min of ultrasonication (52 Hz and 2800 W) in solvent mixture (chloroform-methanol, 2:1). This is a much shorter process time (15 min) compared to 12 h that was needed for same extraction efficiency when only solvent extraction was used (Zhang et al., 2014). This method has been also shown high recovery yield of PHA/PHB from bacteria (Madkour et al., 2013). The ultrasound-assisted extraction is promising for bacterial lipid extraction; yet, ultrasonication requires high energy input which remains expensive (Harris et al., 2018).

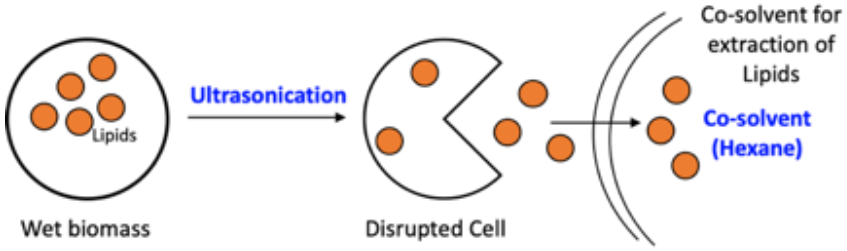

Figure 2.6. Ultrasound-assisted extraction with hexane as a co-solvent (revised from Graphical abstract of (Yao et al., 2018)).

2.5.2. Biological methods for biolipid extraction

2.5.2.1. Enzymatic cell lysis to release lipids

Various enzymes such as lysozyme, glycosidase, peptidase, or protease can be used to degrade bacterial cell wall (Vermassen et al., 2019). Lysozyme can hydrolyze the

peptidoglycan of cell wall structure, and thus it is a common enzyme used to degrade Gram-positive bacterial cell wall (Salazar and Asenjo, 2007). Glycosidase or peptidase hydrolyze the glycosidic linkages or amide bonds in the peptidoglycan chain, respectively. Protease can break down proteins by cleavage the peptide bonds. Complex enzymatic cocktails might be needed for complete hydrolysis of the cell wall of strain PD630 (a TAG-accumulating bacterium), which have a complex cell wall structure including layers of peptidoglycan, arabinogalactan and mycolic acids (Figure 2.5a).

Enzymatic treatment is effective for extracting PHB from Gram-negative, PHB-accumulating bacteria such as *Cupriavidus necator* and *Pseudomonas putida*. Approximately 89% of PHB of *C. necator* DSM545 was recovered by using 2% (mass/biomass) of trypsin (a serine protease) at 50 °C and pH 8.0 (Kapritchkoff et al., 2006). Similarly, more than 88% of P(3HB) was extracted from *C. necator* DSM545 by using commercial enzyme cocktails such as Celumax® BC in acetate buffer at 60 °C and pH 4.0 for 1 h (Neves and Muller, 2012). Ninety-five % of PHA recovery from *P. putida* was achieved by using the combination of alcalase, SDS, and ethylenediaminetetraacetic acid (EDTA) (Madkour et al., 2013). The operating conditions are an important factor to affect the lysis efficiency because of different optimal temperature/ pH of each enzyme (Islam et al., 2017). No research on release TAGs or WEs from bacteria by enzymatic treatment has been reported. The advantages of enzymatic cell disruption are low energy input and effective under mild operating conditions. However, commercial enzymes are expensive, making application of enzymes for cell disruption not cost-effective (Demuez et al., 2015).

2.5.2.2. Phage-based extraction for lipids

Although previous and current research efforts have been heavily placed on biolipid extraction from microalgae, a novel bacteriophage-based approach to release bacterial lipids (TAGs and PHB) has been recently reported (Gill et al., 2018; Hand et al., 2016).

Bacteriophage (phage) is a virus that only infects host bacterial cell. Following infection (lytic cycle), phage takes over host genetic replication machinery and rapidly produces new phage particles, which are then released from the host cell by lysing the host cell envelope. This lysis process leads to release of intracellular components and phage particles together (Cahill and Young, 2019; Doss et al., 2017). Phage's ability to disrupt host cell has received considerable research interest in clinical and environmental applications (Pires et al., 2016; Young, 2014). The phage lytic proteins - holin, endolysin (LysA), and mycolate esterase (LysB) - are responsible for host cell lysis process. Holin disrupts the cytoplasmic membrane by generating lethal holes and controls the cell lysis timing, LysA hydrolyzes peptidoglycan of cell wall, and LysB degrades ester bonds between arabinogalactan and mycolic acids. Holin and LysA are needed to lyse cell wall without mycolic acid layer, while all three lytic proteins are needed to lyse bacterial cell wall containing mycolic acids. Similar to mycobacterium, three lytic proteins are needed to lyse TAG-accumulating *Rhodocossus* bacteria (Kamilla and Jain, 2016) (Figure 2.5b).

Researchers have demonstrated PHAs extraction using engineered PHA-producing bacterium with an ability to produce phage lytic proteins (Martinez et al., 2011;

Naranjo et al., 2013) or using bacteriophage infection (Hand et al., 2016). A self-lytic *Pseudomonas putida* was able to express two lytic proteins of phage EJ-1 to lyse the cell for PHA release, and PHA can be directly extracted from the wet lysed cell (Martinez et al., 2011). By infecting PHB-accumulating *Pseudomonas oleovorans* with phage Ke14, granule PHB was successfully released from the infected strain (Hand et al., 2016). Results of these studies suggest that phages-based approach would be useful to extract TAGs from TAG-accumulating bacterium. More recently, our laboratory demonstrated TAGs extraction from a TAG-accumulating bacterium *Rhodococcus opacus* PD631 (referred as PD631) by using a novel phage Toil (Gill et al., 2018). About 30% of intracellular TAGs was released from PD631 comparing to those without Toil infection. The phage-based technology opens a new means to release bacterial lipids. Given that several factors such as incubation times, operating conditions, and ratios of phage to cell are important factors to increase the extraction efficiencies when using whole phages for biolipid extraction, more studies, perhaps by integrating phage-based technologies with some chemical-based extraction methods, are needed to improve the overall TAGs yield.

2.5.2.3. Advanced biological techniques to release lipids

Autolysis of cells and secretion of TAGs/PHB can be effective ways to harvest biolipids from bacteria, since this approach does not require cell lysis (Rahman et al., 2013). A recombinant *E. coli* MG1655 harboring *phbCAB* genes from *Alcaligenes eutrophus* was able to grow with 2X LB medium with 21% of glucose with ampicillin to release up to 80.2% of PHB upon autolysis of the strain (Jung et al., 2005). Using type I

secretion system and phasin proteins to reduce PHB granule size for secretion, an engineered *E. coli* strain was able to secret about 36% of total PHB into its growth medium (Rahman et al., 2013). These engineered bacterial strains have demonstrated promising strategies to recover PHB without using conventional biolipid extraction methods. No research on spontaneous secretion of TAGs has been reported.

2.6. Challenges and future directions

Lipids from prokaryotes are promising renewable feedstocks for lipid-based biofuel production. Yet, there are still several challenges, mainly the high cost of lipid extraction, preventing industrial production of lipid-based biofuel. The estimated minimum production cost of biodiesel from microalgal lipids (3.96 $/L) remains much higher than those produced from plant-based lipids such as derived from sunflower (0.62 $/L) or derived from oil palm (0.68 $/L) (Pardo-Cárdenas et al., 2013). This cost analysis does not consider important factors such as feedstock types and biolipid productivity. If bacterial lipids from oleaginous *Rhodococcus* strains are used, the biodiesel production cost might be potentially reduced to 0.79 $/L because the *Rhodococcus* strains can achieve a high cell density which is approximately five-fold higher than that of oleaginous microalgae (Perin et al., 2015; Thanapimmetha et al., 2017).

Solvent extraction is commonly used in industry, and the cost of extraction solvent was estimated to be 10% of total operation cost (Sun et al., 2019). Additionally, approximately 50% of the total energy consumption for algal biodiesel production was used for solvent-based lipid extraction (Dassey et al., 2014). A brief summary and

comparison of extraction methods are listed in Table 2.2. As shown in Table 2.2, to reduce the amounts of solvent, improved methods combining cell disruption and solvent extraction such as ultrasound-assisted or chemical-assisted extraction were introduced. However, applications of these methods into the industry remain challenging due to the high costs. The high costs of these methods are due to the higher energy inputs for ultrasonication steps or higher costs of detergent/surfactants (Madkour et al., 2013; Miazek et al., 2017). Not surprisingly, most of these techniques have not been widely applied for bacterial biolipids extraction. Phage-based or biolipid secretion techniques can be promising effective bacterial lipid extraction approaches to overcome the drawbacks of high cost and energy input associated with solvent extraction and other extraction methods described above. Using advanced biological extraction, the environmental and health impacts associated with extraction solvent can be potentially lessened. Newly reported phage-based extraction technique and biolipid secretion technique are promising in terms of no additional high energy inputs for cell disruption compared to ultrasound-assisted methods and no concerns of solvent toxicity and no needs for subsequence downstream processes compared to solvent and chemical-assisted extraction methods.

Table 2.2. Summary and comparison of various extraction methods.

Method		Extraction efficiency[a]	Energy requirement	Factors	Advantages	Disadvantages	References
Conventional solvent extraction		High	High	- Type/ concentration of solvent - Incubation time - Pretreatment for cell disruption	- High efficiency	- Toxicity - Flammability - Volatility - High costs - Drying of microorganism OR cell disruption pretreatment needed	- Harris et al., 2018 - Kumar et al., 2015a - Lee et al., 2017
Cell disruption-assisted solvent extraction	Bead beating	Medium-high	Moderate-high	- Speed of equipment - Size of bead (diameter) - Ratio of bead	- Continuous operation - Applicability - Efficiency	- Depending on several factors - Difficult to scale up	- Patel et al., 2018 - Wang et al., 2020
	Ultrasonication	High	High	- Number of cycles - Interval time on ice - Frequency intensity	- High efficiency - Small amounts of solvent - Short process time	- Energy intensive - High costs for equipment and operation - Difficult to scale up	- Harris et al., 2018 - Patel et al., 2018 - Zhang et al., 2014
	Microwave	High	Moderate-high	- Type of cell - Operation time	- Simple - Small amounts of solvent - Short process time	- Energy intensive - High costs for equipment and operation	- Harris et al., 2018 - Kapoore et al., 2018 - Patel et al., 2018 - Woo et al., 2000
	Freeze-thaw	Medium-low	Moderate-high	- Number of cycles of freeze/thaw - Temperature - Incubation time	- Simple	- Time-consuming - Energy intensive - No suitable for temperature sensitive components	- Islam et al., 2017 - Tang et al., 2003
	Chemical treatment	High	Moderate	- Type/ concentration of solvent - Incubation time - Temperature/ pH	- Simple	- Toxicity - Flammability - Volatility - High costs	- Lee et al., 2017 - Madkour et al., 2013 - Patel et al., 2018
	Enzymatic treatment	Medium-high	Low	- Type of enzyme - Temperature/ pH - Cell density	- Simple - Low energy requirement	- High costs - Long process time	- Demuez et al., 2015 - Islam et al., 2017 - Patel et al., 2018
Phage-based extraction		Low	Low	- Incubation time - Temperature/ pH - Ratio of phage to cell	- Low energy requirement - No need cell disruption pretreatment	- Low extraction yield - Need to find suitable phage - Only for bacterial biolipids extraction - Lack of research	- Gill et al., 2018 - Hand et al., 2016 - Martinez et al., 2011
Autolysis of cells		Medium-high	Low	- Incubation time - Temperature/ pH	- Low energy requirement - No need cell disruption pretreatment	- Lack of research	- Jung et al., 2005 - Rahman et al., 2013
Secretion of biolipids		Medium-low	Low	- Incubation time - Temperature/ pH	- Low energy requirement - No need cell disruption pretreatment	- Low extraction yield - Lack of research	- Rahman et al., 2013

[a] Extraction efficiency was evaluated based on previous studies ranging from 0-30% of efficiency (Low), 31-60% of efficiency (Medium), 61-90% of efficiency (Medium-high), and 91-100% of efficiency (High).

To overcome challenges of biolipid extraction from cells, new approaches to directly convert lipids into lipid-based biofuel have been recently explored. For example, *in-situ* transesterification of TAGs from microalgae biomass into FAMEs has been demonstrated by adding chemical solvents (methanol) and a catalyst with TAG-bearing microalgae so that TAG extraction and transesterification can occur together (Tang et al., 2016). In this process, the produced FAMEs form a lighter separate aqueous phase for easy recovery, lifting the need of solvent extraction for TAGs (Nelson and Viamajala, 2016). This approach can be a new way to reduce lipid-based biofuel production costs due to exclusion of lipid extraction step.

2.7. Conclusions

This review discussed the current and advanced technologies of biolipid extraction for lipid-based biofuels production. Due to several advantages of biolipids from prokaryotes, this review focused on finding a better and effective prokaryotic biolipids extraction. Based on comparing previous biolipid extraction technologies, phage-based approach or biological advanced approach are promising bacterial lipids extraction methods, which can reduce environmental impacts and solvent costs of conventional solvent extraction even the yield of them is still low. Also, the facilities costs or energy inputs of them are smaller than the current extraction methods. Future research is needed directly towards increasing the efficiency of biolipid extraction from these new biological approaches for biolipids-accumulating prokaryotes.

2.8. References

Abdo SM, Ali GH. Analysis of polyhydroxybutrate and bioplastic production from microalgae. Bulletin of the National Research Centre 2019; 43: 97.

Alvarez HM. Relationship between β-oxidation pathway and the hydrocarbon-degrading profile in actinomycetes bacteria. International Biodeterioration & Biodegradation 2003; 52: 35-42.

Alvarez HM, Pucci OH, Steinbüchel A. Lipid storage compounds in marine bacteria. Appl Microbiol Biotechnol 1997; 47: 132-139.

Alvarez HM, Steinbüchel A. Triacylglycerols in prokaryotic microorganisms. Appl Microbiol Biotechnol 2002; 60: 367-376.

Amara S, Seghezzi N, Otani H, Diaz-Salazar C, Liu J, Eltis LD. Characterization of key triacylglycerol biosynthesis processes in *rhodococci*. Scientific Reports 2016; 6: 24985.

Aramvash A, Gholami-Banadkuki N, Moazzeni-Zavareh F, Hajizadeh-Turchi S. An environmentally friendly and efficient method for extraction of PHB biopolymer with non-halogenated solvents. J Microbiol Biotechnol 2015; 25: 1936-1943.

Aramvash A, Moazzeni-Zavareh F, Gholami-Banadkuki N. Comparison of different solvents for extraction of polyhydroxybutyrate from *Cupriavidus necator*. Engineering in Life Sciences 2018; 18: 20-28.

Asiri F, Chen CH, Hwangbo M, Shao Y, Chu KH. From organic wastes to bioplastics: Feasibility of non-sterile polyhydroxybutylate (PHB) production by *Zobellella denitrificans* ZD1. ACS Omega 2020. *In revision*.

Balat M. Potential alternatives to edible oils for biodiesel production – A review of current work. Energy Conversion and Management 2011; 52: 1479-1492.

Benvenuti G, Bosma R, Ji F, Lamers P, Barbosa MJ, Wijffels RH. Batch and semi-continuous microalgal TAG production in lab-scale and outdoor photobioreactors. J Appl Phycol 2016; 28: 3167-3177.

Bertrand JL, Ramsay BA, Ramsay JA, Chavarie C. Biosynthesis of Poly-p-Hydroxyalkanoates from Pentoses by *Pseudomonas pseudoflava*. Appl Environ Microbiol 1990; 56: 3133-3138.

Bormann EJ, Roth M. The production of polyhydroxybutyrate by *Methylobacterium rhodesianum* and *Ralstonia eutropha* in media containing glycerol and casein hydrolysates. Biotechnology Letters 1999; 21: 1059-1063.

Brennan L, Owende P. Biofuels from microalgae—A review of technologies for production, processing, and extractions of biofuels and co-products. Renewable and Sustainable Energy Reviews 2010; 14: 557-577.

Brown RB, Audet J. Current techniques for single-cell lysis. J R Soc Interface 2008; 5: S131-S138.

Budge SM, Iverson SJ. Quantitative analysis of fatty acid precursors in marine samples: direct conversion of wax ester alcohols and dimethylacetals to FAMEs. J Lipid Res 2003; 44: 1802-1807.

Cahill J, Young R. Phage lysis: Multiple genes for multiple barriers. Adv Virus Res 2019; 103: 33-70.

Castro AR, Rocha I, Alves MM, Pereira MA. *Rhodococcus opacus* B4: a promising bacterium for production of biofuels and biobased chemicals. AMB Express 2016; 6: 35.

Catone MV, Ruiz JA, Castellanos M, Segura D, Espin G, Lopez NI. High polyhydroxybutyrate production in *Pseudomonas extremaustralis* is associated with differential expression of horizontally acquired and core genome polyhydroxyalkanoate synthase genes. PLoS One 2014; 9: e98873.

Cea M, Sangaletti-Gerhard N, Acuna P, Fuentes I, Jorquera M, Godoy K, Osses F, Navia R. Screening transesterifiable lipid accumulating bacteria from sewage sludge for biodiesel production. Biotechnol Rep (Amst) 2015; 8: 116-123.

Chen J, Li W, Zhang ZZ, Tan TW, Li ZJ. Metabolic engineering of *Escherichia coli* for the synthesis of polyhydroxyalkanoates using acetate as a main carbon source. Microb Cell Fact 2018; 17: 102.

Chien CC, Chen CC, Choi MH, Kung SS, Wei YH. Production of poly-beta-hydroxybutyrate (PHB) by *Vibrio* spp. isolated from marine environment. J Biotechnol 2007; 132: 259-263.

Choonut A, Yunu T, Pichid N, Sangkharak K. The optimization conditions of polyhydroxybutyrate methyl ester from polyhydroxybutyrate via acid-catalyst. Energy Procedia 2017; 138: 435-440.

Danilevich VN, Petrovskaya LE, Grishin EV. A Highly efficient procedure for the extraction of soluble proteins from bacterial cells with mild chaotropic solutions. Chem. Eng. Technol. 2008; 31: 904-910.

Dassey AJ, Hall SG, Theegala CS. An analysis of energy consumption for algal biodiesel production: Comparing the literature with current estimates. Algal Research 2014; 4: 89-95.

De Andres C, Espuny MJ, Robert M, Mercade ME, Manresa A, Guinea J. Cellular lipid accumulation by *Pseudomonas aeruginosa* 44T1. Appl Microbiol Biotechnol 1991; 35: 813-816.

Demuez M, Mahdy A, Tomas-Pejo E, Gonzalez-Fernandez C, Ballesteros M. Enzymatic cell disruption of microalgae biomass in biorefinery processes. Biotechnol Bioeng 2015; 112: 1955-1966.

Dickinson S, Mientus M, Frey D, Amini-Hajibashi A, Ozturk S, Shaikh F, Sengupta D, El-Halwagi MM. A review of biodiesel production from microalgae. Clean Technologies and Environmental Policy 2017; 19: 637-668.

Doss J, Culbertson K, Hahn D, Camacho J, Barekzi N. A review of phage therapy against bacterial pathogens of aquatic and terrestrial organisms. Viruses 2017; 9.

Du ZY, Alvaro J, Hyden B, Zienkiewicz K, Benning N, Zienkiewicz A, Bonito G, Benning C. Enhancing oil production and harvest by combining the marine alga Nannochloropsis oceanica and the oleaginous fungus Mortierella elongata. Biotechnol Biofuels 2018; 11: 174.

Fernandez-Castillo R, Rodriguez-Valera F, Gonzalez-Ramos J, Ruiz-Berraquero F. Accumulation of poly(b-hydroxybutyrate) by halobacteria. Appl Environ Microbiol 1986; 51: 214-216.

Fixter LM, Nagi MN, McCormack JG, Fewson CA. Structure, distribution and function of wax esters in *Acinetobacter calcoaceticus*. Journal of General Microbiology 1986; 132: 3147-3157.

Franz A, Rehner R, Kienle A, Grammel H. Rapid selection of glucose-utilizing variants of the polyhydroxyalkanoate producer *Ralstonia eutropha* H16 by incubation with high substrate levels. Lett Appl Microbiol 2012; 54: 45-51.

Garay LA, Boundy-Mills KL, German JB. Accumulation of high-value lipids in single-cell microorganisms: A mechanistic approach and future perspectives. J Agric Food Chem 2014; 62: 2709-2727.

Gill JJ, Wang B, Sestak E, Young R, Chu KH. Characterization of a novel *tectivirus* phage Toil and its potential as an agent for biolipid extraction. Scientific Reports 2018; 8: 1062.

Gouda MK, Swellam AE, Omar SH. Production of PHB by a *Bacillus megaterium* strain using sugarcane molasses and corn steep liquor as sole carbon and nitrogen sources. Microbiol Res 2001; 156: 201-207.

Guo M, Song W, Buhain J. Bioenergy and biofuels: History, status, and perspective. Renewable and Sustainable Energy Reviews 2015; 42: 712-725.

Halim R, Danquah MK, Webley PA. Extraction of oil from microalgae for biodiesel production: A review. Biotechnol Adv 2012; 30: 709-732.

Han J, Lu Q, Zhou L, Zhou J, Xiang H. Molecular characterization of the *phaEC*Hm genes, required for biosynthesis of poly(3-hydroxybutyrate) in the extremely halophilic archaeon *Haloarcula marismortui*. Appl Environ Microbiol 2007; 73: 6058-6065.

Hand S, Gill J, Chu KH. Phage-based extraction of polyhydroxybutyrate (PHB) produced from synthetic crude glycerol. Science of the Total Environment 2016; 557-558: 317-21.

Harris J, Viner K, Champagne P, Jessop PG. Advances in microalgal lipid extraction for biofuel production: A review. Biofuels, Bioproducts and Biorefining 2018; 12: 1118-1135.

Hattab MA, Ghaly A, Hammouda A. Microalgae harvesting methods for industrial production of biodiesel: Critical review and comparative analysis. J Fundam Renewable Energy Appl 2015; 5: 1000154.

Heinrich D, Madkour MH, Al-Ghamdi MA, Shabbaj II, Steinbüchel A. Large scale extraction of poly(3-hydroxybutyrate) from *Ralstonia eutropha* H16 using sodium hypochlorite. AMB Express 2012; 2: 59.

Hezayen FF, Rehm BHA, Eberhardt R, Steinbüchel A. Polymer production by two newly isolated extremely halophilic archaea: Application of a novel corrosion-resistant bioreactor. Appl Microbiol Biotechnol 2000; 54: 319-325.

Ibrahim MH, Steinbüchel A. Poly(3-hydroxybutyrate) production from glycerol by *Zobellella denitrificans* MW1 via high-cell-density fed-batch fermentation and simplified solvent extraction. Appl Environ Microbiol 2009; 75: 6222-6231.

Ishige T, Tani A, Sakai Y, Kato N. Wax ester production by bacteria. Current Opinion in Microbiology 2003; 6: 244-250.

Islam MS, Aryasomayajula A, Selvaganapathy PR. A review on macroscale and microscale cell lysis methods. Micromachines 2017; 8.

Jacquel N, Lo CW, Wei YH, Wu HS, Wang SS. Isolation and purification of bacterial poly(3-hydroxyalkanoates). Biochem Eng J 2008; 39: 15-27.

Ji RY, Ding Y, Shi TQ, Lin L, Huang H, Gao Z, Ji XJ. Metabolic engineering of yeast for the production of 3-hydroxypropionic acid. Front Microbiol 2018; 9: 2185.

Jung IL, Phyo KH, Kim KC, Park HK, Kim IG. Spontaneous liberation of intracellular polyhydroxybutyrate granules in *Escherichia coli*. Res Microbiol 2005; 156: 865-873.

Kamilla S, Jain V. Mycobacteriophage D29 holin C-terminal region functionally assists in holin aggregation and bacterial cell death. The FEBS Journal 2016; 283: 173-190.

Kapoore RV, Butler TO, Pandhal J, Vaidyanathan S. Microwave-Assisted extraction for microalgae: From biofuels to biorefinery. Biology (Basel) 2018; 7.

Kapritchkoff FM, Viotti AP, Alli RC, Zuccolo M, Pradella JG, Maiorano AE, Miranda EA, Bonomi A. Enzymatic recovery and purification of polyhydroxybutyrate produced by *Ralstonia eutropha*. J Biotechnol 2006; 122: 453-462.

Kawaroe M, Hwangbo J, Augustine D, Putra HA. Comparison of density, specific growth rate, biomass weight, and doubling time of microalgae *Nannochloropsis* sp. cultivated in Open Raceway Pond and Photobioreactor. AACL BIOFLUX 2015; 8: 740-750.

Kim M, Cho KS, Ryu HW, Lee EG, Chang YK. Recovery of poly(3-hydroxybutyrate) from high cell density culture of *Ralstonia eutropha* by direct addition of sodium dodecyl sulfate. Biotechnol Lett 2003; 25: 55-59.

Klok AJ, Lamers PP, Martens DE, Draaisma RB, Wijffels RH. Edible oils from microalgae: Insights in TAG accumulation. Trends Biotechnol 2014; 32: 521-528.

Koller M. A Review on established and emerging fermentation schemes for microbial production of polyhydroxyalkanoate (PHA) biopolyesters. Fermentation 2018; 4.

Koller M, Salerno A, Muhr A, Reiterer A, Chiellini E, Casella S, Horvat P, Braunegg G. Whey lactose as a raw material for microbial production of biodegradable polyesters. In: Saleh HED, editor. Polyester. InTech, 2012.

Kosa M, Ragauskas AJ. Bioconversion of lignin model compounds with oleaginous *Rhodococci*. Appl Microbiol Biotechnol 2012; 93: 891-900.

Kucera D, Pernicova I, Kovalcik A, Koller M, Mullerova L, Sedlacek P, Mravec F, Nebesarova J, Kalina M, Marova I, Krzyzanek V, Obruca S. Characterization of the promising poly(3-hydroxybutyrate) producing halophilic bacterium *Halomonas halophila*. Bioresour Technol 2018; 256: 552-556.

Kumar RR, Rao PH, Arumugam M. Lipid extraction methods from microalgae: A comprehensive review. Frontiers in Energy Research 2015a; 2.

Kumar S, Gupta N, Pakshirajan K. Simultaneous lipid production and dairy wastewater treatment using *Rhodococcus opacus* in a batch bioreactor for potential biodiesel application. Journal of Environmental Chemical Engineering 2015b; 3: 1630-1636.

Kurosawa K, Radek A, Plassmeier JK, Sinskey AJ. Improved glycerol utilization by a triacylglycerol-producing *Rhodococcus opacus* strain for renewable fuels. Biotechnol Biofuels 2015; 8: 31.

Lee SY, Cho JM, Chang YK, Oh YK. Cell disruption and lipid extraction for microalgal biorefineries: A review. Bioresour Technol 2017; 244: 1317-1328.

Legat A, Gruber C, Zangger K, Wanner G, Stan-Lotter H. Identification of polyhydroxyalkanoates in *Halococcus* and other haloarchaeal species. Appl Microbiol Biotechnol 2010; 87: 1119-1127.

Lenneman EM, Ohlert JM, Palani NP, Barney BM. Fatty alcohols for wax esters in *Marinobacter aquaeolei* VT8: two optional routes in the wax biosynthesis pathway. Appl Environ Microbiol 2013; 79: 7055-7062.

Leong WH, Lim JW, Lam MK, Uemura Y, Ho CD, Ho YC. Co-cultivation of activated sludge and microalgae for the simultaneous enhancements of nitrogen-rich wastewater bioremediation and lipid production. Journal of the Taiwan Institute of Chemical Engineers 2018; 87: 216-224.

Madkour MH, Heinrich D, Alghamdi MA, Shabbaj II, Steinbüchel A. PHA recovery from biomass. Biomacromolecules 2013; 14: 2963-2672.

Markou G, Georgakakis D. Cultivation of filamentous cyanobacteria (blue-green algae) in agro-industrial wastes and wastewaters: A review. Applied Energy 2011; 88: 3389-3401.

Martinez V, Garcia P, Garcia JL, Prieto MA. Controlled autolysis facilitates the polyhydroxyalkanoate recovery in *Pseudomonas putida* KT2440. Microb Biotechnol 2011; 4: 533-547.

Mata TM, Martins AA, Caetano NS. Microalgae for biodiesel production and other applications: A review. Renewable and Sustainable Energy Reviews 2010; 14: 217-232.

McCarthy C. Utilization of palmitic acid by *Mycobcterium avium*. Infection and Immunity 1971; 4: 199-204.

Miazek K, Kratky L, Sulc R, Jirout T, Aguedo M, Richel A, Goffin D. Effect of organic solvents on microalgae growth, metabolism and industrial bioproduct extraction: A review. Int J Mol Sci 2017; 18: 1429.

Mitani Y, Meng X, Kamagata Y, Tamura T. Characterization of LtsA from *Rhodococcus erythropolis*, an enzyme with glutamine amidotransferase activity. J Bacteriol 2005; 187: 2582-2591.

Moore E, Arnscheidt A, Kruger A, Strompl C, Mau M. Simplified protocols for the preparation of genomic DNA from bacterial cultures. Molecular Microbial Ecology Manual 2004; 1.01: 3-18.

Mubarak M, Shaija A, Suchithra TV. Ultrasonication: An effective pre-treatment method for extracting lipid from *Salvinia molesta* for biodiesel production. Resource-Efficient Technologies 2016; 2: 126-132.

Muller EE, Sheik AR, Wilmes P. Lipid-based biofuel production from wastewater. Curr Opin Biotechnol 2014; 30: 9-16.

Murphy DJ. The dynamic roles of intracellular lipid droplets: from archaea to mammals. Protoplasma 2012; 249: 541-585.

Nakazawa M, Ando H, Nishimoto A, Ohta T, Sakamoto K, Ishikawa T, Ueda M, Sakamoto T, Nakano Y, Miyatake K, Inui H. Anaerobic respiration coupled with mitochondrial fatty acid synthesis in wax ester fermentation by *Euglena gracilis*. FEBS Lett 2018; 592: 4020-4027.

Naranjo JM, Posada JA, Higuita JC, Cardona CA. Valorization of glycerol through the production of biopolymers: the PHB case using *Bacillus megaterium*. Bioresour Technol 2013; 133: 38-44.

Nath A, Dixit M, Bandiya A, Chavda S, Desai AJ. Enhanced PHB production and scale up studies using cheese whey in fed batch culture of *Methylobacterium* sp. ZP24. Bioresour Technol 2008; 99: 5749-5755.

Nelson DR, Viamajala S. One-pot synthesis and recovery of fatty acid methyl esters (FAMEs) from microalgae biomass. Catalysis Today 2016; 269: 29-39.

Neves A, Muller J. Use of enzymes in extraction of polyhydroxyalkanoates produced by *Cupriavidus necator*. Biotechnol Prog 2012; 28: 1575-1580.

Ng KS, Ooi WY, Goh LK, Shenbagarathai R, Sudesh K. Evaluation of jatropha oil to produce poly(3-hydroxybutyrate) by *Cupriavidus necator* H16. Polymer Degradation and Stability 2010; 95: 1365-1369.

Nguyen TDP, Nguyen DH, Lim JW, Chang CK, Leong HY, Tran TNT, Vu TBH, Nguyen TTC, Show PL. Investigation of the relationship between bacteria growth and lipid production cultivating of Microalgae *Chlorella vulgaris* in seafood wastewater. Energies 2019; 12.

Norazah MN, Jayasree N, Ahmad SA, Shukor MY, Abdul Latif I. Disrupting *Rhodococcus* sp: A competent method for genomics and proteomics. Journal of Chemical and Pharmaceutical Sciences 2015; 8: 336-341.

Olukoshi ER, Packter NM. Importance of stored triacylglycerols in *Streptomyces*: Possible carbon source for antibiotics. Microbiology 1994; 140: 931-943.

Pardo-Cárdenas Y, Herrera-Orozco I, González-Delgado AD, Kafarov V. Environmental assessment of microalgae biodiesel production in colombia: Comparison of three oil extraction systems. CT&F 2013; 5: 85-100.

Patel A, Mikes F, Matsakas L. An overview of current pretreatment methods used to improve lipid extraction from oleaginous microorganisms. Molecules 2018; 23.

Pathak J, Rajneesh, Maurya PK, Singh SP, Häder D-P, Sinha RP. Cyanobacterial farming for environment friendly sustainable agriculture practices: Innovations and perspectives. Frontiers in Environmental Science 2018; 6.

Peña C, Castillo T, Garcia A, Millan M, Segura D. Biotechnological strategies to improve production of microbial poly-(3-hydroxybutyrate): A review of recent research work. Microb Biotechnol 2014; 7: 278-293.

Perin G, Bellan A, Segalla A, Meneghesso A, Alboresi A, Morosinotto T. Generation of random mutants to improve light-use efficiency of *Nannochloropsis gaditana* cultures for biofuel production. Biotechnol Biofuels 2015; 8: 161.

Pernicova I, Novackova I, Sedlacek P, Kourilova X, Koller M, Obruca S. Application of osmotic challenge for enrichment of microbial consortia in polyhydroxyalkanoates producing thermophilic and thermotolerant bacteria and their subsequent isolation. Int J Biol Macromol 2020; 144: 698-704.

Pfeiffer D, Jendrossek D. PhaM is the physiological activator of poly(3-hydroxybutyrate) (PHB) synthase (PhaC1) in *Ralstonia eutropha*. Appl Environ Microbiol 2014; 80: 555-563.

Pires DP, Cleto S, Sillankorva S, Azeredo J, Lu TK. Genetically engineered phages: A review of advances over the last decade. Microbiology and Molecular Biology Reviews 2016; 80: 523-543.

Qadeer S, Mahmood S, Anjum M, Ilyas N, Ali Z, Khalid A. Synchronization of lipid-based biofuel production with waste treatment using oleaginous bacteria: A biorefinery concept. Process Safety and Environmental Protection 2018; 115: 99-107.

Rabodoarivelo MS, Aerts M, Vandamme P, Palomino JC, Rasolofo V, Martin A. Optimizing of a protein extraction method for *Mycobacterium tuberculosis* proteome analysis using mass spectrometry. J Microbiol Methods 2016; 131: 144-147.

Rahman A, Linton E, Hatch AD, Sims RC, Miller CD. Secretion of polyhyroxybutyrate in *Escherichia coli* using a synthetic biological engineering approach. J Biol Eng 2013; 7: 24.

Ren X, Zhao X, Turcotte F, Deschenes JS, Tremblay R, Jolicoeur M. Current lipid extraction methods are significantly enhanced adding a water treatment step in *Chlorella protothecoides*. Microbial Cell Factories 2017; 16: 26.

Ruhul AM, Kalam MA, Masjuki HH, Fattah IMR, Reham SS, Rashed MM. State of the art of biodiesel production processes: a review of the heterogeneous catalyst. RSC Advances 2015; 5: 101023-101044.

Salakkam A, Webb C. The inhibition effect of methanol, as a component of crude glycerol, on the growth rate of *Cupriavidus necator* and other micro-organisms. Biochemical Engineering Journal 2015; 98: 84-90.

Salazar O, Asenjo JA. Enzymatic lysis of microbial cells. Biotechnol Lett 2007; 29: 985-994.

Santala S, Efimova E, Koskinen P, Karp MT, Santala V. Rewiring the wax ester production pathway of *Acinetobacter baylyi* ADP1. ACS Synth Biol 2014; 3: 145-151.

Sharma PK, Saharia M, Srivstava R, Kumar S, Sahoo L. Tailoring microalgae for efficient biofuel production. Frontiers in Marine Science 2018; 5: 382.

Shields-Menard SA, Amirsadeghi M, Sukhbaatar B, Revellame E, Hernandez R, Donaldson JR, French WT. Lipid accumulation by *Rhodococcus rhodochrous* grown on glucose. J Ind Microbiol Biotechnol 2015; 42: 693-699.

Shimada I, Nakamura Y, Kato S, Mori R, Ohta H, Suzuki K, Takatsuka T. Catalytic cracking of wax esters extracted from *Euglena gracilis* for hydrocarbon fuel production. Biomass and Bioenergy 2018; 112: 138-143.

Silva LF, Taciro MK, Michelin Ramos ME, Carter JM, Pradella JG, Gomez JG. Poly-3-hydroxybutyrate (P3HB) production by bacteria from xylose, glucose and sugarcane bagasse hydrolysate. J Ind Microbiol Biotechnol 2004; 31: 245-254.

Silva RA, Grossi V, Olivera NL, Alvarez HM. Characterization of indigenous *Rhodococcus* sp. 602, a strain able to accumulate triacylglycerides from naphthyl compounds under nitrogen-starved conditions. Res Microbiol 2010; 161: 198-207.

Singhvi MS, Chaudhari S, Gokhale DV. Lignocellulose processing: A current challenge. RSC Advances 2014; 4: 8271-8277.

Sun J, Xiong X, Wang M, Du H, Li J, Zhou D, Zuo J. Microalgae biodiesel production in China: A preliminary economic analysis. Renewable and Sustainable Energy Reviews 2019; 104: 296-306.

Swain K, Casabon I, Eltis LD, Mohn WW. Two transporters essential for reassimilation of novel cholate metabolites by *Rhodococcus jostii* RHA1. J Bacteriol 2012; 194: 6720-6727.

Tan JS, Lee SY, Chew KW, Lam MK, Lim JW, Ho SH, Show PL. A review on microalgae cultivation and harvesting, and their biomass extraction processing using ionic liquids. Bioengineered 2020; 11: 116-129.

Tan XB, Lam MK, Uemura Y, Lim JW, Wong CY, Lee KT. Cultivation of microalgae for biodiesel production: A review on upstream and downstream processing. Chinese Journal of Chemical Engineering 2018a; 26: 17-30.

Tan XB, Lam MK, Uemura Y, Lim JW, Wong CY, Ramli A, Kiew PL, Lee KT. Semi-continuous cultivation of *Chlorella vulgaris* using chicken compost as nutrients source: Growth optimization study and fatty acid composition analysis. Energy Conversion and Management 2018b; 164: 363-373.

Tang S, Hettiarachchy NS, Eswaranandam S, Crandall P. Protein extraction from heat-stabilized defatted rice bran: II. The role of amylase, celluclast, and viscozyme. Journal of Food Science 2003; 68: 471-475.

Tang Y, Zhang Y, Rosenberg JN, Betenbaugh MJ, Wang F. Optimization of one-step in situ transesterification method for accurate quantification of EPA in *Nannochloropsis gaditana*. Applied Sciences 2016; 6: 343.

Taran M, Amirkhani H. Strategies of poly(3-hydroxybutyrate) synthesis by *Haloarcula* sp. IRU1 utilizing glucose as carbon source: Optimization of culture conditions by Taguchi methodology. Int J Biol Macromol 2010; 47: 632-634.

Thanapimmetha A, Suwaleerat T, Saisriyoot M, Chisti Y, Srinophakun P. Production of carotenoids and lipids by *Rhodococcus opacus* PD630 in batch and fed-batch culture. Bioprocess Biosyst Eng 2017; 40: 133-143.

Vermassen A, Leroy S, Talon R, Provot C, Popowska M, Desvaux M. Cell wall hydrolases in bacteria: Insight on the diversity of cell wall amidases, glycosidases and peptidases toward peptidoglycan. Front Microbiol 2019; 10: 331.

Wältermann M, Hinz A, Robenek H, Troyer D, Reichelt R, Malkus U, Galla HJ, Kalscheuer R, Stöveken T, von Landenberg P, Steinbüchel A. Mechanism of lipid-body formation in prokaryotes: How bacteria fatten up. Molecular Microbiology 2005; 55: 750-763.

Wang B, Rezenom YH, Cho KC, Tran JL, Lee DG, Russell DH, Gill JJ, Young R, Chu KH. Cultivation of lipid-producing bacteria with lignocellulosic biomass: effects of inhibitory compounds of lignocellulosic hydrolysates. Bioresour Technol 2014; 161: 162-170.

Wang B, Sharma-Shivappa RR, Olson JW, Khan SA. Production of polyhydroxybutyrate (PHB) by *Alcaligenes latus* using sugarbeet juice. Industrial Crops and Products 2013; 43: 802-811.

Wang M, Chen S, Zhou W, Yuan W, Wang D. Algal cell lysis by bacteria: A review and comparison to conventional methods. Algal Research 2020; 46.

Wang Y, Ling C, Chen Y, Jiang X, Chen GQ. Microbial engineering for easy downstream processing. Biotechnol Adv 2019; 37: 107365.

Woo IS, Rhee IK, Park HD. Differential damage in bacterial cells by microwave radiation on the basis of cell wall structure. Appl Environ Microbiol 2000; 66: 2243-2247.

Wu H, Fan Z, Jiang X, Chen J, Chen GQ. Enhanced production of polyhydroxybutyrate by multiple dividing *E. coli*. Microb Cell Fact 2016; 15: 128.

Xu L, Wang L, Zhou XR, Chen WC, Singh S, Hu Z, Huang FH, Wan X. Stepwise metabolic engineering of *Escherichia coli* to produce triacylglycerol rich in medium-chain fatty acids. Biotechnol Biofuels 2018; 11: 177.

Yao S, Mettu S, Law SQK, Ashokkumar M, Martin GJO. The effect of high-intensity ultrasound on cell disruption and lipid extraction from high-solids viscous slurries of Nannochloropsis sp. biomass. Algal Research 2018; 35: 341-348.

Yellapu SK, Bharti, Kaur R, Kumar LR, Tiwari B, Zhang X, Tyagi RD. Recent developments of downstream processing for microbial lipids and conversion to biodiesel. Bioresour Technol 2018; 256: 515-528.

Young R. Phage lysis: three steps, three choices, one outcome. J Microbiol 2014; 52: 243-258.

Zhang B, Li W, Guo Y, Zhang Z, Shi W, Cui F, Lens PNL, Tay JH. Microalgal-bacterial consortia: From interspecies interactions to biotechnological applications. Renewable and Sustainable Energy Reviews 2020; 118.

Zhang X, Yan S, Tyagi RD, Drogui P, Surampalli RY. Ultrasonication assisted lipid extraction from oleaginous microorganisms. Bioresour Technol 2014; 158: 253-61.

Zhu C, Nomura CT, Perrotta JA, Stipanovic AJ, Nakas JP. Production and characterization of poly-3-hydroxybutyrate from biodiesel-glycerol by *Burkholderia cepacia* ATCC 17759. Biotechnol Prog 2010; 26: 424-430

3. EFFECTIVE ONE-STEP SACCHARIFICATION OF LIGNOCELLULOSIC BIOMASS USING MAGNETITE-BIOCATALYSTS CONTAINING SACCHARIFYING ENZYMES*

3.1. Summary

Lignocellulosic biomass, packed with sugars, is one of the most available renewable resources for biofuels and bioproducts production. To release the sugars for the production, enzymatic hydrolysis (saccharification) of pretreated lignocellulosic biomass are required. However, the saccharification process is costly, inefficient, and requires multi-step operations. This is in part due to the high cost and the limited selection of commercial enzymes which commonly have different optimal pH and temperatures. Here we reported a one-step saccharification of pretreated lignocellulosic biomass using immobilized biocatalysts containing five different saccharifying enzymes (SEs) with a similar optimum pH and temperature. The five SEs - endo-1,4-β-D-glucanase (an endoglucanase, eglS), cellobiohydrolase (an exoglucanase, cbhA), and β-glucosidase (bglH), endo-1,4-β-xylanase (an endoxylanase, xynC) and β-xylosidase (bxlB) – were successfully expressed and produced by *E. coli* BL21. Better saccharification of pretreated corn husks was observed when using the five crude SE enzymes than those using two commonly used SEs, endo-1,4-β-D-glucanase and β-glucosidase. The five

* Reprinted from "Effective one-step saccharification of lignocellulosic biomass using magnetite-biocatalysts containing saccharifying enzymes" by Hwangbo, M., Tran, J.L., and Chu, K.H., 2019, *Science of the Total Environment*, Vol. 647, pp 806-813, Copyright 2019, with permission by Elsevier.

SEs were cross-linked in the absence or the presence of magnetic nanoparticles (hereafter referred as SE-CLEAs and M-SE-CLEAs, respectively). By using SE-CLEAs, the highest amount of reduced sugar (250 mg/g biomass) was measured. The activity of immobilized SEs is better than free crude SEs. The M-SE-CLEAs can be reused at least 3 times for effective saccharification of pretreated lignocellulosic biomass.

Graphical Summary

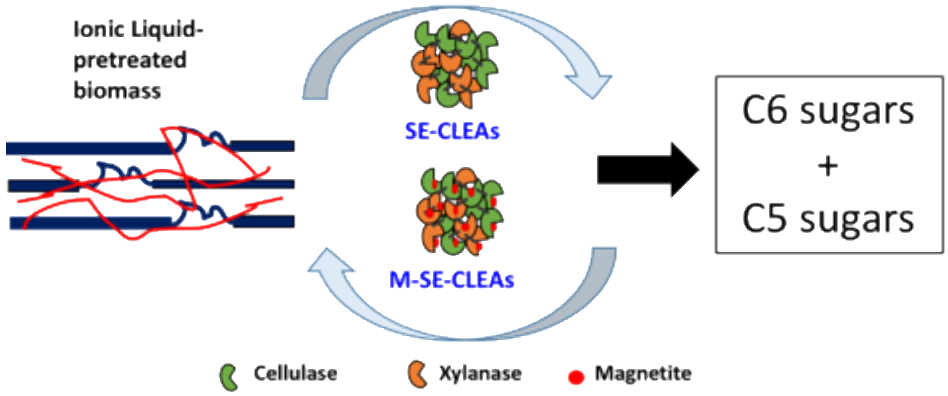

Figure 3.0. Graphical summary of Chapter 3.

Highlights

- Saccharifying enzymes (SEs) with similar optimal pH and temperature were produced.
- The produced SEs enabled a simple one-step enzymatic hydrolysis.
- Using the SEs resulted in 100% more sugar release than using commercial cellulases.
- Higher amounts of reduced sugar were observed using immobilized SEs than crude SEs.

- Magnetic-cross-linked enzyme aggregates allow for rapidly recover and reuse of SEs.

3.2. Introduction

Lignocellulosic biomass, one of the most abundant renewable resources, is available for producing various biofuels and bioproducts (Billion-Ton, 2016). Lignocellulosic biomass contains 40-50% cellulose, 25-30% hemicellulose, and 15-25% lignin (Kumar et al., 2009; Limayem and Ricke, 2012). Cellulose and hemicellulose are sugar polymers protected by a complex non-sugar, phenolic alcohol-based polymer, lignin. To extract sugars from lignocellulosic biomass for biofuels and bioproducts production, physical/chemical pretreatment followed by enzyme hydrolysis (so-called saccharification) is required (Kumar et al., 2009; Nlewem and Thrash, 2010; Wang et al., 2014). Many studies have reported that pretreatment process alone cannot achieve complete saccharification of hemicellulose (Agbor et al., 2011; Yang et al., 2011). Enzyme hydrolysis using commercial enzymes (endoglucanase and beta-glucosidase) on NaOH- or ionic liquid-pretreated biomass can release 71% of the sugars in the biomass (Xu et al., 2010). However, saccharification is costly and inefficient, in part, due to the high cost and the limited selection of commercial enzymes (Bhattacharya and Pletschke, 2014; Khare et al., 2015). The cost of commercial enzymes required for saccharification is estimated to be approximately 36% of total bioethanol production cost (i.e., $0.78 of enzyme cost to produce one gallon of ethanol from biomass) (Johnson, 2016; Lynd et al., 2008).

Cellulose is a polysaccharide consisting of repeating D-glucose (C6 sugar) with β-1,4 glycosidic bonds in a linear amorphous and/or crystalline form. Complete depolymerization of cellulose into sugar monomers requires endoglucanase to cleave amorphous cellulose, exoglucanase to cleave the crystalline cellulose, and β-glucosidase to cleave the dimers into monomer sugars (Iakiviak et al., 2016). Endoglucanase and β-glucosidase are two common commercial cellulases used in enzymatic hydrolysis for pretreated lignocellulosic biomass. Different from cellulose, hemicellulose consists various 5-and 6-carbon sugars (xylose, arabinose, galactose, mannose, glucose, and uronic acid) with β-1,4 and β-1,3 glycosidic bonds (Caes et al., 2013; Rubin, 2008) and xylan is the major component in hemicellulose (Podkaminer et al., 2012). Accordingly, different enzymes are needed to depolymerize different hemicellulose (Gupta et al., 2016). Similar to cellulose, xylan consists of repeating xylose. Depolymerization of xylan requires two types of xylanases, endoxylanase and β-xylosidase. Endoxylanase hydrolyzes (1->4)-β-D-xylosidic linkages in xylan backbones, and β-xylosidase hydrolyzes (1->4)-β-D-xylan units to produce xylose units by eliminating D-xylose residues (Terrasan et al., 2016). Endoxylanase produced from *Trichoderma viride* or from *Bacillus subtilis* are commercially available but their prices are much more higher than those for commercial cellulase. In addition, as these commercial cellulase and xylanase have different optimal pH and temperature, multiple steps are needed to adjust to the optimal operating conditions when using these enzymes for hydrolysis.

Cellulase and xylanase (collectively referred as saccharifying enzymes (SEs) hereafter in this study) can be produced by wild-type or genetically-modified strains

(Elkins et al., 2010; Yang et al., 2011). More recently, SEs (endocellulase, β-glucosidase, endoxylanase, and xylobiosidase) have been produced by engineered *E. coli* in quantity (Bokinsky et al., 2011). However, due to the sensitivity of each of SEs to pH and temperature, there have been several trials to optimize an operating condition for saccharification (Verardi et al., 2012). Most commercial cellulase have similar optimal pH (4.0 – 5.0) and temperature (50 – 60 °C), however, commercial xylanases have various optimal conditions, with pH ranging from 4.5 to 6.0 and temperature from 30 to 50 °C. Thus, multi-step saccharification is needed when using commercial SEs for complete depolymerization of pretreated lignocellulosic biomass. A simple one-step saccharification for pretreated lignocellulosic biomass would be favorable and can be potentially achieved by using SEs that are active at pH 5.5 – 6.5 and 50 – 60 °C.

Reuse of SEs is another means to reduce the overall cost of the saccharification (Huang et al., 2015). Immobilization of enzymes not only enable reuse but also increase the activity and stability of the enzymes (Ranjbakhsh et al., 2012; Šulek et al., 2011). When commercial endoglucanase (brand name Celluclast, derived from *Trichoderma reesei*) was immobilized as cross-linked enzyme aggregates (CLEAs), the CLEAs could be reused for four times, where 40% of enzyme activity was retained at the end of the 4th cycle (Perzon et al., 2017). Previous studies have also suggested that such immobilization method would not block the active site of enzymes nor reduce the enzyme activity of SEs (Dalal et al., 2007; Sheldon, 2011). Magnetic nanoparticles (MNPs) have been recently introduced to prepare magnetic cross-linked enzyme aggregates (M-CLEAs) for easy separation between enzymes and substrates (Cui et al., 2016). M-CLEAs of bacterial

xylanase (endoxylanase and β-xylosidase, respectively) from *Bacillus gelatini* ABBP-1 show 1.35-fold higher activity than the free endoxylanase or β-xylosidase (Bhattacharya and Pletschke, 2014) and M-CLEAs of lipase B can be reused up to 10 cycles by recovering easily showing a similar activity of the enzyme (Cruz-Izquierdo et al., 2014).

To address above challenges in saccharification of pretreated biomass, in this study, we reported one-step saccharification of lignocellulosic biomass using five different SEs (endoglucanase, exoglucanase, β-glucosidase, endoxylanase, and β-xylosidase) with a similar optimum pH and temperature. Xylanase were chosen in this study because xylan is a major hemicellulose. These SEs were further immobilized as reusable biocatalysts without and with MNPs (referred hereafter as SE-CLEAs and M-SE-CLEAs, respectively). SE-CLEAs, M-SE-CLEAs, and commercial enzymes were used to saccharify pretreated biomass and the effectiveness were compared based on the amount of sugars released. The reusability of SE-CLEAs and M-SE-CLEAs were also investigated.

3.3. Materials and methods

3.3.1. Chemicals

Ammonium hydroxide ($NH_3 \cdot H_2O$) was purchased from Fisher Scientific (Pittsburgh, PA). Isopropyl-β-D-1-thiogalactopyranoside (IPTG) and ammonium sulfate $(NH_3)_2SO_4$ were purchased from MP Biomedicals (Santa Ana, CA). Luria-Bertani medium and xylose were purchased from Thermo Fisher Scientific (Waltham, MA). Endo-1,4-β-D-glucanase, 0.24 U/mg from *Aspergillus niger* was purchased from TCI

America (Portland, OR). β-glucosidase, 1,000 U/mg from sweet almonds was purchased from MP Biomedicals (Santa Ana, CA). Xylan was purchased from Carbosynth (Berkshire, United Kingdom). All other chemicals used in this study including 1-Ethyl-3-methylimidazolium chloride ([Emin][Cl]) were purchased from Sigma-Aldrich (St. Louis, MO).

3.3.2. Strains and selection of genes encoding SEs

To implement one-step enzymatic hydrolysis under mild conditions, cellulases and xylanases having a similar optimum pH and temperature (pH 6.0 and temperature at 50°C) were chosen. Based on these criteria, endo-1,4-β-D-glucanase (an endoglucanase, eglS, EC 3.2.1.6), cellobiohydrolase (an exoglucanase, cbhA, EC 3.2.1.91), and β-glucosidase (bglH, EC 3.2.1.21) for cellulase and endo-1,4-β-xylanase (an endoxylanase, xynC, EC 3.2.1.8) and β-xylosidase (bxlB, EC 3.2.1.37) for xylanase were selected. Endoglucanase (*eglS*), β-glucosidase (*bglH*), and endoxylanase (*xynC*) were derived from *Bacillus subtilis* 168 (hereafter referred as strain 168) (Bagudo et al., 2014; St John et al., 2006; Wolf et al., 1995), and exoglucanase (*cbhA*) and β-xylosidase (*bxlB*) were derived from *Aspergillus fumigatus* Af293 (hereafter referred as strain Af293) (Adav et al., 2013; Grajek, 1986). Table 3.1 summarizes the information of the genes encoding these enzymes.

Table 3.1. Selection of cellulase and xylanases with a similar optimal pH at 6 and temperature at 50°C.

Gene	Enzyme	Origin	Size (kB)	Size (amino acids)	MW (kDa)
eglS	endo-1,4-β-D-glucanase (endoglucanase)	*Bacillus subtilis* 168	1.5	500	55
bglH	β-glucosidase	*Bacillus subtilis* 168	1.4	469	54
cbhA	cellobiohydrolase (exoglucanase)	*Aspergillus fumigatus* Af293	1.4	452	48
xynC	endo-1,4-β-xylanase (endoxylanase)	*Bacillus subtilis* 168	1.2	422	47
bxlB	β-xylosidase	*Aspergillus fumigatus* Af293	2.3	771	84

3.3.3. Plasmid construction for SEs expression

The genes encoding the SEs described above were used to construct recombinant plasmids using In-Fusion® HD Cloning Kit (Clontech, Mountain View, CA) (Figure 3.1a). The genomic DNA of strains 168 was extracted using FastDNA SPIN KIT (MP Biomedicals, Santa Ana, CA) after growing in LB medium at 37 °C for overnight, and cDNA of strains Af293 was directly used for PCR amplification. The PCR primers were designed based on the sequence of strains 168 and Af293, and each gene was amplified using 10 primers as listed in Table 3.2.

Table 3.2. Primer sets used in this chapter. All primers were designed by primer design tool for In-fusion cloning.

Primer name	Sequence (5' -> 3')	Primer length (bp)	Melting temperature (°C)
eglS_FW	CACCAGTCATGCTAGCTAATTTGGTTCTGTTCCCC	35	64.1
eglS_RV	AAGGAGATATACATAATGAAACGGTCAATCTCTATT	36	57.4
bglH_FW	CACCAGTCATGCTAGTCAGAGACTCTCTCCGTTT	34	64.1
bglH_RV	AAGGAGATATACATAATGAGTTCAAATGAAAAACGAT	37	57.1
cbhA_FW	AAGGAGATATACATATGATGCATCAACGCGCGCTC	35	70.9
cbhA_RV	CACCAGTCATGCTAGCTTAACCTTCGTAGGTCGAACCAATG	41	70.8
xynC_FW	AAGGAGATATACATATGATGATTCCACGCATAAAAAAAA	39	58.5
xynC_FW	CACCAGTCATGCTAGCTTAACGATTTACAACAAATGTTG	39	61.8
bxlB_RV	AAGGAGATATACATATGATGGCTCACATCACGTCATGG	38	68.9
bxlB_FW	CACCAGTCATGCTAGCTCACCGAGTTTTCGGAGGC	35	75

A 25-µL of PCR reaction included 12.5 µL of 2X CloneAmp Hifi PCR Premix, 3 µL of 70-80 ng/µL template DNA, 1 µL each of 10 µM forward and reverse primers, and 7.5 µL of nuclease-free water. PCR reaction was carried out by denaturing at 98 °C for 2 minutes, followed by 35 cycles at 98 °C for 10 seconds, 55 °C for 15 seconds, and 72 °C for 1.5 minutes (*eglS, bglH, cbhA, and xynC*), or 2 minutes (*bxlB*), with final incubation at 72 °C for 10 minutes for final extension.

The PCR products were cloned into pET11a plasmids between the NdeI-NheI cloning sites. The 10 µL ligation mixture for all cellulase and xylanase (*eglS, bglH, cbhA, xynC,* and *bxlB*) included 3 µL of 90 ng/µL linearized pET11a vector, 2 µL of 5X In-Fusion Cloning HD Enzyme Premix, 1 µL of purified PCR product, and 4 µL of deionized water. The mixtures were incubated at 50 °C during 15 minutes. After ligation, the recombinant plasmids were transformed into NEB 5-alpha competent *E. coli*, screened on LB agar with 100 mg/L ampicillin as a selective marker, and extracted using QIAprep Spin Miniprep Kit (Quiagen, Hilden, Germany). To verified recombinant plasmid

sequences, the plasmid was digested with unique restriction enzyme (BamH1 and EcoRV or EcoR1 and BamH1) (Table 3.3) at 37 °C for 1 hour and visualized by agarose gel electrophoresis. The plasmids with correct size fragments were sequenced (Eton Bioscience, San Diego, CA) over the entire saccharifying gene and analyzed by APE, a plasmid editor tool (http://biologylabs.utah.edu/jorgensen/wayned/ape). After that, the correct recombinant plasmid DNA was transformed into *E. coli* BL21 (DE3).

(a)

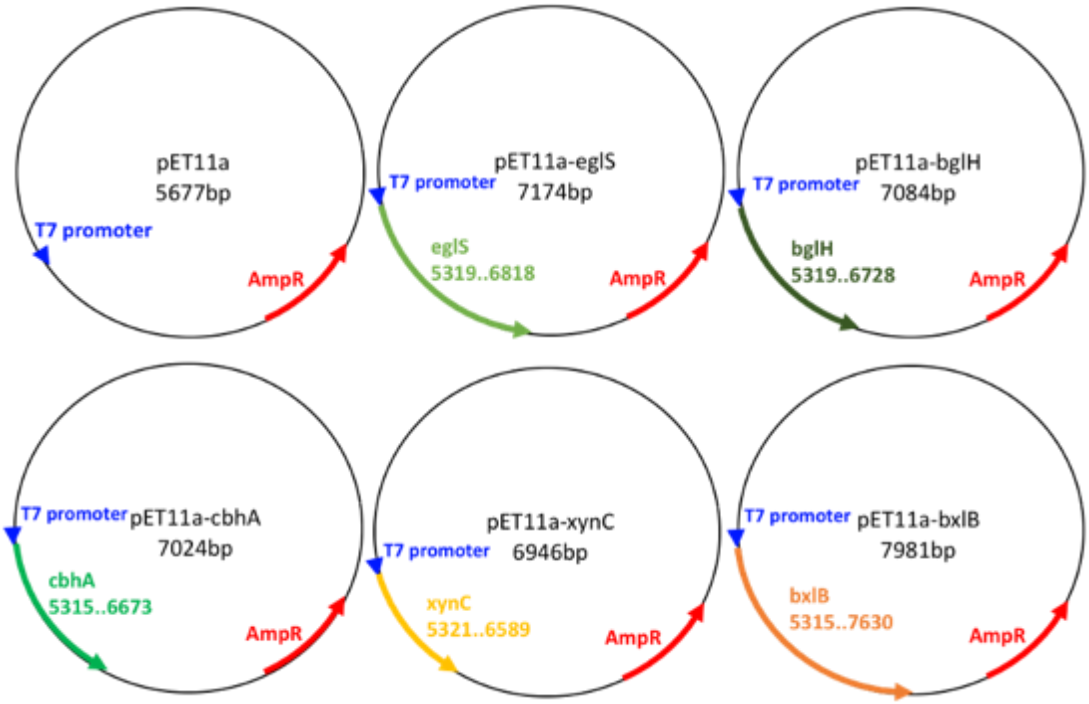

Figure 3.1. Map of recombinant plasmids and expression of recombinant proteins. (a) Map of constructed recombinant plasmids (b) SDS-PAGE analysis of recombinant protein in E. coli BL21 (DE3) after 2 hours of induction with 1mM IPTG.

(b)

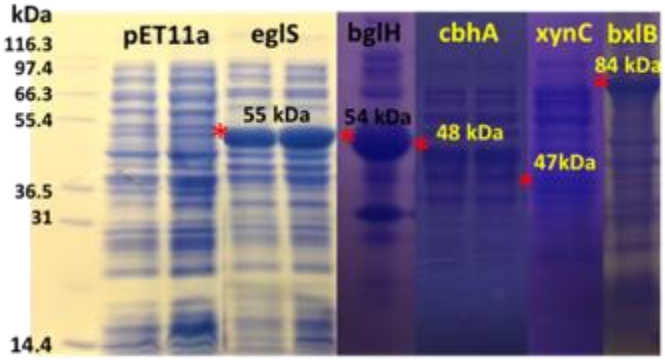

Figure 3.1. Continued.

Table 3.3. Expected plasmid DNA fragment sizes after restriction digestion (a) pET11a-eglS, bglH, and xynC digested with BamH1 (1 cut) and EcoRV (2 or 3 cuts) or without enzymes (No cut) (b) pET11a-cbhA digested with EcoRV (2 cuts) and BamH1 (3 cuts) or without enzymes (No cut) (c) pET11a-bxlB digested with EcoR1 (1 cuts) and BamH1 (2 cuts) or without enzymes (No cut).

(a)

	No cut [kB]	1 cut [kB]	2 or 3 cuts [kB]
pET11a-eglS	3.5	7.0	3.0, 4.0
pET11a-bglH	4.1	7.1	4.2, 1.5, 1.4
pET11a-xynC	3.4	7.0	4.3, 2.7

(b)

	No cut [kB]	2 cuts [kB]	3 cuts [kB]
pET11a-cbhA	4.0	4.2, 2.8	6.0, 0.7, 0.3

(c)

	No cut [kB]	1 cuts [kB]	2 cuts [kB]
pET11a-bxlB	5.3	8.0	7.3, 0.7

3.3.4. Protein expression and western blotting

Expression of the recombinant saccharifying gene in each transformed *E. coli* BL21(DE3) following induction with 0.1 mM IPTG was confirmed using western blotting. First, a fresh transformed colony was grown overnight in 5 mL LB medium containing 100 mg/L ampicillin at 37 °C at 200 rpm. The overnight culture was then

transferred into 50 mL fresh LB medium containing 100 mg/L ampicillin and incubated at 37 °C at 200 rpm until the OD_{600} reached 0.4 to 0.7 (exponential growth of cells). To induce expression of desired proteins, 0.1 mM IPTG was added to the cell suspension and incubated at 37 °C at 200 rpm for additional 2 hours.

Cell pellets were harvested by centrifugation at 10,000 g at 4 °C for 10 minutes and resuspended in 2 mL of phosphate buffer solution (PBS) (pH 7.0) for western blotting. Production of cellulase and xylanase were visualized by sodium dodecyl sulfate polyacrylamide gel electrophoresis (SDS-PAGE), which was performed on 14% Tris-Glycine Gel in the Surelock Minicell apparatus (Thermo Scientific, Waltham, MA) at 90 voltages for 2.5 hours. Then, the gel was stained in Coomassie Blue dye for 4 hours before destained in a destaining solution containing 45% of methanol, 10% of acetic acid, and 45% of DI water for one hour.

3.3.5. Enzyme activity assays

The amount of each protein expressed by the recombinant cell was determined based on the difference of total protein content in *E. coli* with constructed pET11a vector and that with a pET11a empty vector (i.e., by subtracting the total protein content of the recombinant cell from that of the cells with an empty pET11a vector). The content of total cellular proteins was determined using a Pierce BCA protein assay kit (ThermoFisher Scientific, Waltham, MA). After the induction, cell cultures were centrifuged and resuspended in 1/50 volume of PBS buffer (pH 7.0). Cells were lysed by using FastPrep lysis beads and matrix (MP Biomedicals, Santa Ana, CA). Briefly, the responded solution

was transferred to a lysing matrix E tube and homogenized using the FastPrep instrument (Thermo Scientific, Waltham, MA) at a speed setting of 6.0 for 40 second twice. The cell lysates were then centrifuged at 14,000 g for 10 minutes, and the supernatants were collected and tested for enzyme activities. All enzyme activity tests were conducted in triplicate.

Endoglucanase (eglS) activity was measured by 3,5-Dinitrosalicylic acid (DNS) Reducing Sugar Method using carboxymethyl cellulose (CMC, 1%, w/v) as a substrate and D-glucose as a standard (Miller, 1959). The CMC solution was prepared in 0.05 M Na-citrate buffer (pH 6.0). Commercial cellulase (endo-1,4-β-D-glucanase, 0.24 U/mg from *Aspergillus niger*) in 0.05 M Na-citrate buffer (pH 6.0) was used as a positive control for the activity assays. The cell cultures (200 μL) mixed with 800 μL of 0.05 M Na-citrate buffer (pH 6.0) or 1 mL of commercial cellulase was added to 1 mL of 1% CMC in 16-mm glass vials and incubated at 50 °C during 20 minutes. 2 mL of modified DNS Reagent (1% 3,5-dinitrosalicylic acid, 1% NaOH, 0.2% phenol, and 0.05% sodium sulfite) was added into the mixture, and the mixture was then boiled for 15 minutes. Then, 1 mL of 40% Rochelle salt solution was added to the mixture to stop the reaction. The mixture was cooled down to room temperature, and the absorbance of the mixture at OD_{560} was determined using a microplate reader (Tecan GENIOS, Männedorf, Switzerland). One unit (U) of endoglucanase activity was 1 μmole of glucose produced per minute per mL of the culture.

Exoglucanase (cbhA) activity was measured by Phenol-Sulfuric Acid assay using avicel (1.25%, w/v) as a substrate and D-glucose as a standard (Zhang et al., 2009). The

avicel solution was prepared in 0.1 M acetate buffer (pH 4.8). Cell suspension (0.4 mL in PBS (pH 7.0)) was added into a 16 mm test tube containing 1.6 mL of 1.25% avicel. The test tube was then incubated at 50 °C for 2 hours. Following the incubation, the hydrolysate (1 mL) was centrifuged at 13,000 g for 3 minutes in a microcentrifuge tube. The supernatant (0.3 mL) was mixed with 0.3 mL of 5% phenol solution, followed by adding 1.5 mL of concentrated sulfuric acid. The total sugar content in the mixture was determined by the absorbance at 490 nm after cooling down. Controls containing no enzyme or substrate were used. Substrate only (i.e., avicel (1.25%, w/v)) was used as absorbance blank. The unit (U) of exoglucanase activity was 1 μmole of glucose produced per minute per mL of the cell suspension.

β-glucosidase (bglH) activity was measured by a colorimetric assay using *p*-Nitrophenyl-*β*-D-glucopyranoside (*β*-PNPGLU, 5 mM) as a substrate and *p*-nitrophenol (PNP) as the standards (Mfombep et al., 2013). The *β*-PNPGLU solution was prepared in 50 mM sodium acetate buffer (pH 5.0). Cell suspension (0.5 mL of in PBS (pH 7.0)) was added into a 15-mL centrifuge tube containing 2 mL of 5 mM *β*-PNPGLU. The tube was incubated at 37 °C for 30 minutes before adding 1.5 mL of 0.5 M Na_2CO_3. The absorbance of the mixture was measured at 400 nm after cooling down. The sodium acetate buffer was used as absorbance blank. Enzyme free and substrate free were also used as controls.

The activities of xylanase (xynC and bxlB) were measured by DNS reducing sugar method using xylan (0.05%, w/v) as a substrate and xylose as a standard (Bailey et al., 1992). Xylan solution was prepared in 0.05 M Na-citrate buffer (pH 6.0). The positive controls were prepared by adding 1 to 10 μg/mL commercial xylanase (endo-1-4-β-

xylanase from *Trichoderma longibrachiatum*) in 0.05 M Na-citrate buffer (pH 6.0). Forty μL of cell culture and 160 μL of 0.05 M Na-citrate buffer (pH 6.0) was added in a 16-mm glass vial containing 1.8 mL of 0.05% xylan. The mixture in the vial was incubated at 50 °C for 5 minutes, followed by adding 3 mL of modified DNS Reagent. Then, the mixture was boiled for 5 minutes. The absorbance of the mixture was deterimed at OD_{540} using a microplate reader after the mixture was cooled down to room temperature. One unit (U) of xylanase activity was 1 μmole of xylose produced per minute per mL of the cell culture.

3.3.6. Preparation of cross-linked enzyme aggregates (CLEAs)

The SE-CLEAs, consisting of cellulase (eglS, bglH, and cbhA) and xylanase (xynC and bxlB), was prepared as described previously (Cui et al., 2016). Briefly, 0.5 mL of each of five crude enzyme solutions (produced by *E. coli* BL21 (DE3) as described above in section 3.2.5 (i.e., a total of 2.5 mL)) was mixed with 50 mM sodium phosphate buffer (pH 7.5). The enzymes in the mixture were precipitated by adding 80% ammonium sulfate at 4 °C for 1 hour, followed by adding 0.8% glutaraldehyde (25% v/v) for another 2 hours. During the precipitation process, the mixture was shaking continuously at 200 rpm at 4 °C. Then, the mixture was centrifuged at 10,000g at 4 °C for 10 minutes to obtain CLEAs of SEs (SE-CLEAs). The SE-CLEAs were washed with 50 mM sodium phosphate buffer (pH 7.5) three times and then stored in 0.05 M Na-citrate buffer (pH 6.0) at 4 °C until use.

3.3.7. Preparation of magnetite-CLEAs (M-CLEAs)

Magnetite-CLEAs of SEs (M-SE-CLEAs) were prepared similarly as described above for SE-CLEAS with some modifications. Magnetite nanoparticles (MNPs) were prepared by adding 0.625 g of $FeCl_2 \cdot 4H_2O$ and 1.02 g of $FeCl_3$ in 50 mL of DI water with purging by N_2 gas and shake at 150 rpm at room temperature. Then, 25% $NH_3 \cdot H_2O$ (3 mL) was added slowly into the mixture via a syringe, and the mixture was shaken at 50 rpm for 30 minutes to form MNPs. The MNPs were recovered using a strong magnet and then washed with DI water 3 to 5 times. To make M-SE-CLEAs, five crude enzyme solutions (0.5 mL of each, a total of 2.5 mL) were first mixed with 5 mL of MNPs, followed by adding 80% ammonium sulfate for 1 hour and then 0.8% glutaraldehyde (25% v/v) for 2 hours as described above. The M-SE-CLEAs were then recovered using a strong magnet, washed with DI water three times, and then stored in the 0.05 M Na-citrate buffer (pH 6.0) at 4 °C until use.

Morphology of SE-CLEAs, MNPs, and M-SE-CLEAs were observed by a field scanning electron microscope (FE-SEM, JEOL JSM-7500F, Tokyo, Japan) at Materials Characterization Facility, Texas A&M University. An accelerating voltage of 1 kV and emission current of 10 μA were used for image of SE-CLEAs, MNPs, and M-SE-CLEAs.

3.3.8. Pretreatment of lignocellulosic biomass

Corn husks, obtained from a local supermarket at College Station, Texas, US, were used as a model lignocellulosic biomass in this study. The corn husks were washed with DI water 3 times, dried at 50 °C for 24 hours, and then ground to fine particles using a

coffee grinder (Wang et al., 2014). The ground biomass was stored in a sealed plastic bag at 4 °C until experimental use.

Two different pretreatment methods - alkali (NaOH) treatment and ionic liquid (IL) treatment - were used to remove lignin from the ground biomass. All experiments were conducted in duplicate. For alkali treatment, 0.5 g of corn husk was added to 10 mL of 1% sodium hydroxide solution at 30 °C for 1 day, washed with DI water three times, and then dried at 50 °C for 24 hours (Sills and Gossett, 2011; Wang et al., 2014). For IL treatment, 2.82 g of ionic liquid 1-Ethyl-3-methylimidazolium chloride ([Emim][Cl]) was added to 0.5 g of corn husk in a 10-mL glass test tube with a rubber stopper. The mixture was heated at 120 °C in a Hach DRB200 reactor block (Hach, Loveland, CO) for 3 hours with manually stirring every 30 minutes with a glass rod. Then, 30 mL of DI water was added to the mixture followed by centrifugation at 10,000 g for 10 minutes. The supernatant was discarded, and the solid portion was dried at 50 °C for 24 hours. The pretreated biomass was used in all the saccharifying experiments with free or immobilized commercial enzymes and crude enzymes produced in this study.

3.3.9. Saccharification of pretreated biomass using crude enzymes and immobilized enzymes (SE-CLEAs and M-SE-CLEAs)

The pretreated corn husk was saccharified through enzyme hydrolysis by using free crude cellulase and xylanase produced from *E. coli* BL21 (DE3) as described above. Cells were grown, harvest (as stated in section 3.2.4), and resuspended in 0.05 M Na-citrate buffer (pH 6.0) to lyse the cells as stated in section 3.2.5. The supernatant that

containing crude enzyme was applied to the biomass as follows. Crude eglS and xynC were added as 2.5 U/g biomass and 0.35 U/g biomass, respectively. Other bglH, cbhA, and bxlB were added as 0.1 U/g biomass. Note that the activity of these crude enzymes applied in the tests were much lower than that of commercial pure enzyme bglH (64 U/g biomass). Because the optimal condition of all enzymes produced in this study is similar, the hydrolysis of the pretreated biomass was incubated at pH 6.0 at 50 °C at 200 rpm for 48 hours.

IL-pretreated corn husks were added with commercial enzymes (endo-1,4-β-D-glucanase and β-glucosidase), SE-CLEAs, or M-SE-CLEAs to demonstrate one-step enzymatic hydrolysis. For comparison, the amount of free commercial enzymes, endo-1,4-β-D-glucanase (EC 3.2.1.4, equivalent to eglS, 2.5 U/g biomass) and β-glucosidase (equivalent to bglH, 20 U/g biomass) were used. Briefly, the mixtures (with free commercial enzyme, or SE-CLEAS, or M-SE-CLEAS) were incubated at pH 6.0 at 50 °C at 200 rpm for 48 hours. The hydrolysate was then separated from the solid portion via centrifugation at 10,000 g for 10 minutes (4 °C), collected, and used for reduced sugar measurements. To determine the reusability of SE-CLEAs or M-SE-CLEAs, these biocatalysts were recovered via centrifugation or via application of a strong magnet. The recovered biocatalysts were then washed two times with the 0.05 M Na-citrate buffer and used in a new saccharification experiment containing IL-pretreated biomass. The reusability of the biocatalysts was determined based on the amount of reduced sugar produced at the end of each cycle.

3.3.10. Reduced sugars analysis

The amounts of reduced sugars in the hydrolysates was determined by DNS reducing sugar method (Miller, 1959). Briefly, 2 mL of diluted hydrolysates was mixed with 2 mL of modified DNS Reagent in 16-mm glass vials. The vials were boiled for 15 minutes, and 1 mL of 40% Rochelle salt solution was added to stop the reaction. After cooling down the mixture, reduced sugar amounts were measured as a glucose equivalence at OD_{560} color-metrically using the microplate reader.

3.4. Results and discussion

3.4.1. Cloning, transformation, and expression of SEs in E. coli.

The PCR products were confirmed by the size on an agarose gel. The band of 1.5 kilo-base pairs (kB) for endoglucanase (*eglS*) was observed clearly, 1.4 kB for β-glucosidase (*bglH*), 1.4 kB for exoglucanase (*cbhA*), 1.2 kB for endoxylanase (*xynC*), and 2.3 kB for β-xylosidase (*bxlB*) were observed on the agarose gel (Figure 3.2).

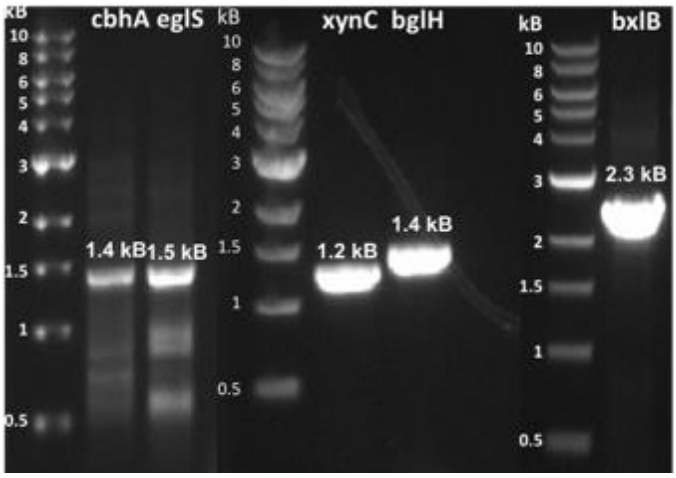

Figure 3.2. Agarose gel showing amplified PCR products of genes encoding saccharifying enzymes.

The cloning results were confirmed by the unique fragment size using restriction enzymes and visualized on the agarose gel (Figure 3.3). Also, to visualize the expression of SEs in *E. coli* BL21 (DE3), the concentrated whole cell cultures were analyzed on SDS-PAGE (Figure 3.1b) showing protein profiles. A large 84 kilodalton (kDa) band were observed on the polyacrylamide gel. This indicated significant β-xylosidase (bxlB) enzyme production from *E. coli* BL21 (DE3), and thicker bands for all cellulase (eglS, bglH, cbhA) while a fainter 47 kDa for endoxylanase (xynC) was observed (Figure 3.1b).

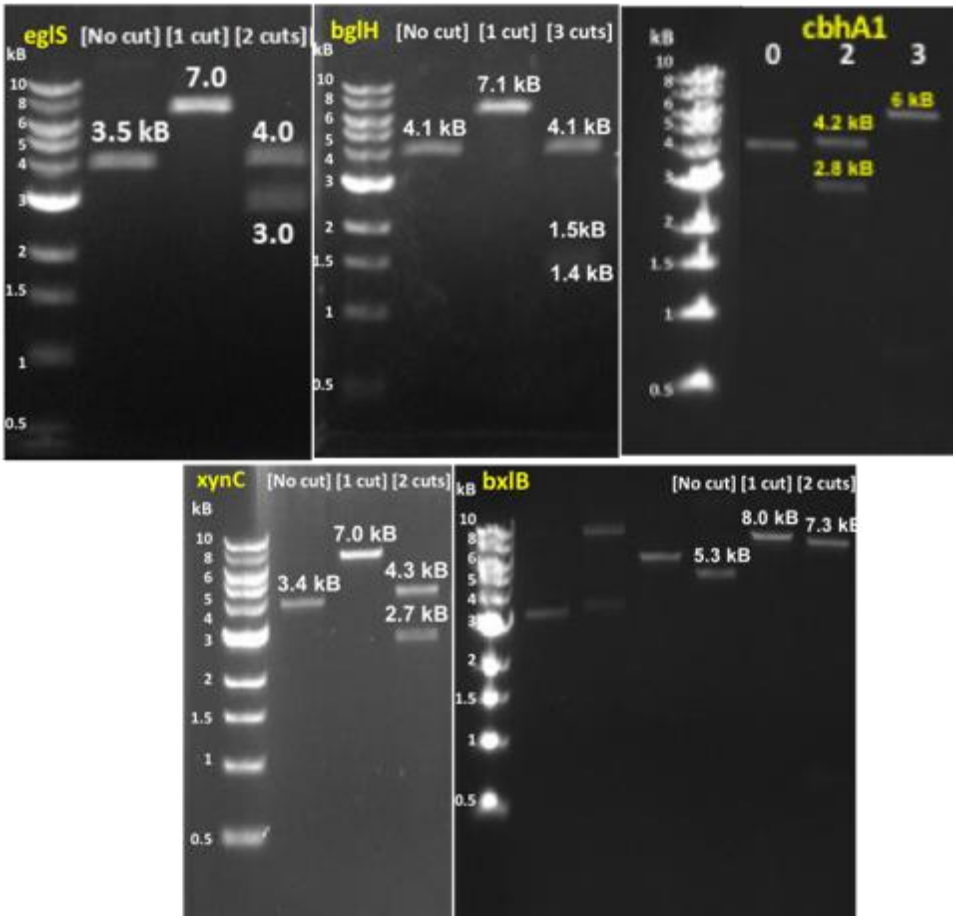

Figure 3.3. Agarose gel showing cut and uncut recombinant plasmids extracted from NEB 5-alpha competent E. coli.

3.4.2. Activities of recombinant proteins

The amounts of proteins expressed by the *E. coli* was determined based on the method described in section 3.2.5. Approximately 80% of expressed proteins were released into the supernatant after cell lysis (i.e., by subtracting the protein concentrations measured from the whole cell from that in the supernatant). The concentrations of expressed enzymes in the *E. coli* were as follows: eglS 7.1 mg/mL, bglH 8.6 mg/mL, cbhA 5.9 mg/mL, xynC 3.4 mg/mL, and bxlB 5.0 mg/mL (Figure 3.4a).

(a)

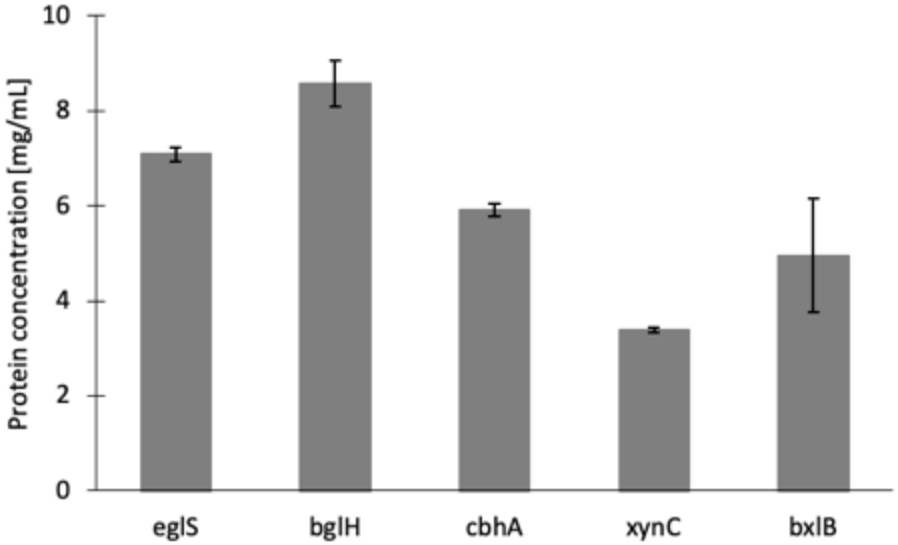

(b)

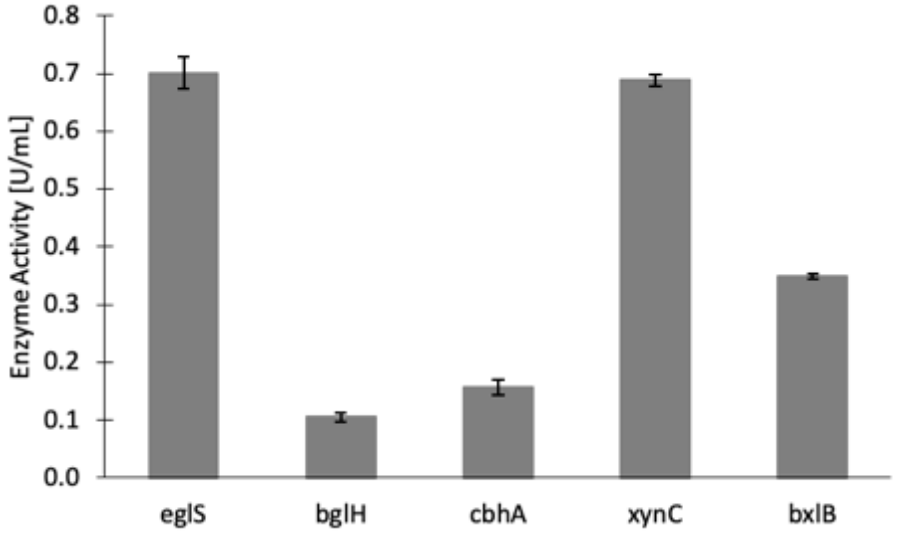

Figure 3.4. Concentrations and activities of saccharifying enzymes (SEs) expressed by E. coli BL21 (DE3) (a) Enzyme concentration of each SE detected in the supernatant of lysed E. coli BL21 (DE3) (b) Activity of saccharifying enzymes (SEs) in the cell free supernatant.

The activity of each of SEs in the supernatant was determined. Endoglucanase (eglS) activity was estimated at 0.71 U/mL (from the supernatant of 50 mL of cell suspension (OD_{600} at 1.0)). This estimated activity is equivalent to the activity of 3 g of commercial cellulase (0.24 U/mg activity) (Figure 3.4b). Endoxylanase (xynC) activity in the supernatant was estimated to be 0.69 U/mL, equivalent to the activity of 0.28 g of commercial endoxylanase (2.5 U/mg activity) (Figure 3.4b). The activity of other enzymes was lower than endoglucanase and endoxylanase; 0.16 U/mL for cbhA, 0.11 U/mL for bglH, and 0.35 U/mL for bxlB (Figure 3.4b).

3.4.3. Hydrolysis of pretreated corn husks with crude enzymes and SE-CLEAs

Both free and immobilized crude enzymes produced in this study could hydrolyze two pretreated corn husks to different degrees. As shown in Figure 3.5a, using free crude enzymes, a higher reduced sugar amount (170 mg/g biomass) was observed for IL-pretreated biomass than that for NaOH-pretreated biomass (114 mg/g biomass). The previous study reported a release of 156 - 600 mg of sugars per 1 g NaOH-pretreated corn husk after incubating with commercial enzymes (endoglucanase and β-glucosidase) for 6 to 45 hours (Hang and Woodams, 1999). Using the same commercial enzymes (endoglucanase and β-glucosidase) for NaOH and CaO- pretreated corn stover released similar amounts of sugar (300 – 600 mg/g biomass) (Zhang et al., 2011). The amounts of sugar released observed in our study were at the lower end of the reported results.

(a)

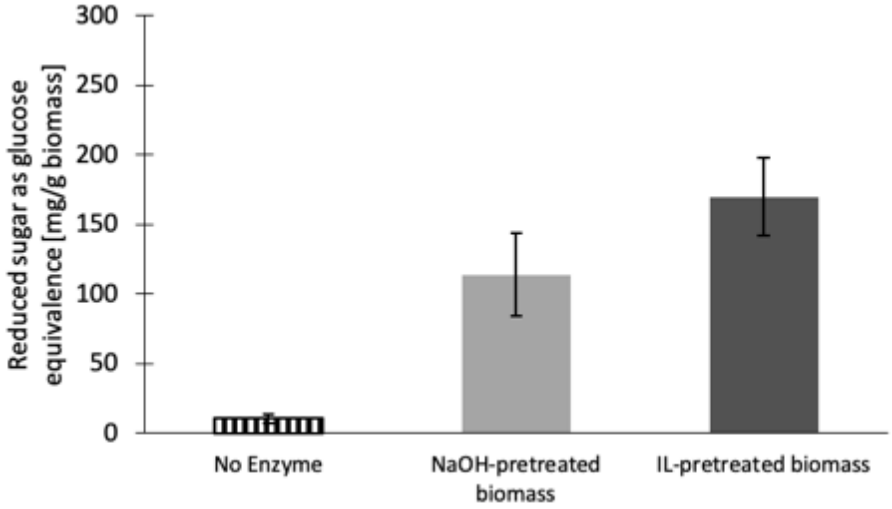

(b)

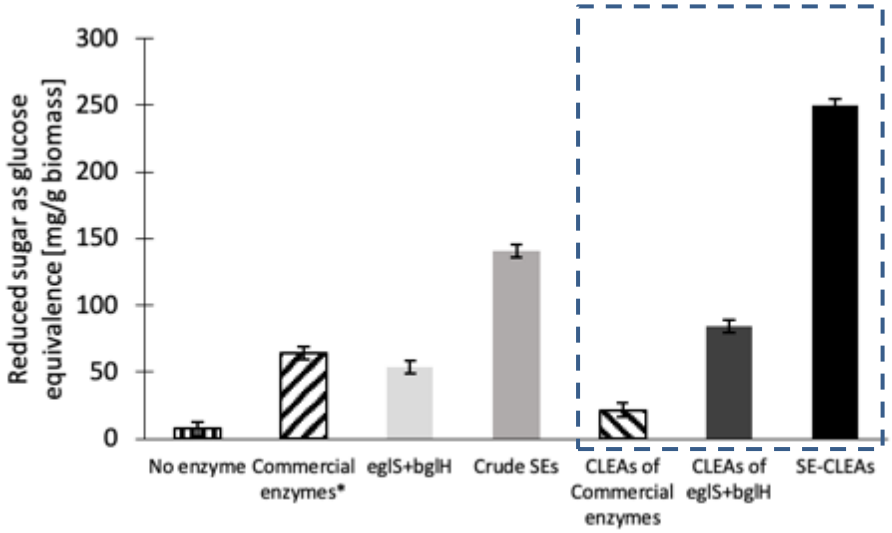

Figure 3.5. Enzymatic hydrolysis of pretreated corn husk to release reduced sugars. (a) Application of SEs to release sugars from two different pretreated corn husks: NaOH-pretreated and IL-pretreated, using a combination of five crude SEs produced in this study. (b) Reduced sugar released from IL-pretreated corn husk following enzymatic hydrolysis. Commercial enzymes (free enzymes), eglS+bglH (free enzymes), crude SEs (free enzymes), CLEAs of commercial enzymes (immobilized enzymes), CLEAs of eglS+bglH (immobilized enzymes), or SE-CLEAs (immobilized enzymes) were used for enzymatic hydrolysis. *Commercial enzymes: endoglucanase (endo-1,4-β-D-glucanase) and β-glucosidase. The function of these two commercial enzymes are similar to eglS and bglH, respectively.

However, such comparison appears less meaningful, as many factors including sugary contents and genetic traits of the biomass, pretreatment methods, and types of enzymes used for hydrolysis can all contribute to the discrepancies. For example, a previous study used corn stover as biomass (Zhang et al., 2011), but our study used corn husks. The sugar contents of corn stover is different with corn husks, since corn husks is composed with glucose (47%), xylose (28%), arabinose (4%), and cellobiose (21%) (Hang and Woodams, 1999) and corn stover is composed with glucose (51%), xylose (27%), and arabinose (22%) (Wang et al., 2014). Our study used crude enzymes for the scarification, while others used high purity commercial enzymes. Unlike the finding of decreased enzyme activity following immobilization reported in the most studies (Perzon et al., 2017), enhanced enzyme activity of immobilized crude enzymes was observed in our study (Figure 3.5b). Applications of crude enzymes directly for saccahrification is advantageous since it is simple and eliminates the tedious and expensive steps needed for enzyme purification. Additionally, our enzymatic hydrolysis approach is simpler, since only one operating condition, pH 6.0 at 50 °C for 48 hours is required.

The FE-SEM images allow for morphological analysis of SE-CLEAs, MNPs, and M-SE-CLEAs (Figure 3.6). SE-CLEAs showed aggregated forms with several layers on the surface but with no defined morphology (Figure 3.6a). In contrast, the FE-SEM image of MNPs in Figure 3.6b showed that the MNPs were small and round shapes particles. The FE-SEM image of the M-SE-CLEAs showed that MNPs were attached on the surface of the SEs (Figure 3.6c), and some SEs were completely covered with MNPs (Figure 3.6d). The location of MNPs in our M-SE-CLEAs was on the surface of the CLEAs, not

inside the CLEAs as reported previously (Huang et al., 2015). The discrepancy of the locations of MNPs might be due to the different precipitation method used for preparing the M-CLEAs.

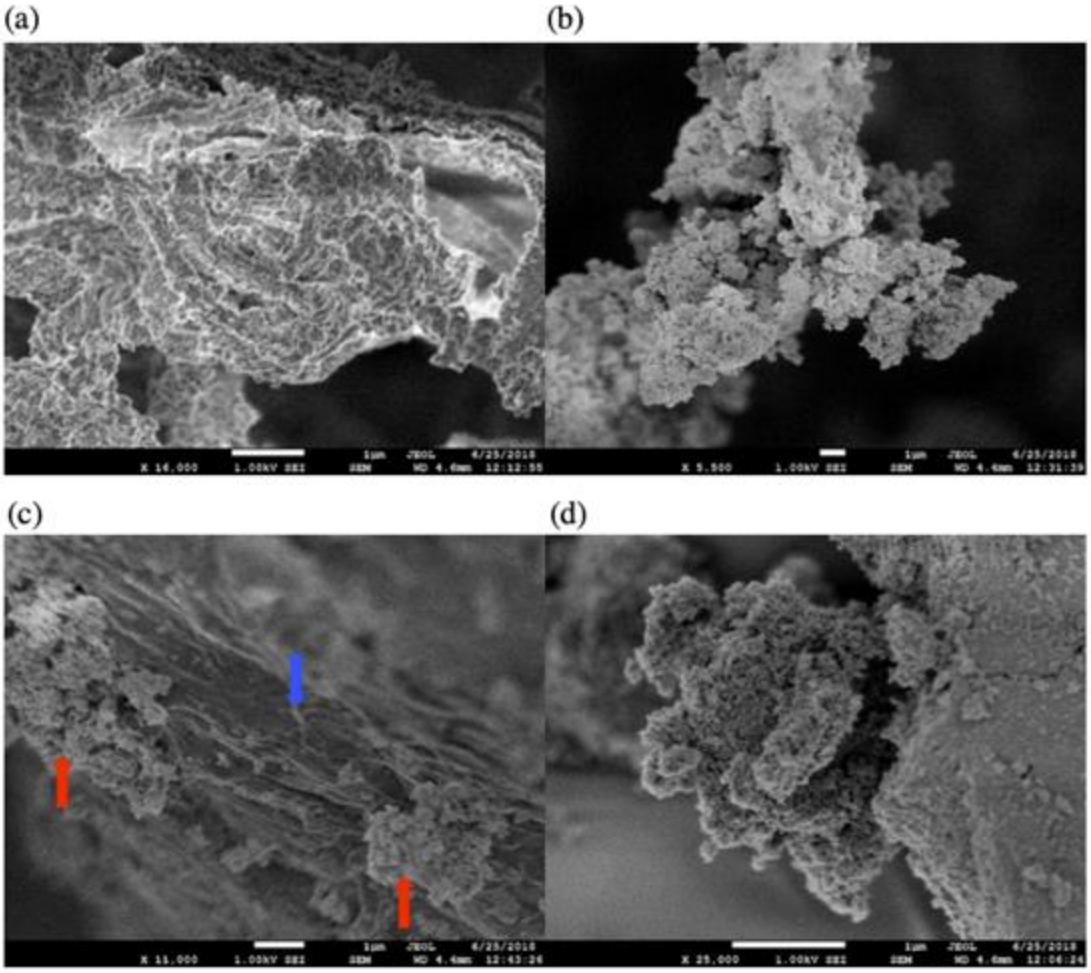

Figure 3.6. SEM images of (a) SE-CLEAs magnified 16,000x, (b) MNPs magnified 5,500x, (c) M-SE-CLEAs magnified 11,000x; red arrow: MNPs, blue arrow: SE-CLEAs, and (d) M-SE-CLEAs magnified 25,000x.

As higher reduced sugars from IL pretreated corn husks was observed in this study (Figure 3.5a), IL-pretreated biomass was used in the rest of experiments in this study. In Figure 3.5b, commercial enzymes, the combination of crude eglS and bglH (same as

commercial enzymes), five crude SEs, CLEAs of commercial enzymes, CLEAs of eglS and bglH, or SE-CLEAs were applied to IL-pretreated corn husks. The amounts of reduced sugars (54 mg/g biomass) in the samples added with free crude eglS and bglH was much lower than that observed in the samples added with all five free crude SEs (eglS, bglH, cbhA, xynC, and bxlB, 142 mg/g biomass) (Figure 3.5b). These results indicated that better and more complete saccharification of pretreated biomass could be achieved by using all types of cellulase and xylanase produced in this study.

The enzyme activity of the CLEAs of commercial enzymes was reduced by 3 times of free commercial enzymes (Figure 3.5b). The result was similar to the previous study (Perzon et al., 2017) reported that commercial enzymes could be reusable as the CLEAs but the enzyme activity of the CLEAs was reduced. In contrast, the highest amount of reduced sugar (250 mg/g biomass) was detected when SE-CLEAs was used (Figure 3.5b), which was about 1.7 times higher than that in the samples added with same 5 crude SEs. Using the crude SEs, without purification step, might contribute to the higher activity of SE-CLEAs than crude SEs. A previous study reported that CLEAs had no effects on the binding site of lignocellulose for the enzymes, despite that CLEAs and biomass are all insoluble materials (Bhattacharya and Pletschke, 2014). The results of our study were consistent with previous findings and suggested that the immobilization of SEs has led to improvement of saccharification as evident by higher amount of sugar released in the hydrolysate. Understanding the mechanism that may or may not affect the binding site of lignocellulose for the free and immobilized enzyme is an interesting research topic and requires in depth investigation in the future.

3.4.4. Reusability of SE-CLEAs and M-SE-CLEAs

The reusability of enzymes is a critical aspect of cost reduction of lignocellulos-based biofuel. In this study, the crude SEs were immobilized as SE- CLEAs and M-SE-CLEAs. The reusability of SE-CLEAs and M-SE-CLEAs were determined based on the amounts of reduced sugar released from the corn husk in each cycle. As shown in Figure 3.7a, no sugars were released when the SE-CLEAs was reused in the third cycle. During the experiment, incomplete recovery of SE-CLEAs after centrifugation was observed (much less of SE-CLEAs mass was recovered based on visual inspection). Because both SE-CLEAs and spent biomass are insoluble materials, it was possible that SE-CLEAs remained on the spent biomass, leading to the recovery of SE-CLEAs from the supernatant difficult (Bhattacharya and Pletschke, 2014). On the other hand, the M-SE-CLEAs allow for recovery after enzyme hydrolysis of the pretreated biomass by using magnet bars. As shown in Figure 3.7b, the M-SE-CLEAs maintained their activity until the 3rd cycle. However, their activity was reduced dramatically after the 4th cycle. The amounts of the M-SE-CLEAs after the 1st, 2nd, and 3rd cycles looked similar to the original M-SE-CLEAs based on visual inspection while the recovery of M-SE-CLEAs from the solution was not successful after the 4th cycle (i.e., about 90% of M-SE-CLEAs were lost based on visual inspection after the 4th cycle). The reasons for the failure of M-SE-CLEAs recovery were unclear and were not further investigated. It might be due to the loss of magnetic nanoparticles (numbers) and/or magnetic property from the M-SE-CLEAs. However, this

result indicates that M-SE-CLEAs can be reused at least three times for releasing sugars from the IL-pretreated lignocellulosic biomass.

(a)

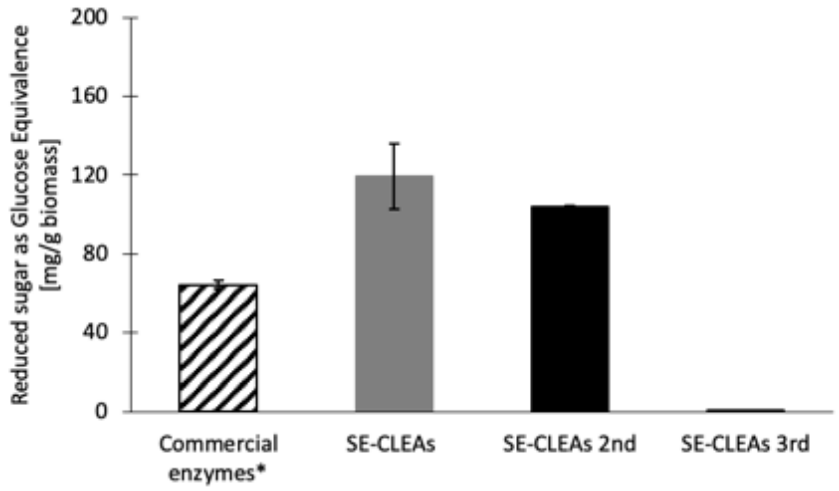

(b)

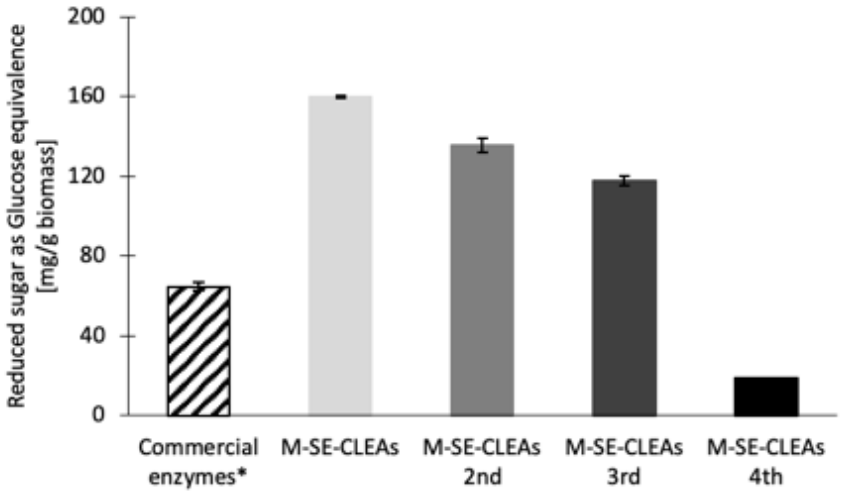

Figure 3.7. Reusability of crude enzymes by making SE-CLEAs or M-SE-CLEAs. (a) SE-CLEAs (b) M-SE-CLEAs.

3.4.5. Discussion

Effective release of reduced sugars from lignocellulose is a key step to enabling cost-effective biofuels and bioproducts production from lignocellulosic biomass. However, commercial enzymes are costly and offer a limited selection of SEs with different optimal pH and temperature (Bhattacharya and Pletschke, 2014). Compared to the results from previous enzymatic hydrolysis studies (Alvarez et al., 2016; Huang et al., 2015), our approach - using all types of crude SEs (without purification step) with a similar optimal condition - is much more effective, quicker, and easier. Using all types of SEs to achieve effective hydrolysis is supported by our results as shown in Fig. 3b, i.e., more reduced sugar content was detected in the pretreated biomass added with all SEs that those with only two commercial cellulases, endo-1,4-β-D-glucanase and β-glucosidase.

This study also demonstrated that it is possible to use crude SEs to create immobilized SE-CLEAs and M-SE-CLEAs, for enzyme reuse. Reusable biocatalysts like M-SE-CLEAs are favorable since it can potentially reduce the cost of biofuels and bioproducts production. Previous studies have shown that M-CLEAs can be recovered more quickly and easily when compared to another immobilization method, CELAs (Cui et al., 2016) and that M-CLEAs of lipase B retained its similar activity up to 10 cycles for converting olive oil into biodiesel (Cruz-Izquierdo et al., 2014). Also, the immobilized cellulase from *Aspergillus niger* (endo-1,4-β-D-glucanase) by magnetic nanoparticles was reusable total 16 times in the hydrolysis of powered rice straw (Huang et al., 2015). In this study, the SE-CLEAs and the M-SE-CLEAs maintained their enzyme activity until 2^{nd} and 3^{rd} cycles, respectively. Unlike the high numbers of reuse cycles of M-CELAs

reported previously (Cruz-Izquierdo et al., 2014; Huang et al., 2015), in this study, the reusability of SEs is low. Several factors might contribute the low reusability of the M-SE-CLEAs. For example, in this study, the corn husks were only ground to fine particles, not into powder as used in previous studies. Thus, it is possible that both our CLEAs were attached to the fine particles of the biomass, making recovery of CLEAs from the spent biomass even much more difficult through centrifugation or by application of a weak magnetic field. Based on FE-SEM images of M-SE-CLEAs (Fig. S4c), the MNPs were attached on the surface of immobilized SEs, not located inside of immobilized enzymes as reported previously (Huang et al., 2015). The difference of the locations of MNPs on the immobilized SEs might be due to different preparation methods of MNPs and M-SE-CLEAs used. In our study, in addition to the attachment on the surface of SEs, the NMPs were not covalently bonded to the SEs. Both factors might contribute to the loss of the magnetic properties after several cycles of CLEAs reuse, leading to the failure to CLEAs recovery. However, more studies are needed to determine the effects of biomass sizes, the strength of magnetic power needed, and amounts of magnetic nanoparticles required for effective recovery to improve the reuse of M-SE-CLEAs.

3.5. Conclusions

In this study, lignocellulose-saccharifying genes were successfully cloned into pET11a vector. This study verified that crude SEs could be produced using *E. coli* in quantity, and concentration and activity of crude SEs were measured. It was shown that the all five crude SEs could saccharify lignocellulose biomass more effectively and simply

because there is no a tedious purification step for the enzymes, and the amounts of reduced sugar were the highest when the SE-CLEAs was applied. This application is efficient because the optimal conditions of all enzymes are similar (pH 6.0 and temperature 50 °C). Furthermore, immobilized enzymes by magnetite-biocatalysts (M-SE-CLEAs) can be reused at least three times.

3.6. References

Adav SS, Ravindran A, Sze SK. Proteomic analysis of temperature dependent extracellular proteins from *Aspergillus fumigatus* grown under solid-state culture condition. Journal of Proteome Research 2013; 12: 2715-2731.

Agbor VB, Cicek N, Sparling R, Berlin A, Levin DB. Biomass pretreatment: Fundamentals toward application. Biotechnol Adv 2011; 29: 675-685.

Alvarez C, Reyes-Sosa FM, Diez B. Enzymatic hydrolysis of biomass from wood. Microbial biotechnology 2016; 9: 149-156.

Bagudo AI, Argungu AU, Aliero AA, Aliero S, Suleiman N, Kalpana S. *Bacillus subtilis* as an alternative source of beta-glucosidase. International Journal of Modern Cellular and Molecular Biology 2014; 3: 1-9.

Bailey MJ, Biely P, Poutanen K. Interlaboratory testing of methods for assay of xylanase activity. Journal of Biotechnology 1992; 23: 257-270.

Bhattacharya A, Pletschke BI. Magnetic cross-linked enzyme aggregates (CLEAs): A novel concept towards carrier free immobilization of lignocellulolytic enzymes. Enzyme Microb Technol 2014; 61-62: 17-27.

Billion-Ton. Advancing domestic resources for a thriving bioeconomy. U.S. Department of Energy, 2016.

Bokinsky G, Peralta-Yahya PP, George A, Holmes BM, Steen EJ, Dietrich J, Lee TS, Tullman-Ercek D, Voigt CA, Simmons BA, Keasling JD. Synthesis of three advanced biofuels from ionic liquid-pretreated switchgrass using engineered *Escherichia coli*. Proceedings of the National Academy of Sciences of the United States of America 2011; 108: 19949-19954.

Caes BR, Van Oosbree TR, Lu F, Ralph J, Maravelias CT, Raines RT. Simulated moving bed chromatography: Separation and recovery of sugars and ionic liquid from biomass hydrolysates. ChemSusChem Communications 2013; 6: 2083-2089.

Cruz-Izquierdo A, Pico EA, Lopez C, Serra JL, Llama MJ. Magnetic cross-linked enzyme aggregates (mCLEAs) of *Candida antarctica* lipase: An efficient and stable biocatalyst for biodiesel synthesis. PLoS One 2014; 9: e115202.

Cui J, Cui L, Jia S, Su Z, Zhang S. Hybrid cross-linked lipase aggregates with magnetic nanoparticles: A robust and recyclable biocatalysis for the epoxidation of oleic acid. Journal of Agricultural and Food Chemistry 2016; 64: 7179-7187.

Dalal S, Sharma A, Gupta MN. A multipurpose immobilized biocatalyst with pectinase, xylanase and cellulase activities. Chemistry Central Journal 2007; 1: 16-20.

Elkins JG, Raman B, Keller M. Engineered microbial systems for enhanced conversion of lignocellulosic biomass. Current Opinion in Biotechnology 2010; 21: 657-662.

Grajek W. Temperature and pH optima of enzyme activities produced by cellulolytic thermophilic fungi in batch and solid-state cultures. Biotechnology Letters 1986; 8: 587-590.

Gupta VK, Kubicek CP, Berrin JG, Wilson DW, Couturier M, Berlin A, Filho EXF, Ezeji T. Fungal enzymes for bio-products from sustainable and waste biomass. Trends in Biochemical Sciences 2016; 41: 633-645.

Hang YD, Woodams EE. Enzymatic production of soluble sugars from corn husks. Food science and technology 1999; 32: 208-210.

Huang PJ, Chang KL, Hsieh JF, Chen ST. Catalysis of rice straw hydrolysis by the combination of immobilized cellulase from *Aspergillus niger* on beta-cyclodextrin-Fe3O4 nanoparticles and ionic liquid. BioMed Research International 2015; 2015: 409103.

Iakiviak M, Devendran S, Skorupski A, Moon YH, Mackie RI, Cann I. Functional and modular analyses of diverse endoglucanases from *Ruminococcus albus* 8, a specialist plant cell wall degrading bacterium. Scientific Reports 2016; 6: 29979.

Johnson E. Integrated enzyme production lowers the cost of cellulosic ethanol. Biofuels, Bioproducts and Biorefining 2016; 10: 164-174.

Khare SK, Pandey A, Larroche C. Current perspectives in enzymatic saccharification of lignocellulosic biomass. Biochemical Engineering Journal 2015; 102: 38-44.

Kumar P, Barrett DM, Delwiche MJ, Stroeve P. Methods for pretreatment of lignocellulosic biomass for efficient hydrolysis and biofuel production. Industrial and Engineering Chemistry Research 2009; 48: 3713-3729.

Limayem A, Ricke SC. Lignocellulosic biomass for bioethanol production: Current perspectives, potential issues and future prospects. Prog Energy Combust Sci 2012; 38: 449-467.

Lynd LR, Laser MS, Bransby D, Dale BE, Davison B, Hamilton R, Himmel M, Keller M, McMillan JD, Sheehan J, Wyman CE. How biotech can transform biofuels. Nature Biotechnology 2008; 26: 169-172.

Mfombep PM, Senwo ZN, Isikhuemhen OS. Enzymatic activities and kinetic properties of β-glucosidase from selected white rot fungi. Advances in Biological Chemistry 2013; 03: 198-207.

Miller GL. Use of dinitrosalicylic acid reagent for determination of reducing sugar. Analytical Chemistry 1959; 31: 426-428.

Nlewem KC, Thrash MEJ. Comparison of different pretreatment methods based on residual lignin effect on the enzymatic hydrolysis of switchgrass. Bioresour Technol 2010; 101: 5426-5430.

Perzon A, Dicko C, Çobanoğlu Ö, Yükselen O, Eryilmaz J, Dey ES. Cellulase cross-linked enzyme aggregates (CLEA) activities can be modulated and enhanced by precipitant selection. Journal of Chemical Technology & Biotechnology 2017; 92: 1645-1649.

Podkaminer KK, Guss AM, Trajano HL, Hogsett DA, Lynd LR. Characterization of xylan utilization and discovery of a new endoxylanase in *Thermoanaerobacterium saccharolyticum* through targeted gene deletions. Applied and Environmental Microbiology 2012; 78: 8441-8447.

Ranjbakhsh E, Bordbar AK, Abbasi M, Khosropour AR, Shams E. Enhancement of stability and catalytic activity of immobilized lipase on silica-coated modified magnetite nanoparticles. Chemical Engineering Journal 2012; 179: 272-276.

Rubin EM. Genomics of cellulosic biofuels. Nature 2008; 454: 841-845.

Sheldon RA. Characteristic features and biotechnological applications of cross-linked enzyme aggregates (CLEAs). Applied Microbiology and Biotechnology 2011; 92: 467-477.

Sills DL, Gossett JM. Assessment of commercial hemicellulases for saccharification of alkaline pretreated perennial biomass. Bioresource Technology 2011; 102: 1389-1398.

St John FJ, Rice JD, Preston JF. Characterization of XynC from *Bacillus subtilis* subsp. *subtilis* strain 168 and analysis of its role in depolymerization of glucuronoxylan. Journal of Bacteriology 2006; 188: 8617-8626.

Šulek F, Fernández DP, Knez Ž, Habulin M, Sheldon RA. Immobilization of horseradish peroxidase as crosslinked enzyme aggregates (CLEAs). Process Biochemistry 2011; 46: 765-769.

Terrasan CRF, Guisan JM, Carmona EC. Xylanase and β-xylosidase from *Penicillium janczewskii* : Purification, characterization and hydrolysis of substrates. Electronic Journal of Biotechnology 2016; 23: 54-62.

Verardi A, Bari ID, Ricca E, Calabro V. Hydrolysis of lignocellulosic biomass: Current status of processes and technologies and future perspectives. IntechOpen, 2012.

Wang B, Rezenom YH, Cho KC, Tran JL, Lee DG, Russell DH, Gill JJ, Young R, Chu KH. Cultivation of lipid-producing bacteria with lignocellulosic biomass: effects of inhibitory compounds of lignocellulosic hydrolysates. Bioresour Technol 2014; 161: 162-170.

Wolf M, Geczi A, Simon O, Borriss R. Genes encoding xylan and *β*-glucanhydrolysing enzymes in *Bacillus subtilis*: characterization, mapping and construction of strains deficient in lichenase, cellulase and xylanase. Microbiology 1995; 141: 281-290.

Xu J, Cheng JJ, Sharma-Shivappa RR, Burns JC. Sodium hydroxide pretreatment of switchgrass for ethanol production. Energy & Fuels 2010; 24: 2113-2119.

Yang B, Dai Z, Ding SY, Wyman CE. Enzymatic hydrolysis of cellulosic biomass. Biofuels 2011; 2: 421-450.

Zhang X, Xu J, Cheng JJ. Pretreatment of corn stover for sugar production with combined alkaline reagents. Energy and Fuels 2011; 25: 4796-4802.

Zhang YH, Hong J, Ye X. Cellulase assays. Methods in Molecular Biology 2009; 581: 213-231.

4. DEVELOPMENT OF NON-STERILE CULTIVATION AND SOLVENT-FREE BIOLIPID BIOEXTRACTION TO REDUCE PRODUCTION COST OF BIOLIPID-BASED BIOFUEL

4.1. Summary

Triacylglycerols (TAGs) are starting materials for production of biolipid-based fuels such as biodiesel and biojet fuel. While TAGs can be produced from various microorganisms with renewable resources, cultivation of TAG-producing microorganisms under sterile conditions to avoid microbial contamination and application of solvent to extract TAGs from the TAG-filled microorganisms are costly. To overcome these challenges, this study reports non-sterile cultivation of an oleaginous bacterium *Rhodococcus opacus* PD631SpAHB with glucose under saline conditions, followed by use of a solvent-free, phage-lysis-protein-based bioextraction approach for TAGs release. The engineered strain PD631SpAHB is a salt-tolerant strain with a plasmid carrying an inducible phage lytic gene cassette to enable TAGs release into the supernatant upon induction. Cell lysis of PD631SpAHB was confirmed by decrease of optical density of cell suspension, by loss of the integrity of cell membrane, and by detection of TAGs released into the supernatant. Up to 38% of the total TAGs accumulated in the strain PD631SpAHB was released into supernatant after the expression of the lytic genes. PD631SpAHB strain is a promising candidate to produce TAGs from non-sterile growth medium and release of its TAGs without solvent extraction - a new approach to reduce the overall cost of biolipid-based biofuel production.

Graphical Summary

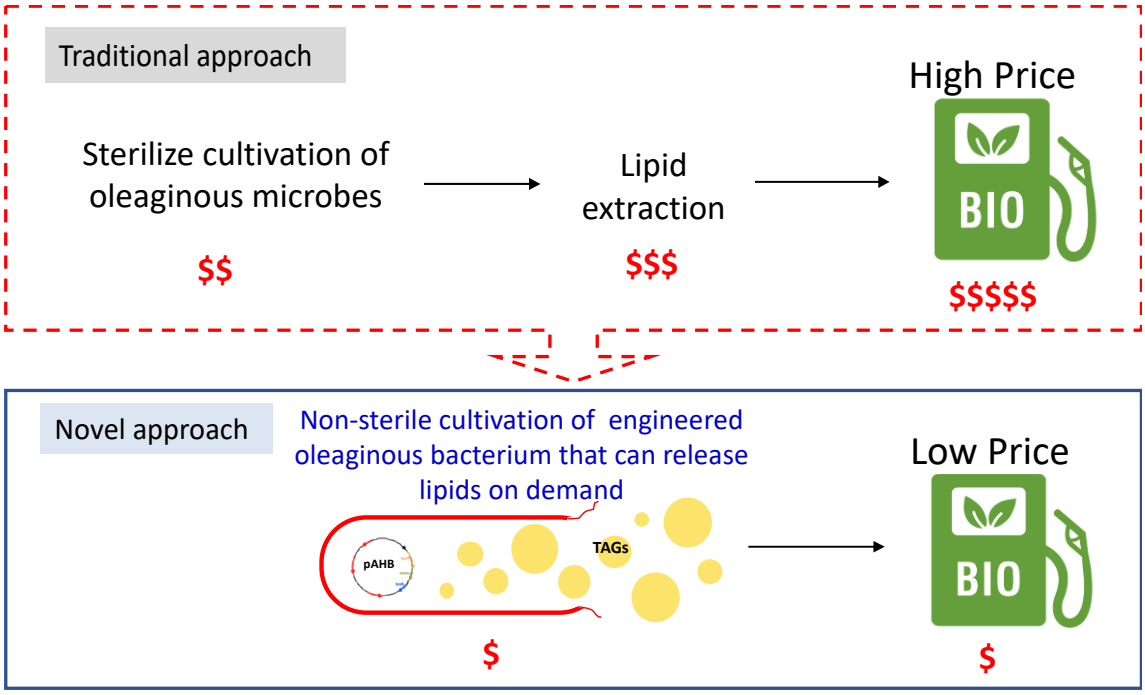

Figure 4.0. Graphical summary of Chapter 4.

Highlights

- PD631pAHB was engineered with phage lytic genes to enable cell lysis on demand.
- PD631S and PD631SpAHB accumulated TAGs in non-sterilize saline growth media.
- PD631SpAHB produced and released its TAGs into supernatant on demand.
- PD631SpAHB is a proof-of-principle construct to be optimized for biofuel production.

4.2. Introduction

Triacylglycerols (TAGs), one type of biolipids, are starting materials for producing biolipid-based biofuels such as biodiesel and biojet fuel (EPA, 2018; Kim et al., 2017). TAGs can be produced from various microorganisms including microalgae, yeast, and bacteria (Amara et al., 2016; Gujjala et al., 2019; Lee et al., 2017; Patel et al., 2018; Tanimura et al., 2014). Compared to microalgae or yeast, cultivation of TAG-accumulating bacteria is much easier and sustainable as higher TAG yields can be produced from various inexpensive and renewable organic wastes (Davila Costa et al., 2017). For example, *Rhodococcus opacus* PD630 (referred as PD630 hereafter), a model strain capable of accumulating TAGs up to 76% of the cell dry weight (Alvarez and Steinbüchel, 2002), has been shown to produce TAGs from hydrolysates of renewable lignocellulosic biomass (Wang et al., 2014). However, production cost of lipid-based biofuels remains high, in part, due to two additional major obstacles: high cost of cultivation under sterilized conditions to avoid microbial contamination and expensive downstream process for extracting TAGs from the TAG-filled microorganisms.

Sterilization of growth medium accounts for 16.4% of the total energy consumption of biolipid-based biofuel production (Soccol et al., 2017). Accordingly, non-sterile cultivation of biolipid-producing microorganisms is attractive and has been received considerable attention (Santamauro et al., 2014). One promising strategy to implement non-sterile cultivation is to leverage or create growth advantages for the desired strains to outgrow non-desired ones during the cultivation. For example, cultivation of salt-tolerant polyhydroxyburyrate (PHB)-accumulating strains in non-sterilized salt media

for production of PHB, a type of biolipids, has been successfully demonstrated (Asiri et al., 2020; Tan et al., 2011; Wu et al., 2019; Yue et al., 2014). The success of these studies relied on the fact that these salt-tolerant PHB-accumulating microbial strains can accumulate osmolytes such as glutamate, ectoine, or trehalose to survive under high saline conditions and outgrow those non-salt tolerant and non PHB-accumulating strains. Accordingly, a similar strategy will be applicable to oleaginous strains for non-sterile cultivation in saline growth medium, if the oleaginous strains becomes salt-tolerant. However, no study has explored this aspect – non-sterile saline cultivation of oleaginous bacterial strains for TAG production.

High cost of extraction of biolipids from oleaginous microbes is another major obstacle, making the price of biolipid-based biofuels less competitive to those of petroleum-based fuels. While solvent extraction is a common method for biolipid extraction (Hwangbo and Chu, 2020), this extraction method is considered as a bottleneck for commercial production of biolipid-based biofuels due to toxicity of chlorinated solvent, requirement of additional energy input to separate biolipids from the solvent mixture, and treatment cost for the spent solvent (Harris et al., 2018; Madkour et al., 2013; Ren et al., 2017).

A novel bioextraction method using bacteriophage (phage) to lyse cells to release biolipids like PHB (Hand et al., 2016) and TAGs (Gill et al., 2018) has been recently reported. Bacteriophage, also called phage, is a host-specific bacterial virus. Once its DNA has invaded the bacterial host cell, the phage can enter a lytic cycle to degrade the cell envelope using phage-encoded lytic proteins, leading to release of the intracellular

components upon cell lysis (Cahill and Young, 2019; Pires et al., 2016; Young, 2014). However, achieving synchronous infection of the culture under the conditions of biomass growth is problematic.

In this study we explored the development of a salt-tolerant TAG-accumulating bacterium with an ability to express phage lysis proteins on demand to achieve non-sterile cultivation for TAG production and solvent-free bioextraction of accumulated TAGs from the bacterium (as shown in Figure 4.1). First, an engineered TAG-producing bacterium with an ability to lyse cell on demand was developed by introducing an inducible phage lytic gene cassette into a known TAG-producing *R. opacus* PD631. Then, the engineered strain (referred as PD631pAHB hereafter) was further developed via an adaptive evolution strategy to become a high-salt tolerant strain, PD631SpAHB. This PD631SpAHB strain was characterized and capable of outgrowing non-TAG-producing microorganisms in non-sterilized salt media and release of its TAGs into the supernatant upon induction.

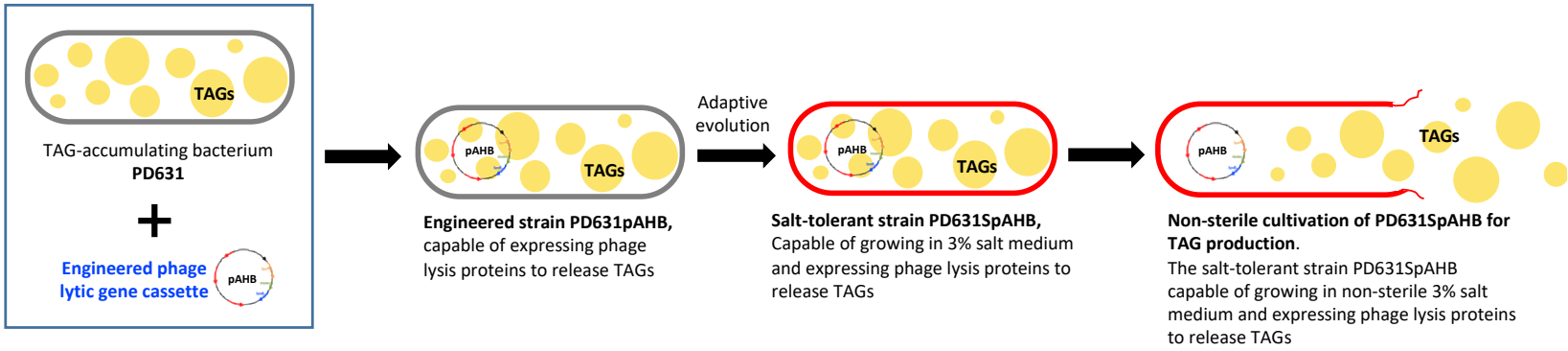

Figure 4.1. Proposed experimental approach of this study.

4.3. Materials and Methods

4.3.1. Bacterial strain, culture conditions, and chemicals

R. opacus PD631 (referred as PD631 hereafter), a domesticated derivative of PD630, was used in this study. The strain PD631 was developed by subculturing on Reasoner's 2A (R2A) agar plates for six months and showed a similar TAG-accumulating ability to PD630 (Gill et al., 2018). The strain PD631 was maintained aerobically in R2A or Luria-Bertani (LB) broth medium at 200 rpm at 30 °C. Amido black, hexane, methanol, and Imperial^{TM} protein stain were purchased from Fisher Scientific (Hampton, NH, USA). R2A broth was purchased from Teknova (Hollister, CA, USA). Difco LB broth, Difco LB agar, and Difco R2A agar were purchased from VWR (Radnor, PA, USA). Diethyl ether, glyceryl trioleate (TL), chloroform, thiostrepton, chloramphenicol (CAM), and all other chemicals used in this study were purchased from Millipore Sigma (Burlington, MA, USA).

4.3.2. Construction of a plasmid with a phage lytic gene cassette under inducible control

To express phage lysis proteins in TAG-accumulating *Rhodococcus* strains, the lytic genes of mycobacterium phage D29 were selected because *Mycobacterium* and *Rhodococcus* have similar cell envelope structure. The phage D29 lytic gene cassette consists of the genes *lysA-holin-lysB* (Table 4.1a). Phage D29 was provided from Center for Phage Technology at Texas A&M University (College Station, TX). The genomic DNA of phage D29 was prepared, purified by Promega Wizard DNA cleanup kit

(Promega, Madison, WI), and then used for PCR amplification. The lytic gene cassette was amplified using 2 primers as listed in Table 4.1b. A 25-µL of PCR reaction - including 12.5 µL of 2X PCR Master Mix (Promega, Madison, WI, USA), 1 µL of template phage DNA, 1 µL each of 10 µM forward and reverse primers, and 9.5 µL of nuclease-free water - was used. The PCR reaction was carried out as follows: denaturing at 98 °C for 2 min, followed by 35 cycles at 98 °C for 30 sec, 57 °C for 1 min, and 72 °C for 2 min and 42 sec, and then a final extension cycle at 72 °C for 10 min. The PCR product for lysis gene cassette (*lysA-holin-lysB*) was clearly observed as a band of 2.7 kilo-base pairs (kB) on the agarose gel (Figure 4.2a). The PCR product was purified by QiAquick Gel Extraction Kit (Qiagen, Hilden, Germany).

Table 4.1. (a) Names and sizes of phage lysis enzymes and associated phage lytic genes of mycobacterium phage D29. (b) Primer sets used for traditional cloning of the phage lytic gene cassette (*lysA-holin-lysB*) into the plasmid pTipQC2 as plasmid pAHB.

(a)

Target gene	Enzyme	Size (kb)	# of Amino acids	MW (kDa)
lysA	Endolysin A	1.5	493	55
holin	Holin	0.5	141	15
lysB	Mycolate esterase (Endolysin B)	0.8	254	29

(b)

Primers	Sequence	Primer length (bp)	Tm (°C)
AHB_NdeIFW	5'- TAAGGGCATATGATGACGCTCATAGTCACACGC -3'	33	64
AHB_NcoIRV	5'- TGCTTACCATGGTCAGATCTGTCGTAGGAA -3'	30	62

(a)

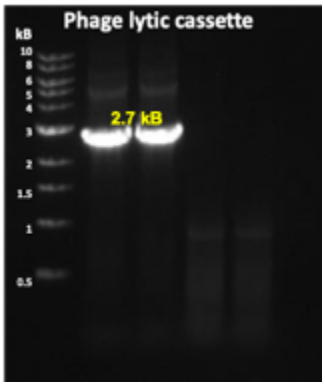

(b)

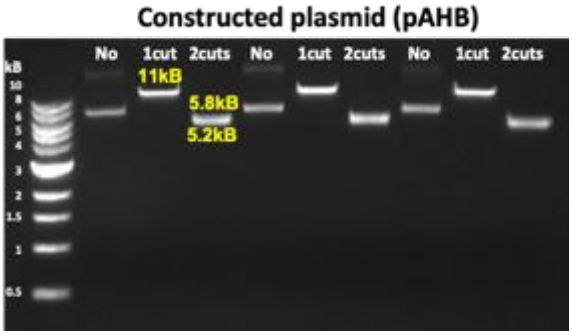

Figure 4.2. (a) An agarose gel showing PCR products of a phage lytic gene cassette (*lysA-holin-lysB*) (2.7 kb), (b) An agarose gel showing restriction digestion of the constructed plasmid (pAHB) containing a phage lytic gene cassette (pAHB). The plasmids were extracted from NEB 5-alpha competent *E. coli*. The plasmid (pAHB) was digested with EcoRV (1 cut, expected size: 11 kb), EcoRV and NotI (2 cuts, expected sizes: 5.2 and 5.8 kb), or without enzymes (No: no restriction digestion, 7.0 kb).

The PCR product was cloned into a pTipQC2 plasmid (AIST Japan, Tokyo, Japan) using the NdeI-NcoI cloning site. The 20-µL of ligation mixture included 3 µL of linearized pTipQC2 vector (about 50 ng), 2 µL of 10X T4 DNA ligase buffer, 1 µL of purified PCR product (a molar ratio of 1:3 vector to insert), 1 µL of T4 DNA ligase, and 13 µL of deionized water. The mixture was incubated at 23 °C for 2 h, followed by inactivation of enzymes at 65 °C for 10 min. A 2-µL of reaction mixture was used for

chemical transformation into competent NEB 5-alpha *Escherichia coli* cells (Product No. C2987H, New England Biolabs, Ipswich, MA, USA) by heat-shock, according to the manufacturer's instructions. The transformed culture was plated on LB agar with 100 mg/L of ampicillin as a selective marker. About 80 colonies in a ten-time diluted plate were screened and transformation efficiency was 3.2 x 10^5 cfu/μg. The candidate plasmid constructs were prepared by QIAprep Spin Miniprep Kit (Qiagen, Hilden, Germany) and was confirmed by (i) observation of expected fragment sizes of restriction enzymes digested plasmids on the agarose gel (Figure 4.2b), and by (ii) verification of plasmid sequence (Eton Bioscience, San Diego, CA, USA). This inducible plasmid containing the phage lytic gene cassette is referred hereafter as pAHB (Figure 4.3).

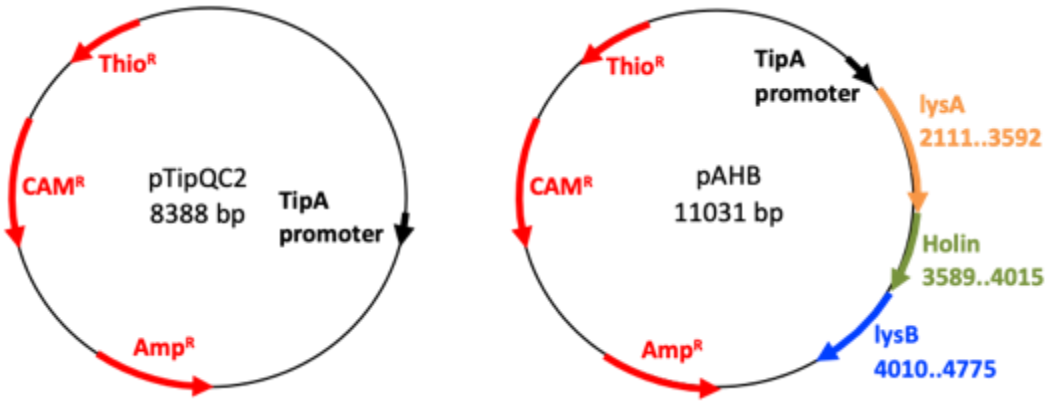

Figure 4.3. Maps of the pTipQC2 vector and the constructed recombinant plasmid (pAHB) containing a phage lytic gene cassette.

4.3.3. Development of PD631pAHB by transformation of recombinant plasmid

The verified recombinant plasmid (pAHB) was transformed into PD631 via electroporation to obtain a new engineered strain, PD631pAHB. Transformation was

done as described previously (Gill et al., 2018). Briefly, the recombinant plasmid (about 300 ng) was mixed with electrocompetent cells of PD631 and preincubated at 4 °C for 5 min. The electroporation was performed in electrocuvettes (gaps of 2mm) by micropulser (Bio-Rad, Hercules, CA, USA) with the following settings: ec2: 2.5 kV, 600 ohm, and 25 μF. The electroporated cells were recovered outgrown in NB medium at 30 °C for 4 h, and then plated on an NB agar plate with 35 mg/L of CAM as a selective marker. The transformant colonies were visible after 3 to 5 days incubation at 30 °C. About 45 colonies were screened and transformation efficiency was 3.8×10^2 cfu/μg.

4.3.4. Development of a salt-tolerant engineered strain (PD631SpAHB) via adaptive evolution

Ectoine and glutamate are the two most common osmolytes in salt-tolerant bacteria (Burg and Ferraris, 2008; Ikeuchi et al., 2003; Kuhlmann and Bremer, 2002). An ectoine synthesis gene cluster (*ectA, ectB*, and *ectC*) encoding ectoine synthesis proteins were found in PD630 genome based on Blast-P results against to the genome of a known salt-tolerant strain *Zobellella denitrificans* ZD1 (Wu et al., 2019). Additionally, six possible glutamate synthases genes encoding glutamate synthesis proteins were directly identified in the genome of PD630 (CP003949.1 as an accession number of GenBank databases). Table 4.2 lists names of these enzymes and genes. Since these osmolyte-producing genes are present in strain PD630, we hypothesized that both the domesticated strain PD631 and the engineered strain PD631pAHB also contain these genes.

Accordingly, an adaptive evolution approach was used to develop PD631SpAHB, a salt-tolerant version of PD631pAHB. Briefly, PD631pAHB was successively subcultured on LB medium agar containing 35 mg/L of CAM and 3% (w/v) NaCl and incubated at 30 °C. After 3 days of incubation, colonies were observed and re-streaked on a new plate containing LB agar medium with 35 mg/L of CAM and 3% NaCl. This process was repeated ten times over a month. Similarly, PD631S, a salt-tolerant version of PD631, was developed by ten times of successive subculturing of PD631 on LB medium agar containing 3% NaCl. These newly developed salt-tolerant strains PD631S and PD631SpAHB were allowed to adjust to the high saline liquid medium.

Table 4.2. Primer sets used in RT-qPCR analysis. These primer sets target housekeeping gene (16S rRNA), three possible ectoine synthesis genes, and six possible glutamate synthesis genes in PD630.

Target gene	Enzyme	Primers	Sequence	Product length (bp)	Tm (°C)
16S rRNA		16S-F	5'-AGGCGATACGGGCAGACTTG-3'	131	60
		16S-R	5'-CGCTCCTCAGCGTCAGTTAC-3'		58
ectA	L-2,4-diaminobutyric acid acetyltransferase	ectA-F	5'-CGTGGGATTCGTATCAGGGTTC-3'	150	58
		ectA-R	5'-GTAATCCCTTCGGGTGCAAGTC-3'		58
ectB	Diaminobutyrate-2-oxoglutarate transaminase	ectB-F	5'-TGATCGTCGAGACCGTGCAG-3'	163	60
		ectB-R	5'-CGGCGATCTCGAAGGAGAAG-3'		58
ectC	L-ectoine synthase	ectC-F	5'-ACAAAGTGGGCTTCTCGTTCC-3'	145	58
		ectC-R	5'-AGTTCGTAGACCTTGTCGTTGTCG-3'		59
LPD00054	Ferredoxin-dependent glutamate synthase 1	1LPD00054-F	5'- CAGCGGTCAACCCGTACATG -3'	146	59
		1LPD00054-R	5'- GCCCATCTTGGACATCACCTTG -3'		58
LPD00055	Glutamate synthase (NADPH), homotetrameric	2LPD00055-F	5'- AGGAACTCCATCGCCTGGTG -3'	153	60
		2LPD00055-R	5'- CAAGACGGGTGTCAACGTGG -3'		59
gltD	glutamate synthase (NADPH), small chain	3gltD-F	5'- CTTGTTCGAGGTGACGAGGTG -3'	132	58
		3gltD-R	5'- CAGATGCGCGAGAACTTCGAC -3'		58
LPD05102	Ferredoxin-dependent glutamate synthase 1	4LPD05102-F	5'- TGACGGTGCCCTTGAAGTAC -3'	151	57
		4LPD05102-R	5'- CGGAACTATCTCACCGCTCTCG -3'		59
LPD05956	Glutamate synthase (NADPH), large chain	5LPD05956-F	5'- TCGACCGCTTCGAGATCACC -3'	154	59
		5LPD05956-R	5'- CCCATCTGCTTGCGGAACTC -3'		59
gltS	Glutamate synthase large subunit-like protein	6gltS-F	5'- TCGCGGAGTTCGATGATCTTG -3'	136	57
		6gltS-R	5'- TGCTGGGACAGAAGATCACC -3'		57

4.3.5. Assessment of cell lysis after induction of pAHB in the engineered strains

The success of cell lysis after induction of pAHB in the engineered strains (i.e., PD631pAHB and PD631SpAHB) was determined by observation of decrease of optical density and detection of lactate dehydrogenase (LDH) in the supernatant. LDH is a cytosolic enzyme in cells. When cell membranes are damaged and/or cells are lysed, LDH will be released into growth medium. As LDH remains stable extracellularly in solution, presence of LDH in the supernatant can be used as an indication of cell lysis (Henein et al., 2016).

Experiments to examine the success of cell lysis of PD631pAHB and PD631SpAHB upon induction were conducted as follows. These engineered strains were first grown in LB medium containing 35 mg/L of CAM with or without 3% NaCl, respectively, at 200 rpm at 30 °C. Optical density (OD_{600}) of the cell suspension was monitored over time. When reaching exponential growth phase (OD_{600} ~0.5 - 0.7), 1 μg/mL of thiostrepton was added to induce the expression of phage lytic genes cassette in pAHB. Presence of LDH in supernatant was determined as extracellular LDH activity using Pierce LDH cytotoxicity assay kit (Thermo Fisher Scientific, Waltham, MI, USA) according to the manufacturer's instructions. The amount of LDH released in the supernatant is directly proportional to the formation of formazan as determined by absorbance at 560 nm (A_{560}) using a microplate reader (Tecan GENIOS, Männedorf, Switzerland). PD631 and PD631pTipQC2 (carrying pTipQC2) were used as negative controls (i.e. these strains contain no pAHB).

4.3.6. Sodium dodecyl sulfate polyacrylamide gel electrophoresis (SDS-PAGE) analysis

The phage lysis proteins produced by PD631pAHB and PD631SpAHB were visualized using sodium dodecyl sulfate polyacrylamide gel electrophoresis (SDS-PAGE). After induction, the cell suspensions were collected and centrifuged at 10,000 g at 4 °C for 10 min to pellet cells and cell-debris. The supernatant was collected and used for SDS-PAGE analysis. Briefly, the cell pellet was resuspended in 2 mL of sodium phosphate buffer (MP Biomedicals, Santa Ana, CA, USA), at OD_{600} ~ 16.7. A 15 µL aliquot of the cell suspension was mixed with 15 µL of 2X SDS buffer and boiled for 10 min. The 30 µL samples were used for SDS-PAGE analysis. SDS-PAGE was performed on Novex™ wedge well 14% tris-glycine gel (Invitrogen, Carlsbad, CA, USA) in XCellSureLock™ Mini-Cell equipment (Novel Experimental Technology, San Diego, CA, USA) at 90 V for 2.5 h. Five µL of Mark12 Unstained Standard (Invitrogen, Carlsbad, CA, USA) and 300 mL of 1X Tris-Glycine (MP Biomedicals, Santa Ana, CA, USA) running buffer were used. After electrophoresis, the gel was stained with Imperial™ protein stain for 1 h, and destained with deionized water for 2 h. To establish total cell controls, cell pellets of PD631 and PD631pTipQC2 were lysed by sonication, conducted in 6 rounds of 20 sec of sonication (50% amplification) and 20 sec on ice.

4.3.7. Expression levels of genes encoding enzymes responsible for producing known osmolytes

Experiments were designed to quantify the expression of genes encoding osmolytes-producing enzymes in PD631S grown in medium with or without 3% NaCl. Briefly, the strain was aerobically grown in 50 mL of ammonium mineral salts (AMS) medium (Hand et al., 2015) with 10 g/L of glucose in the presence or absence of 3% NaCl at 200 rpm at 30 °C. When the cell density reached an OD_{600} of 2.0, cells were harvested for total RNA extraction, followed by cDNA synthesis using the extracted RNA and quantification of targeted genes using the synthesized cDNA. The total RNA in the samples was extracted by FastRNA™ Pro Blue Kit (MP Biomedicals, Santa Ana, CA, USA) according to the manufacturer's protocol. Gene quantification from the synthesized cDNA was conducted as described previously (Wu et al., 2019). Briefly, the cDNA was synthesized from extracted total RNA using QIAGEN OneStep Ahead reverse transcription (RT)-PCR kit (Quiagen, Hilden, Germany). A 25-μL of reaction mixture included 10 μL of 2.5X OneStep Ahead RT-PCR Master Mix, 1 μL of 25X OneStep Ahead RT-Mix, each 1.25 μL of 10 μM forward and reverse primers (listed in Table 2), 10.5 μL of RNase-Free Water, and 1 μL of total RNA (about 1 μg). The cDNA was synthesized by the following RT-PCR cycling conditions: 10 min of reverse transcription at 50 °C, 5 min of initial PCR activation at 95 °C, followed by 40 three-step cycles of 95 °C for 10 sec, 53 °C for 20 sec and 72 °C for 20 sec, and 2 min of final extension at 72 °C. The cDNA products were stored at -80 °C before use.

The cDNA was diluted 200-fold to serve as templates for RT-qPCR to quantify a housekeeping gene (16S rRNA) and osmolyte synthesis genes. A 20-μL RT-qPCR reaction mixture consisted of 1 μL of diluted cDNA, each of 1 μL of 10 μM forward and reverse primers (listed in Table 2), 7 μL of RNase-Free Water, and 10 μL of PowerSYBR Green PCR Master Mix (Applied Biosystem, Foster City, CA, USA). The RT-qPCR cycling conditions are as follows: 10 min of denaturation at 95 ºC, followed by 35 three-step amplification cycles of 95 °C for 30 sec, 55 °C for 45 sec and 72 °C for 45 sec using an IQ5 multicolor real-time PCR detection system (Bio-Rad, Hercules, CA, USA). During the amplification cycle, the fluorescence intensity was measured. For the endpoint of RT-qPCR quantification, the cycle threshold (Ct) value was used, which is defined as the number of PCR cycles required for crossing an arbitrary signal threshold. Each gene expression was calculated using Double delta Ct method as described previously (Wu et al., 2019). The expression as measured in PD631S grown without 3% NaCl was normalized to 1.0 as the baseline.

4.3.8. Non-sterile cultivation of PD631S for TAG production

Experiments were conducted to examine whether TAGs can be produced from non-sterile cultivation of PD631 and PD631S. Non-sterile cultivation of both strains for TAG production were conducted via two-stage cultivation process as described previously (Gill et al., 2018), except that non-sterile saline (3% NaCl) growth medium was used. Strains (PD631 and PD631S) were cultured with 10 g/L of glucose in AMS medium at 200 rpm at 30 °C until stationary growth phase (above OD_{600} of 2.0). These saturated

cultures were used as inocula for non-sterile cultivation experiments. An aliquot of the saturated culture was added to 50 mL of sterile or non-sterile AMS medium containing 10 g/L of glucose with or without 3% NaCl, resulting an initial OD600 ~0.02. After the inoculated cultures were grown at 200 rpm at 30 °C until early stationary phase, the cell suspension was pelleted, resuspended in sterile or non-sterile nitrogen-free mineral salts medium (MS) containing 10 g/L of glucose, and then incubated at 30 °C without shaking for 24 h. This process was to allow TAG accumulation while minimize TAG utilization. After 24 h of incubation, 50 mL of cell culture was pelleted by centrifugation at 10,000 g for 10 min and the cell pellet was used for TAG measurement using thin layer chromatography (TLC) analysis as described previously (Wang et al., 2014).

4.3.9. Non-sterile cultivation of PD631SpAHB for TAG production and release

TAG production under non-sterile conditions and TAGs release were investigated using PD631SpAHB along with PD631pTipQC2 used as a positive control. The experiments were conducted similarly as described in section 4.3.8 with some modification. Most protein expression from cloning vector are generally induced by adding an inducer at OD_{600} of 0.6 - 1.0 (Berrow et al., 2006; Rahmanpour and Bugg, 2013). However, PD631 can only accumulate TAGs during stationary phase under nitrogen limited conditions (Alvarez et al., 2000). Due to this limitation, the previous study cultivated TAG-filled PD631 under nitrogen-limit conditions first, followed by promoting cell growth through nitrogen source addition before infecting with Toil phages (Gill et al., 2018). The infected cells were then able to produce lysis enzymes that resulted in cell

lysis to release of TAGs to supernatant. Similarly, in this study, after accumulation of TAGs from the strain under nitrogen limited conditions, the cell cultures returned to the active growth by adding additional nitrogen content (0.7761 g/L of $(NH_4)_2SO_4$) and 1 μg/mL of thiostrepton to induce phage lytic genes in PD631SpAHB. Following overnight induction, the cell pellet and suspension were collected respectively by centrifugation at 10,000 g for 10 min and used for TAG measurement using TLC analysis.

4.3.10. Measurement of TAGs using TLC analysis

TAG contents in the cell pellet were extracted and analyzed as described previously (Gill et al., 2018; Wang et al., 2014). Briefly, the cell pellet was washed with deionized (DI) water, resuspended in 1 mL of DI water, and then extracted with 10 mL of chloroform/methanol mixture (2:1, v/v) overnight. For supernatant samples, 30 mL of chloroform/methanol mixture (2:1, v/v) was used. After overnight extraction, the chloroform layer (i.e., the bottom layer) was collected, dried, and then reconstituted in hexane. The TAGs contents in the reconstituted extracts (i.e. in hexane) were visualized on a silica gel TLC plate (Product No. 99570, Millipore Sigma, Burlington, MA, USA) and determined using ImageJ software (National Institutes of Health, Bethesda, MD) as described previously (Gill et al., 2018; Wang et al., 2014).

4.4. Results and discussion

4.4.1. Demonstration of cell lysis of PD631pAHB via induction of its phage lytic gene cassette

An inducible plasmid pAHB for expressing phage lysis proteins was constructed by cloning the phage D29 lytic gene cassette (consisting of genes *lysA-holin-lysB*) into the thiostrepton-inducible expression plasmid pTipQC2. The pAHB was then used to construct strain PD631pAHB for cell lysis on demand. Cell lysis of PD631pAHB was confirmed by monitoring changes of cell density after inducing the expression of the phage lytic genes. As shown in Figure 4.4a, PD631pTipQC2 and PD631pAHB both grew more slowly than PD631. This might be due to CAM in the growth medium as a selective marker for both plasmids. However, PD631pAHB grew even more slowly than cells carrying an empty vector pTipQC2, presumably due to leaky gene expression from the inducible promoter. After thiostrepton induction (1 μg/mL), cells carrying the empty vector continued to grow. However, the induced PD631pAHB culture showed decreased optical density after 6 h. The final optical density of PD631pAHB was ~ 0.3 after overnight induction.

Additional experiments were conducted to characterize the lysis of the PD631pAHB cells using the release of a cytosolic enzyme, LDH into the growth medium. After pelleting cell debris and unlysed cells, the supernatant of the induced PD631pAHB cells had about 74% of the total LDH activity (Figure 4.4b).

(a)

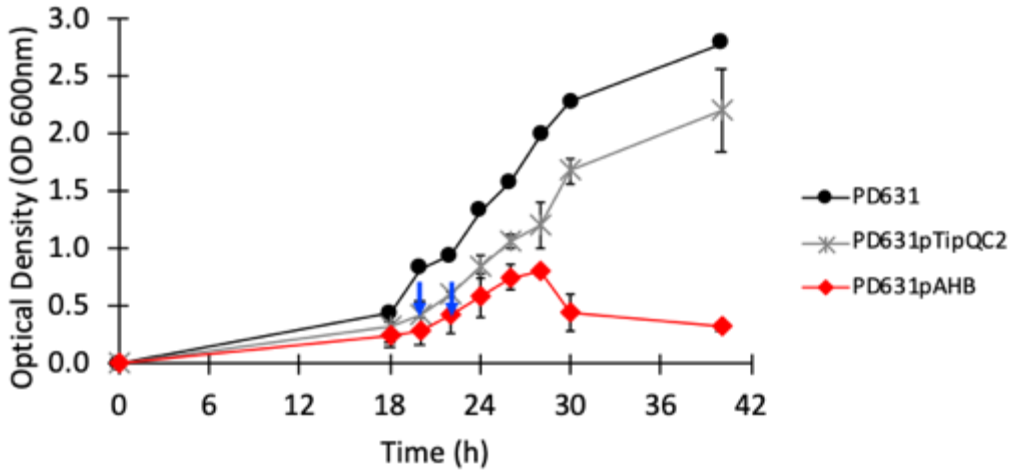

(b)

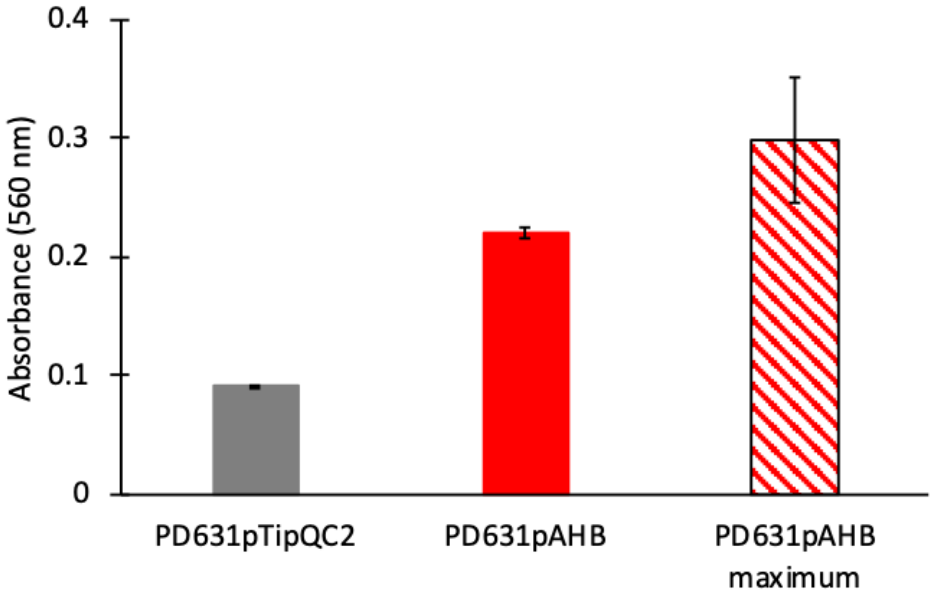

Figure 4.4. Demonstration of inducible lysis of PD631pAHB. (a) Profile of the optical density before and after induction. Blue arrows indicate the time points (around OD_{600} = 0.5 - 0.7) where 1 μg/mL of thiostrepton was added as an inducer. (b) Lactate dehydrogenase (LDH) activity detected in the culture medium of PD631pTipQC2, PD631pAHB after induction, and PD631pAHB maximum. PD631pAHB maximum: referred to PD631pAHB lysed by sonication artificially. (c) SDS-PAGE analysis of proteins in induced cells collected at 40 h. The induced cultures at the final point (T=40 h as shown in (a)) were harvested by centrifugation as described in Methods. Mark12 Unstained Standard was used as a protein ladder. All experiments were conducted in duplicate.

(c)

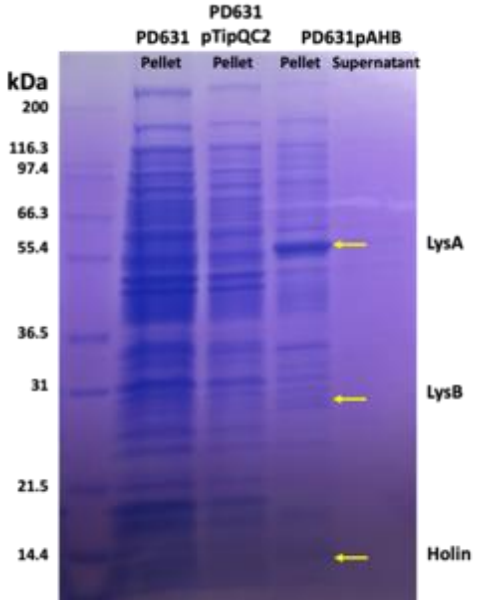

Figure 4.4. Continued.

Moreover, expression of phage lytic genes in PD631pAHB was confirmed by visualizing production of these lysis proteins on the SDS-PAGE gel. The protein profiles obtained from the concentrated whole cell cultures and supernatant of PD631, PD631pTipQC2, and PD631pAHB were compared on the SDS-PAGE gel (Figure 4.4c). Based on the predicted molecular masses of LysA, Holin, and LysB listed in Table 1a, three bands of the appropriate sizes were present in the sample from the induced cells carrying pAHB (lane 3) that were not present in the sample from the control: a thicker band for LysA (55 kDa) and two fainter bands for Holin (15 kDa) and LysB (29 kDa). Also, the sample of PD631pAHB after induction did not need additional cell lysis step (i.e., sonication), suggesting successful expression of the lytic gene cassette upon

induction that led to cell lysis. However, we only confirmed the overexpression for LysA. The difference of Shine-Dalgarno (SD) sequence of these three genes in the plasmid pAHB might explain the low expression levels for LysB and Holin. The SD sequence plays a key role during a translation initiation as a ribosomal binding site, and a positive correlation between SD sequence and gene expression level has been identified in prokaryotes (Ma et al., 2002). The consensus SD sequence (AGGAGG) of *E. coli* is more effective than the shorter SD sequence, leading to a high level of gene expression (Vimberg et al., 2007). This correlation might be applied to the gene expression characteristics of *Rhodococcus* (Kan et al., 2020). In the plasmid pAHB, the *lysA* gene has the SD sequence of pTipQC2 (GAAGGAG), which is strong for protein expression in *Rhodococcus* (Nakashima and Tamura, 2004), leading to the high expression of LysA. However, the *lysB* and holin genes possess the shorter and weaker SD sequences, derived from phage D29, AGGA and GGA, respectively. This difference of SD sequence might result in overexpression of *lysA* than the other two lytic genes, resulting in thicker band of LysA on the SDS-PAGE gel. In any case, despite of the low expression of LysB and Holin, PD631pAHB exhibited cell lysis and release of the intracellular components upon induction.

4.4.2. Characterization of newly developed salt-tolerant strain PD631S and PD631SpAHB

Two salt-tolerant strains PD631S and PD631SpAHB were developed after ten times of successively subculturing PD631 and PD631pAHB on LB agar containing 3%

NaCl or 3% NaCl and 35 mg/L CAM, respectively. The growth rates and doubling times of these strains were compared to those of non-salt-tolerant strains PD631 and PD631pAHB (Figure 4.5 and Table 4.3). PD631S was able to grow in liquid medium containing 3% NaCl, with a decreasing doubling time of 5.8 h for the 1st subculture to 3.9 h for the 3rd subculture (Table 4.3). When grown without 3% NaCl, PD631S showed a similar growth rate to that of strain PD631, i.e., a doubling time of 2.1 h for PD631S vs. a doubling time of 2.2 h for strain PD631 (Table 4.3). This indicated that PD631S are able to survive under high saline conditions for non-sterile cultivation and TAGs production. PD631pAHB and PD631SpAHB also grew slower than that of strain PD631, as evident by their doubling times (i.e., 3.2 h for both PD631pAHB and PD631SpAHB and 2.2 h for PD631 as shown in Table 4.3). To examine the stability of the plasmid pAHB in the newly constructed strain PD631SpAHB, this strain was successively cultured in LB medium without CAM for five generations. The plasmid pAHB was detected in the 5th generation culture (data not shown), suggesting that pAHB was stable in strain PD631SpAHB without CAM.

(a)

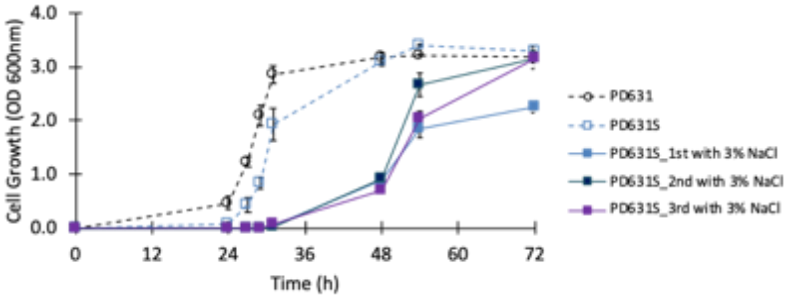

(b)

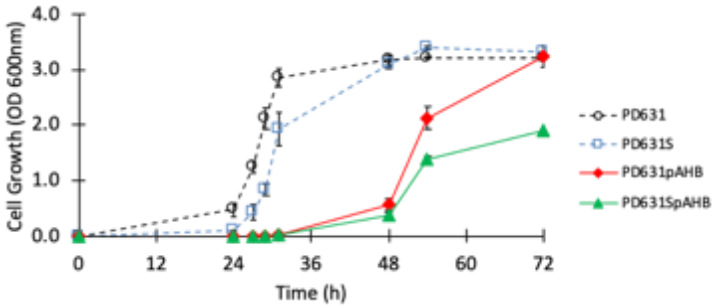

Figure 4.5. (a) Cell growth curves of PD631S and subcultures of PD631S in liquid AMS medium containing 1% of glucose with or without 3% NaCl. (b) Cell growth curves of PD631, PD631S, PD631pAHB, and PD631SpAHB in liquid AMS medium containing 1% of glucose and 35 mg/L of chloramphenicol for PD631pAHB and PD631SpAHB. Optical density was measured at 600 nm. All experimental conditions were listed in Table 4.3.

Table 4.3. Doubling times of strains grown under different conditions. All experiments were conducted in duplicate. All cultures were grown aerobically at 200 rpm at 30 °C. AMS: Ammonium Mineral Salts (AMS) medium, CAM: Chloramphenicol.

Sample Name	Strains	Medium	Doubling time (h)
PD631	PD631	AMS+1% glucose	2.2
PD631S	PD631S	AMS+1% glucose	2.1
PD631S 1st with 3% NaCl	PD631S	AMS+1% glucose+3% NaCl	5.8
PD631S 2nd with 3% NaCl	PD631S	AMS+1% glucose+3% NaCl	3.9
PD631S 3rd with 3% NaCl	PD631S	AMS+1% glucose+3% NaCl	3.9
PD631pAHB	PD631pAHB	AMS+1% glucose+35 mg/L of CAM	3.2
PD631SpAHB	PD631SpAHB	AMS+1% glucose+35 mg/L of CAM+3% NaCl	3.2

4.4.3. Effects of salts on non-sterile cultivation of strain PD631S and its TAG production

Experiments were conducted to determine the enzymes involved in synthesis of common osmolytes were made in strain PD631S under high salt conditions. Among the osmolytes, ectoine is commonly used to provide osmotic balance under extreme conditions (Lang et al., 2011). Three genes involved in ecotine synthesis are *ectA*, *ectB*, and *ectC* encoding diaminobutyric acid acetyltransferase, diaminobutyrate-2-oxoglutarate transaminase, and ectoine synthesase, respectively (Figure 4.6a) (Stoveken et al., 2011). Glutamate is another common osmolyte that can be increased as a counter-ion in cells in response to hyperosmotic stress (Burg and Ferraris, 2008).

Different transcription levels of ectoine synthesis genes in PD631S grown with or without 3% NaCl were observed. Interestingly, as shown in Figure 4.6b, the *ectA* expression level in saline grown PD631S was two-fold higher than that in the non-saline grown PD631S. The mRNA levels encoding *ectB* were slightly increased while the *ectC* expression level was slightly decreased in saline grown PD631S. Unlike those observed for ectoine synthesis genes, the expression levels of glutamate synthesis genes (i.e., mRNA levels encoding glutamate synthesis) in saline-grown PD631S were similar to those in non-saline grown PD631S (Figure 4.7), suggesting that glutamate might not play a key role in PD631S when grown under saline conditions. The gene expression levels for ectoine and glutamate synthesis proteins suggested that ectoine was the key osmolyte

produced in PD631S under high salts conditions. However, the reasons for the decreased expression levels of *ectC* are unclear and need to be further investigated.

(a)

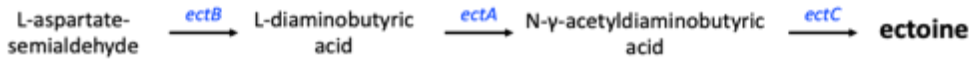

(b)

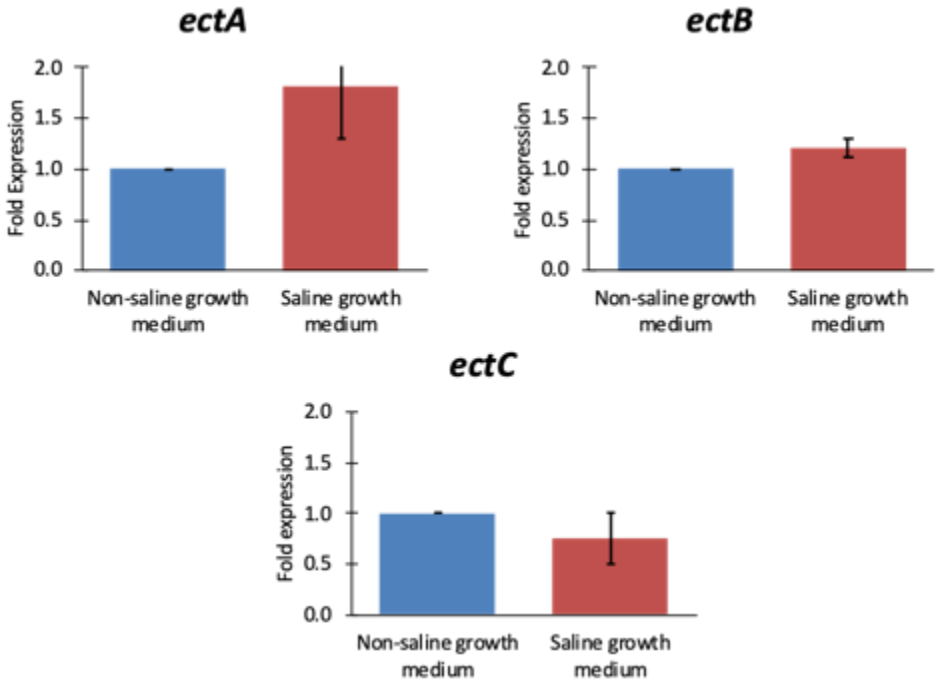

Figure 4.6. (a) Ectoine synthesis pathway starts from the conversion of L-asparate-semialdehyde to L-diaminobutyric acid, N-gama-acetyldiaminobutyric acid, and then to ectoine. The genes involved in the synthesis steps in this pathway are: *ectA* encoding diaminobutyric acid acetyltransferase, *ectB* encoding diaminobutyrate-2-oxoglutarate transaminase, and *ectC* encoding ectoine synthesis. (b) Salt effects on expression of three ectoine synthesis genes in strain PD631S. Blue bars: PD631S grown on glucose as a carbon source in non-saline AMS medium. Red bars: PD631S grown on glucose as a carbon source in AMS medium with 3% NaCl. All experiments were conducted in duplicate.

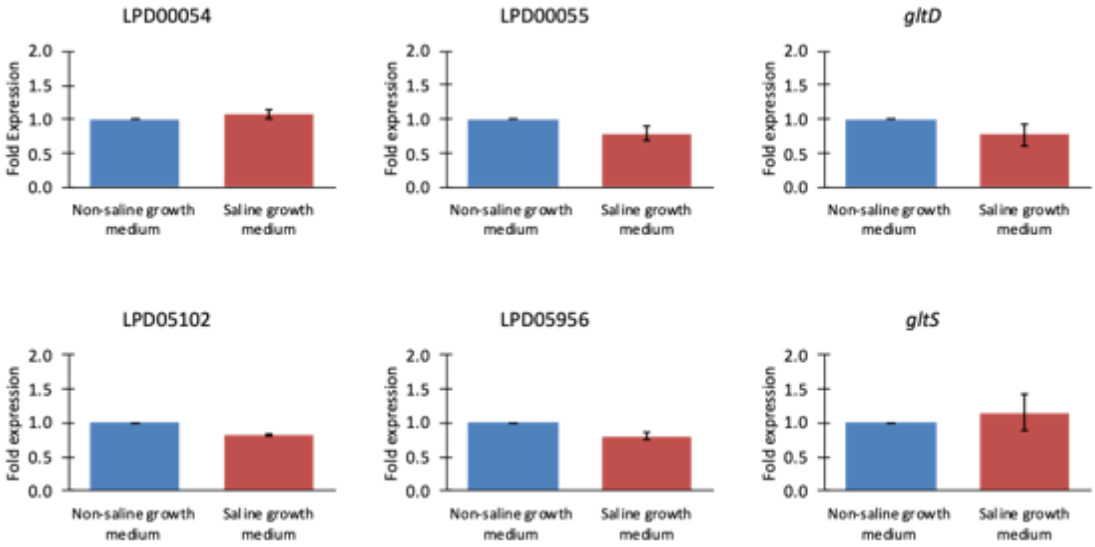

Figure 4.7. Salt effects on expression of six possible glutamate synthesis genes in strain PD631S. Blue bars: PD631S grown on glucose as a carbon source in non-saline AMS medium. Red bars: PD631S grown on glucose as a carbon source in AMS medium with 3% NaCl. All experiments were conducted in duplicate.

The effects of two cultivation variables, sterilization of growth medium and presence of 3% NaCl, on the growth of and TAG production by PD631 and PD631S (Figure 4.8, Table 4.4) were examined. In sterilized salt-free media, which is AMS media in the absence of 3% NaCl, PD631 produced 22.9 mg/L TAG under the conditions of the experiment; the addition of 3% NaCl reduced the production of TAG to 15 mg/L and significantly retarded the growth rate from 0.08 h^{-1} to 0.04 h^{-1}. The final optical density of PD631 in salt media was about two times lower than that of PD631 in salt-free media (Figure 4.8). Also, in the preliminary experiment, only inoculated PD631 from the saturated culture could grow with 3% NaCl while it could not grow directly from a single colony (data not shown). In contrast, the amounts of TAG production by PD631S in

sterilized salt-free media was slightly less (15.5 mg/L) but maintained its growth rate in the high salts as 0.05 h^{-1} from 0.06 h^{-1}.

(a)

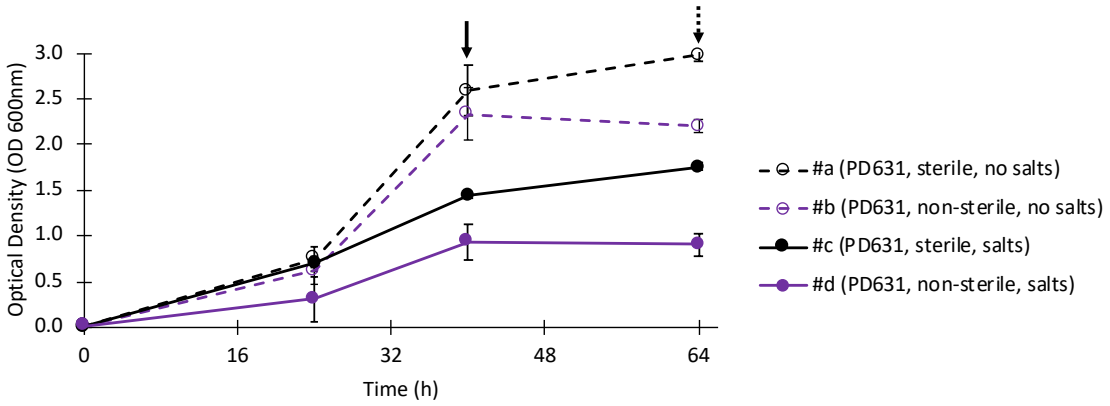

Figure 4.8. Production of TAGs from a newly developed salt-tolerant strain PD631 (PD631S) in non-sterile growth medium. (a) Cell growth curves of PD631 grown under different conditions as listed in Table 4.4. (b) TLC analysis of TAG distribution from PD631 grown under different conditions listed in Table 4.4. (c) Cell growth of PD631S grown under different conditions as listed in Table 4.4. (d) TLC analysis of TAG distribution from PD631S grown under different conditions listed in Table 4.4. Optical density was measured at 600 nm. The arrow indicates the point that cell culture was resuspended with carbon-rich and nitrogen-free medium. The dotted arrow indicates the point that the sample was collected for TAGs measurements. Glyceryl trioleate (TL) was used as standard and different quantities of TL, ranging from 1-100 μg (shown as numbers on the bottom of the Standard panel), were used to develop a calibration curve for estimating TAG. All experiments were conducted in duplicate. 1 and 2 represents duplicate samples of each tested condition.

(b)

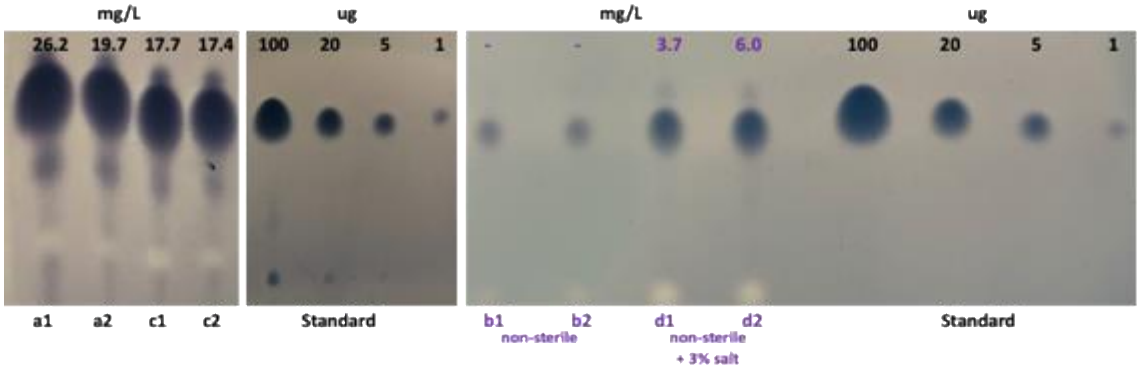

(c)

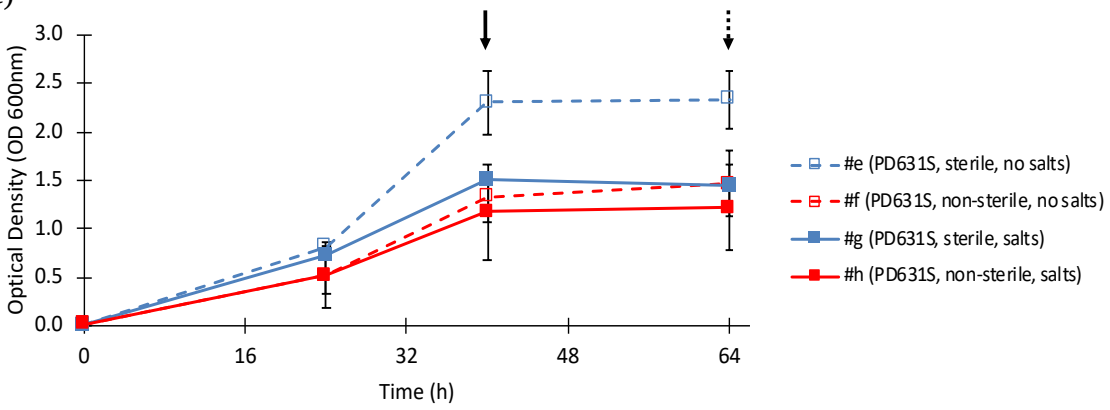

(d)

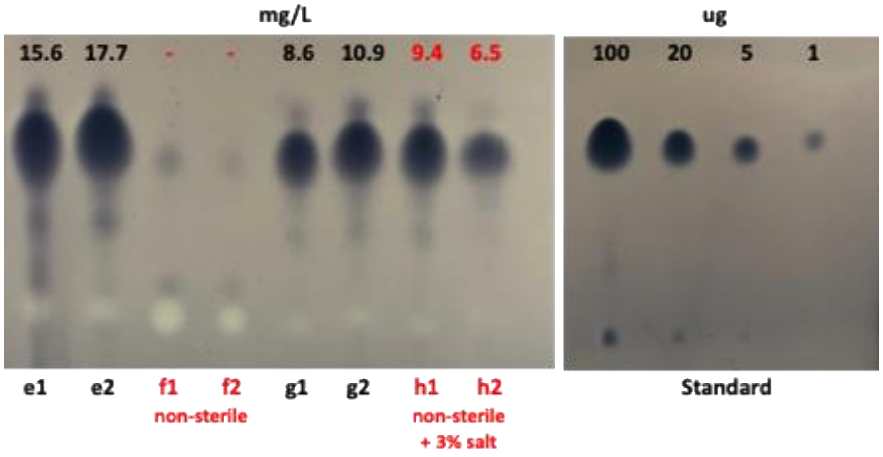

Figure 4.8. Continued.

Table 4.4. TAG production from PD631 or PD631S cultivated with 1% of glucose in AMS medium with or without salts under sterile or non-sterile conditions. All experiments were conducted in duplicate.

Experiment	Variables			Growth rate (h^{-1})	TAG (mg/L)	Total TAG mass (mg)
	Culture	% NaCl (w/v)	Sterilization			
# a	PD631	0	Yes	0.08	22.9 ± 4.6	1.2 ± 0.2
# b	PD631	0	No	0.08	0	0
# c	PD631	3	Yes	0.04	15.0 ± 0.4	0.8 ± 0.0
# d	PD631	3	No	0.07	4.9 ± 1.6	0.2 ± 0.1
# e	PD631S	0	Yes	0.06	15.5 ± 0.9	0.8 ± 0.0
# f	PD631S	0	No	0.06	0	0
# g	PD631S	3	Yes	0.05	9.8 ± 1.6	0.5 ± 0.1
# h	PD631S	3	No	0.05	8.0 ± 2.1	0.4 ± 0.1

The advantage of using PD631S for TAG production is that under non-sterile high salt conditions it is not necessary to sterilize the growth media to achieve efficient TAG accumulation. PD631S in non-sterilized salt media produced 8.0 mg/L TAGs (52% of that achieved in sterilized salt-free media) while PD631S in non-sterilized salt-free media did not produce any TAGs. In contrast, PD631 in non-sterilized salt media only produced 4.9 mg/L TAGs (22% of that achieved in sterilized salt-free media) while there was no TAGs production from PD631 in non-sterilized salt-free media. This indicates that PD631S showed a better ability to survive in non-sterilized salt media than PD631 due to adaptive evolution. Accordingly, PD631S can outcompete the growth of non-TAG-accumulating microorganism under high salt conditions. Generally, under 3% NaCl conditions, not many microorganisms can survive except halophilic bacteria (Ikeuchi et al., 2003). This reflects the ability of PD631S to maintain its normal growth rate in high salt, unlike the parental PD631 and other contaminating bacteria. Also, PD631S can be a

potential candidate for non-sterile TAGs production to reduce the overall costs and energy inputs for cultivation of TAG-accumulating bacteria.

4.4.4. Demonstration of cell lysis of PD631SpAHB and TAGs release from PD631SpAHB

Cell lysis of PD631SpAHB was confirmed based on decrease of cell density following induction with thiostrepton. As shown in Figure 4.9, in the absence of 3% NaCl, PD631SpAHB grew slower than those of PD631pTipQC2. When grown in saline medium, PD631SpAHB showed a long lag phase of 48 h. The long lag phase might be due to a hyperosmotic pressure to the strain, as the strain might need to adapt to sudden change from non-saline to saline conditions. After addition of thiostrepton (1 μg/mL) at 28 h (Figure 4.9), PD631pTipQC2 continued to grow up to an optical density of 2.5. However, 6 h after induction with thiostrepton (1 μg/mL), the optical density of PD631SpAHB (regardless of the cultivation conditions) decreased from 0.8 to 0.3. The decrease of optical density after induction was similar to those observed in the induction experiments using PD631pAHB (Figure 4.4a). Also, after overnight induction, cell debris of PD631SpAHB were found in the cell culture (data not shown). Phage lysis proteins in the supernatants of induced PD631SpAHB were also observed on SDS-PAGE gels (Figure 4.10), providing evidence that phage lysis proteins produced in PD631SpAHB caused cell lysis. Similar to the SDS-PAGE results of induced PD631pAHB, Figure 4.10 shows overexpression of LysA and expression of Holin and LysB in induced PD631SpAHB. Overall, the results showed that cell lysis of PD631SpAHB can be

effectively controlled by expressing the phage lytic gene cassette at the desired time, preferably after cells have accumulated a high level of TAGs.

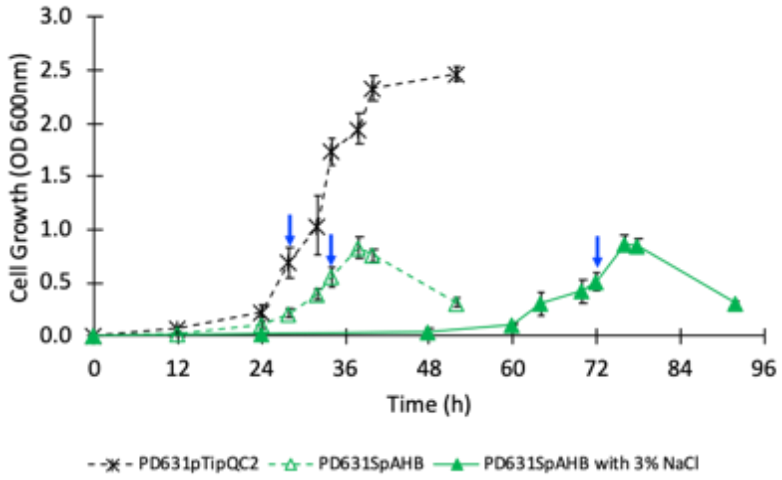

Figure 4.9. Delayed growth of PD631SpAHB in saline growth was observed. Inducible lysis of PD631SpAHB grown in either non-saline or saline medium was observed, based on decrease of optical density 6 h following addition of thiostrepton (an inducer). PD631pTipQC2 was used as a control. Blue arrows indicate the time point in the OD_{600} = 0.5 - 0.7, growth stage where 1 µg/mL of thiostrepton was added to induce expression of phage lytic genes. All experiments were conducted in duplicate.

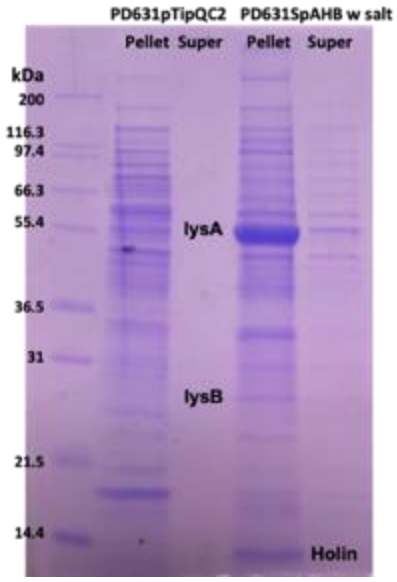

Figure 4.10. SDS-PAGE analysis of phage lytic proteins expressed in PD631SpAHB with 3% NaCl. PD631pTipQC2 was used as a negative control. Mark12 Unstained Standard used as a protein ladder.

The effects of the phage lytic gene cassette on cell growth, TAG production, and TAG release of PD631SpAHB were examined and are summarized in Table 4.5 and Figure 4.11. PD631pTipQC2 in sterilized salt-free media was used as a control. In sterilized media, PD631SpAHB produced similar amounts of total TAG with that from PD631pTipQC2, but slightly decreased the growth rate to 0.15 h^{-1} in salt media and 0.10 h^{-1} in salt-free media.

TAG was produced by PD631SpAHB in non-sterilized salt media up to 17.6 mg/L while PD631SpAHB in non-sterilized salt-free media did not produce TAG. After adding additional nitrogen source and inducer, PD631SpAHB showed the decreased optical density except PD631SpAHB in non-sterilized salt-free media, suggesting that cell lysis occurred by the expression of phage lytic genes while PD631pTipQC2 could grow up to 3.5 of optical density. Also, 21-38% of the total TAGs were released from PD631SpAHB in sterilized media to the supernatant after the induction of phage lysis proteins while only 6% of the total TAGs were released from PD631SpAHB in non-sterilized salt media. Our results were similar to previous finding that about 30% of the total TAGs were released in the phage infected PD631 culture (Gill et al., 2018). Different from the bacteriophage approach, the timing of cell lysis can be controlled and there is no need to prepare an additional phage culture for infection. However, TLC analysis revealed that most TAGs were still not released into the supernatant but associated with pellet of cell debris, suggesting that TAG granules are trapped with the cell debris or TAGs are attached on the cell membranes (Gill et al., 2018).

Table 4.5. Non-sterile cultivation, TAG production, and TAG release from PD631SpAHB with different growth conditions. All experiments were conducted in AMS medium with 1% of glucose as a carbon source.

Experiment	Variables			Growth rate (h^{-1})	Total TAG (mg/L)	TAG in pallet (mg/L)	Released TAG* (mg/L)
	Culture	% NaCl (w/w)	Sterilization				
i	PD631pTipQC2	0	Yes	0.19	24.2	24.2	0
ii	PD631SpAHB	3	Yes	0.15	24.7	19.4	5.3
iii	PD631SpAHB	0	Yes	0.10	24.2	15.1	9.1
iv	PD631SpAHB	0	No	0.24	0	0	0
v	PD631SpAHB	3	No	0.13	17.6	16.7	0.9

* Released TAG were detected in the supernatant of each culture.

(a)

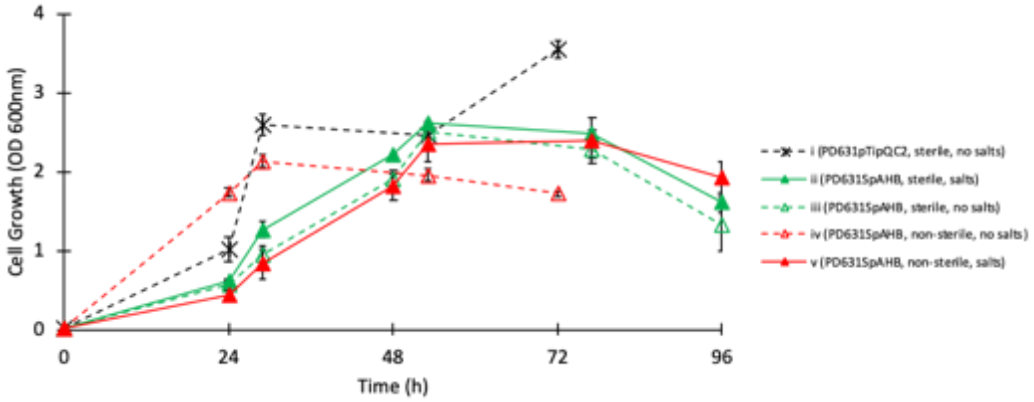

Figure 4.11. Non-sterile cultivation of PD631SpAHB and extraction of TAGs from the TAG-filled PD631SpAHB. (a) Cell growth of PD631pTipQC2 and PD631SpAHB grown in the different conditions. Detailed each condition was shown in Table 4.5. Optical density was measured at 600 nm. The cell culture over 2.0 of optical density was resuspended with carbon-rich and nitrogen-free medium. After 24 h, 1 μg/mL of thiostrepton and additional nitrogen source were added for expression of phage lytic gene cassette. (b) TLC analysis of TAG distribution from each condition (left panel). TL was used as a standard, ranging from 1-100 ug (right panel). All experiments were conducted in duplicate. P stands for the cell pellet and S stands for the supernatant.

(b)

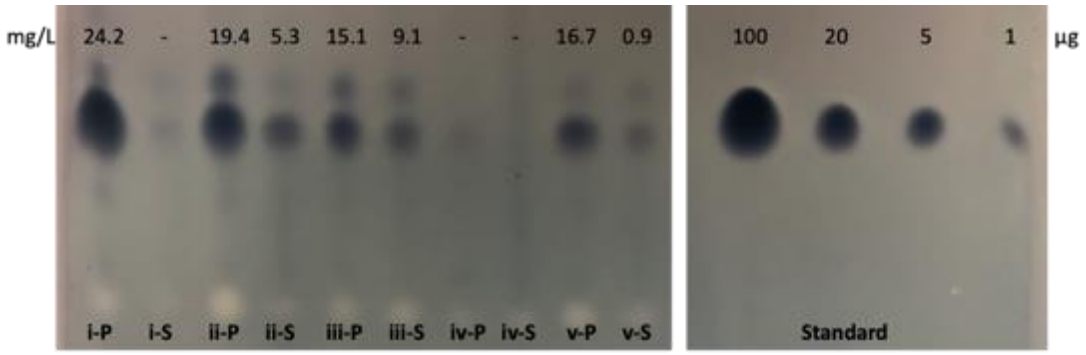

Figure 4.11. Continued.

The lysis results and TAG production suggest that PD631SpAHB as a promising candidate for the non-sterile cultivation for TAGs production and extraction. Given that sterilization cost generally accounts for 16.4% of the total energy costs per liter of biolipid-based biofuels (Soccol et al., 2017), the total TAG production cost can be reduced substantially by cultivating PD631SpAHB in non-sterilized high salt media. This new phage-lytic-protein-based approach to release of TAGs has several advantages compared to traditional solvent extraction, such as no concerns of solvent toxicity and no additional energy inputs for cell disruption step (Harris et al., 2018; Lee et al., 2017). Nevertheless, future studies are needed to optimize the condition for expression of phage lytic genes in order to maximize the overall TAGs yield in the supernatant.

4.5. Conclusions

This study has successfully demonstrated production and release of TAGs from non-sterile growth medium using a newly developed salt-tolerant PD631SpAHB. The

inducible phage lytic gene cassette plasmid (pAHB) enabled lysis of TAG-filled PD631SpAHB to release TAGs into liquid medium. This technique offers a new means for biolipid extraction, potentially leading to a reduction of overall extraction costs of biolipid for biofuel production. Overall, our results indicate that this new strain PD631SpAHB is a promising candidate to address the two major challenges – high costs associated with sterilization cultivation and TAGs extraction – of current biolipid-based biofuel production.

4.6. References

Alvarez, H.M., Kalscheuer, R. and Steinbuchel, A. 2000. Accumulation and mobilization of storage lipids by *Rhodococcus opacus* PD630 and *Rhodococcus ruber* NCIMB 40126. Appl Microbiol Biotechnol 54, 218-223.

Alvarez, H.M. and Steinbüchel, A. 2002. Triacylglycerols in prokaryotic microorganisms. Appl Microbiol Biotechnol 60(4), 367-376.

Amara, S., Seghezzi, N., Otani, H., Diaz-Salazar, C., Liu, J. and Eltis, L.D. 2016. Characterization of key triacylglycerol biosynthesis processes in *rhodococci*. Scientific Reports 6, 24985.

Asiri, F., Chen, C.H., Hwangbo, M., Shao, Y. and Chu, K.H. 2020. From organic wastes to bioplastics: Feasibility of non-sterile polyhydroxybutylate (PHB) production by *Zobellella denitrificans* ZD1. ACS Omega. *In revision*.

Berrow, N.S., Bussow, K., Coutard, B., Diprose, J., Ekberg, M., Folkers, G.E., Levy, N., Lieu, V., Owens, R.J., Peleg, Y., Pinaglia, C., Quevillon-Cheruel, S., Salim, L., Scheich, C., Vincentelli, R. and Busso, D. 2006. Recombinant protein expression and solubility screening in *Escherichia coli*: a comparative study. Acta Crystallogr D Biol Crystallogr 62, 1218-1226.

Burg, M.B. and Ferraris, J.D. 2008. Intracellular organic osmolytes: Function and regulation. J Biol Chem 283(12), 7309-7313.

Cahill, J. and Young, R. 2019. Phage lysis: Multiple genes for multiple barriers. Adv Virus Res 103, 33-70.

Davila Costa, J.S., Silva, R.A., Leichert, L. and Alvarez, H.M. 2017. Proteome analysis reveals differential expression of proteins involved in triacylglycerol accumulation by *Rhodococcus jostii* RHA1 after addition of methyl viologen. Microbiology 163(3), 343-354.

EPA 2018 Biofuels and the Environment. Development, U.S.E.P.A.O.o.R.a. (ed), Washington, DC.

Gill, J.J., Wang, B., Sestak, E., Young, R. and Chu, K.H. 2018. Characterization of a novel *tectivirus* phage Toil and its potential as an agent for biolipid extraction. Scientific Reports 8(1), 1062.

Gujjala, L.K.S., Kumar, S.P.J., Talukdar, B., Dash, A., Kumar, S., Sherpa, K.C. and Banerjee, R. 2019. Biodiesel from oleaginous microbes: Opportunities and challenges. Biofuels 10(1), 45-59.

Hand, S., Gill, J. and Chu, K.H. 2016. Phage-based extraction of polyhydroxybutyrate (PHB) produced from synthetic crude glycerol. Science of the Total Environment 557-558, 317-321.

Hand, S., Wang, B. and Chu, K.H. 2015. Biodegradation of 1,4-dioxane: effects of enzyme inducers and trichloroethylene. Science of the Total Environment 520, 154-159.

Harris, J., Viner, K., Champagne, P. and Jessop, P.G. 2018. Advances in microalgal lipid extraction for biofuel production: A review. Biofuels, Bioproducts and Biorefining 12(6), 1118-1135.

Henein, A.E., Hanlon, G.W., Cooper, C.J., Denyer, S.P. and Maillard, J.Y. 2016. A Partially Purified *Acinetobacter baumannii* Phage Preparation Exhibits no Cytotoxicity in 3T3 Mouse Fibroblast Cells. Front Microbiol 7, 1198.

Hwangbo, M. and Chu, K.H. 2020. Recent advances in production and extraction of bacterial lipids for biofuel production. Science of the Total Environment. 734, 139420.

Ikeuchi, T., Ishida, A., Tajifi, M. and Nagata, S. 2003. Induction of salt tolerance in *Bacillus subtilis* IFO 3025. J. Biosci. Bioeng. 96, 184-186.

Kan, J., Peng, T., Huang, T., Xiong, G. and Hu, Z. 2020. NarL, a novel repressor for CYP108j1 expression during PAHs degradation in *Rhodococcus* sp. P14. Int J Mol Sci 21(3).

Kim, M.Y., Kim, J.K., Lee, M.E., Lee, S.H. and Choi, M.K. 2017. Maximizing biojet fuel production from triglyceride: Importance of the hydrocracking catalyst and separate deoxygenation/hydrocracking steps. ACS Catalysis 7(9), 6256-6267.

Kuhlmann, A.U. and Bremer, E. 2002. Osmotically regulated synthesis of the compatible solute ectoine in *Bacillus pasteurii* and related *Bacillus* spp. Appl Environ Microbiol 68(2), 772-783.

Lang, Y.J., Bai, L., Ren, Y.N., Zhang, L.H. and Nagata, S. 2011. Production of ectoine through a combined process that uses both growing and resting cells of *Halomonas salina* DSM 5928T. Extremophiles 15(2), 303-310.

Lee, S.Y., Cho, J.M., Chang, Y.K. and Oh, Y.K. 2017. Cell disruption and lipid extraction for microalgal biorefineries: A review. Bioresour Technol 244, 1317-1328.

Ma, J., Campbell, A. and Karlin, S. 2002. Correlations between Shine-Dalgarno sequences and gene features such as predicted expression levels and operon structures. J Bacteriol 184(20), 5733-5745.

Madkour, M.H., Heinrich, D., Alghamdi, M.A., Shabbaj, I.I. and Steinbuchel, A. 2013. PHA recovery from biomass. Biomacromolecules 14(9), 2963-2672.

Nakashima, N. and Tamura, T. 2004. Isolation and characterization of a rolling-circle-type plasmid from *Rhodococcus erythropolis* and application of the plasmid to multiple-recombinant-protein expression. Applied and Environmental Microbiology 70(9), 5557-5568.

Patel, A., Mikes, F. and Matsakas, L. 2018. An overview of current pretreatment methods used to improve lipid extraction from oleaginous microorganisms. Molecules 23(7).

Pires, D.P., Cleto, S., Sillankorva, S., Azeredo, J. and Lu, T.K. 2016. Genetically engineered phages: A review of advances over the last decade. Microbiology and Molecular Biology Reviews 80(3), 523-543.

Rahmanpour, R. and Bugg, T.D. 2013. Assembly in vitro of *Rhodococcus jostii* RHA1 encapsulin and peroxidase DypB to form a nanocompartment. The FEBS Journal 280(9), 2097-2104.

Ren, X., Zhao, X., Turcotte, F., Deschenes, J.S., Tremblay, R. and Jolicoeur, M. 2017. Current lipid extraction methods are significantly enhanced adding a water treatment step in *Chlorella protothecoides*. Microbial Cell Factories 16(1), 26.

Santamauro, F., Whiffin, F.M., Scott, R.J. and Chuck, C.J. 2014. Low-cost lipid production by an oleaginous yeast cultured in non-sterile conditions using model waste resources. Biotechnology for Biofuels 7, 34.

Soccol, C.R., Neto, C.J.D., Soccol, V.T., Sydney, E.B., da Costa, E.S.F., Medeiros, A.B.P. and Vandenberghe, L.P.S. 2017. Pilot scale biodiesel production from microbial oil of *Rhodosporidium toruloides* DEBB 5533 using sugarcane juice: Performance in diesel engine and preliminary economic study. Bioresour Technol 223, 259-268.

Stoveken, N., Pittelkow, M., Sinner, T., Jensen, R.A., Heider, J. and Bremer, E. 2011. A specialized aspartokinase enhances the biosynthesis of the osmoprotectants ectoine and hydroxyectoine in *Pseudomonas stutzeri* A1501. J Bacteriol 193(17), 4456-4468.

Tan, D., Xue, Y.S., Aibaidula, G. and Chen, G.Q. 2011. Unsterile and continuous production of polyhydroxybutyrate by *Halomonas* TD01. Bioresour Technol 102(17), 8130-8136.

Tanimura, A., Takashima, M., Sugita, T., Endoh, R., Kikukawa, M., Yamaguchi, S., Sakuradani, E., Ogawa, J., Ohkuma, M. and Shima, J. 2014. *Cryptococcus terricola* is a promising oleaginous yeast for biodiesel production from starch through consolidated bioprocessing. Sci Rep 4, 4776.

Vimberg, V., Tats, A., Remm, M. and Tenson, T. 2007. Translation initiation region sequence preferences in *Escherichia coli*. BMC Mol Biol 8, 100.

Wang, B., Rezenom, Y.H., Cho, K.C., Tran, J.L., Lee, D.G., Russell, D.H., Gill, J.J., Young, R. and Chu, K.H. 2014. Cultivation of lipid-producing bacteria with lignocellulosic biomass: effects of inhibitory compounds of lignocellulosic hydrolysates. Bioresour Technol 161, 162-170.

Wu, Y.W., Yang, S.H., Hwangbo, M. and Chu, K.H. 2019. Analysis of *Zobellella denitrificans* ZD1 draft genome: Genes and gene clusters responsible for high polyhydroxybutyrate (PHB) production from glycerol under saline conditions and its CRISPR-Cas system. PLoS One 14(9), e0222143.

Young, R. 2014. Phage lysis: three steps, three choices, one outcome. J Microbiol 52(3), 243-258.

Yue, H., Ling, C., Yang, T., Chen, X., Chen, Y., Deng, H., Wu, Q., Chen, J. and Chen, G.Q. 2014. A seawater-based open and continuous process for polyhydroxyalkanoates production by recombinant *Halomonas campaniensis* LS21 grown in mixed substrates. Biotechnology for Biofuels 7, 108.

5. DEVELOPEMENT OF NOVEL PROPHAGE-BASED MICROBIAL FACTORY FOR PRODUCTION AND RELEASE OF HIGH TITERS OF LIGNIN PEROXIDASE FOR LIGNOCELLULOSE DEPOLYMERIZATION

5.1. Summary

Lignocellulose is a renewable material for biofuels production. Due to a complex structure of lignocellulose, a pretreatment step of lignocellulose to deconstruct lignin is a necessity. However, current physical/chemical pretreatments are costly and inefficient. While effective lignin depolymerization can be achieved using lignin-modifying enzymes such as lignin peroxidase, commercial enzymes are expensive and production of high titers of the enzymes are challenging. This study investigated the possibility of genome editing of the prophage Mushu4 inside the genome of *Rhodococcus opacus* M213 to produce and release lignin peroxidase in large quantities as a step moving forward the development of a cost-effective biological method for lignin depolymerization. Two homologous recombination approaches, an exogenous recombination system relied on a pair of phage recombinases or natural selection during DNA replication relied on recombinases of Mushu4, were explored to develop engineered Mushu4. The genome annotation of prophage Mushu4 was first conducted to identify its major capsid protein gene as a target site for replacement of lignin peroxidase gene. Results of the first approach showed frequent occurrences of illegitimate insertion (i.e., off-target insertions), and frequent spontaneous deletion of recombinase genes during purification, leading to unsuccessful recombineering. The second approach of homologous recombination was not completed

in part due to the low spontaneous induction rate of Mushu4 from *R. opacus* M213. Although the homologous recombination approaches were not successful at this point, this study reports the first attempt to edit a *Rhodococcus* prophage genome to explore its potential in producing and releasing large quantity of desired enzymes production and release for lignin depolymerization. Overall, the results provide the fundamental knowledge that can be used to further developing prophage harboring *Rhodococcus* as an efficient microbial factory for lignases production and release.

5.2. Introduction

Lignocellulosic biomass is the most abundant renewable material for biofuels and bioproducts production (Billion-Ton, 2016). Lignocellulosic biomass consists of three different polymers: 40-50% of cellulose, 25-30% of hemicellulose, and 15-25% of lignin (Kumar et al., 2009). Lignin is a complex phenolic alcohol-based polymer, which protects two sugar polymers of cellulose and hemicellulose. Due to the complex structure of lignocellulose, a physical/chemical pretreatment to deconstruct lignin followed by a enzymatic hydrolysis of the sugar polymers to release sugars for biofuel production is commonly practiced (Hwangbo et al., 2019; Nlewem and Thrash, 2010; Wang et al., 2014). However, current physical/chemical pretreatments are costly and inefficient due to high energy requirement, toxic chemicals used for lignin removal, and production of inhibitory compounds in lignocellulosic hydrolysates that have been shown to affect growth of biofuel-producing microorganisms (Sun et al., 2016).

Biological pretreatment using ligninolytic microorganisms or lignin-modifying enzymes including lignin peroxidase, manganese peroxidases, and laccase, to degrade lignin can be an attractive alternative to reduce energy costs and toxicity issues associated with physical/chemical pretreatment methods. Lignin peroxidases are known to depolymerize lignin structure efficiently and they can be produced by wild-type ligninolytic enzyme-producing microorganisms (Sun et al., 2016). However, the low production yield of the lignin peroxidase from microorganisms is critical obstacle to apply the enzyme to lignocellulose pretreatment (Chan et al., 2019). Also, the availability of commercial lignin peroxidase is low, and the price is high expensive (Plácido and Capareda, 2015). Therefore, mass production of the enzyme is required for an efficient pretreatment of lignocellulose.

Various research attempts, ranging from using inducible plasmids to genetically modified microorganisms, to increase lignin peroxidase production have been reported (Lambertz et al., 2016). More recently, lignin peroxidase can be produced in quantity from engineered *E. coli* carrying an inducible plasmid with a fungal lignin peroxidase gene (Miki et al., 2010; Santos et al., 2014) or with a bacterial lignin peroxidase gene (Miki et al., 2010; Santos et al., 2014). However, an additional chemical is required to induce over-expression of the enzyme in the engineered *E. coli* strains and a follow-up harvest step is needed to recover the produced enzymes after cell lysis. Therefore, a simple and efficient approach to produce lignin peroxidase in quantity is favorable and needed. To this end, this study explored a new prophase-based technology to produce and release lignin peroxidase in culture medium for effective lignin depolymerization.

Method development and rationale

Genetically modified bacterial strains for production of desired enzymes can be achieved by introducing an inducible plasmid carrying genes of interested or inserting/replacing the target gene fragment inside its bacterial genome. However, the expression level of the target gene is typically limited by copy numbers of plasmids or strength of a transcriptional promoter (Carey et al., 2013; Fakruddin et al., 2013), a major factor limiting the yield of desired enzymes (Carrier et al., 1983). Accordingly, a new way to increase expression level is important to increase yield of desired enzymes.

Bacteriophages (phages) are viruses that only infect bacteria. Virulent phages only follow the lytic cycle during infection, causing lysis of host cells. The expression level of phage particles during its lytic cycle is generally high (Doss et al., 2017; Young et al., 2000). Especially, a major capsid protein (MCP) gene of phage is a highly expressed gene during the lytic cycle, which is normally generated 415 copies per phage containing 30-60 kb genome (Conway et al., 2007; Dunn and Studier, 1983). Temperate phages, unlike virulent phages, integrate their genomes into the chromosome of host cells and can be induced to enter the lytic cycle after multiple generations; the integrated form of the phages is called a prophage. Some temperate phages reenter the lytic cycle when host cell is subject to specific environmental stressful signals such as UV light or antibiotics (mitomycin C) (Doss et al., 2017). Prophages can make up 10-20% of a bacterial genome (Casjens, 2003). The prophage, which is in a bacterial chromosome, can be a suitable candidate for enzyme production due to its potentially high expression level. Accordingly, the genome of prophage can be edited on the bacterial genome, and then engineered

prophage can be induced by specific signals or engineered to induce at a high level constitutively.

Prophage Mushu4, found in the genome of *Rhodococcus opacus* M213 (referred as M213 hereafter), was isolated recently and propagated on *R. opacus* DSM43205 (referred as DSM43205 hereafter) (Wang, 2016). Unlike other common prophages, Mushu4 can be induced spontaneously from a stationary phase culture of M213 without additional energy input (Wang, 2016). Therefore, the selection of MCP gene of Mushu4 as the target site is an efficient way to produce lignin peroxidase because it can be expressed at a high rate from an engineered Mushu4 without an inducer.

In this study, the possibility of engineering prophage DNA on the genome of strain M213 was investigated. We hypothesize that lignin peroxidase can be produced in high quantity from engineered prophage Mushu4 by substituting an MCP gene via homologous recombination. To do this, the MCP gene of Mushu4 was firstly identified by genome annotation of Mushu4 and the characteristics of Mushu4 were recognized. This study is the first trial to edit the prophage genome of *Rhodococcus* by homologous recombination and these two approaches provide the basis of further development of *Rhodococcus* as an efficient and cheaper tool for the pretreatment of lignocellulose.

Proposed prophage engineering approaches

Homologous recombination is a traditional way to edit a bacterial genome. The method relies on recombinases to facilitate insertion of an integration cassette - generally consisting of homologous arms (flanking regions of target site), an inserted gene, and a

selective marker- into the bacterial genome (Capecchi, 1989; Kirchner and Tauch, 2003). However, recombination frequently occurs in an incorrect location of the genome of *Rhodococcus* (illegitimate integration) (DeLorenzo et al., 2018; Desomer et al., 1991). To overcome the illegitimate integration, an improved recombineering strategy using a pair of phage recombinases (an exogenous recombination system) in *R. opacus* PD630 has been recently developed (DeLorenzo et al., 2018). The pair of phage recombinases, Che9c60 and Che9c61 (GC-rich homologs of RecE and RecT) are an exonuclease to create a single-stranded DNA and a single strand DNA binding protein to assist invasion and exchange of DNA strand, respectively. These two recombinases can facilitate double homologous recombination in the correct location (Liang et al., 2020; van Kessel and Hatfull, 2007). Although the exogenous recombination system has been demonstrated in a neutral integration site of *Rhodococcus*, this system has not been applied nor verified in the prophage genome in the *Rhodococcus*. It is also known that prophage generally has its own recombinases to facilitate homology-dependent recombination at a high rate during its DNA replication step when entering lytic cycle in the host bacterium. Therefore, site-specific integration can be occurred at the DNA replication step if the integration cassette exists.

Accordingly, two experimental approaches are used to create engineered prophage Mushu4 in M213 or in DSM43205 lysogen (Figure 5.1). The first approach, as shown in Figure 5.1a, relies on exogenous recombination system for site-directed swapping of the Mushu4 MCP region with a desired gene fragment (in this case is a gene sequence encoding lignin peroxidase gene (*dypB*) and a selection marker gene (gentamycin, Gen))

by using a pair of phage recombinases, Che9c60 and Che9c61. This homologous recombination at the desired site might be facilitated by the expression of this pair of recombinases using a constitutive plasmid that is electroporated into host strain M213.

The second approach relies on the natural recombination processes of phage Mushu4 during spontaneous induction of Mushu4 in M213 and the desired recombinant of prophage Mushu4 is then used to lysogenize the host strain DSM43205 (Figure 5.1.b). We hypothesized that homologous recombination can be facilitated by the recombinases of prophage Mushu4 during its spontaneous induction. In the presence of a plasmid containing the inserted cassette, homologous recombination at a desired site also can occur by Mush4's own recombinases of during its lytic cycle. Accordingly, after spontaneous induction, there would be many phage particles containing wile type Mushu4 DNA and a small number containing the engineered Mushu4 DNA. The induced prophage is used to lysogenize the host strain DSM43205 to produce DSM43205 (ENMushu4). Then, the lysogen containing engineered Mushu4 DNA can be only selected on the agar with gentamycin as a marker.

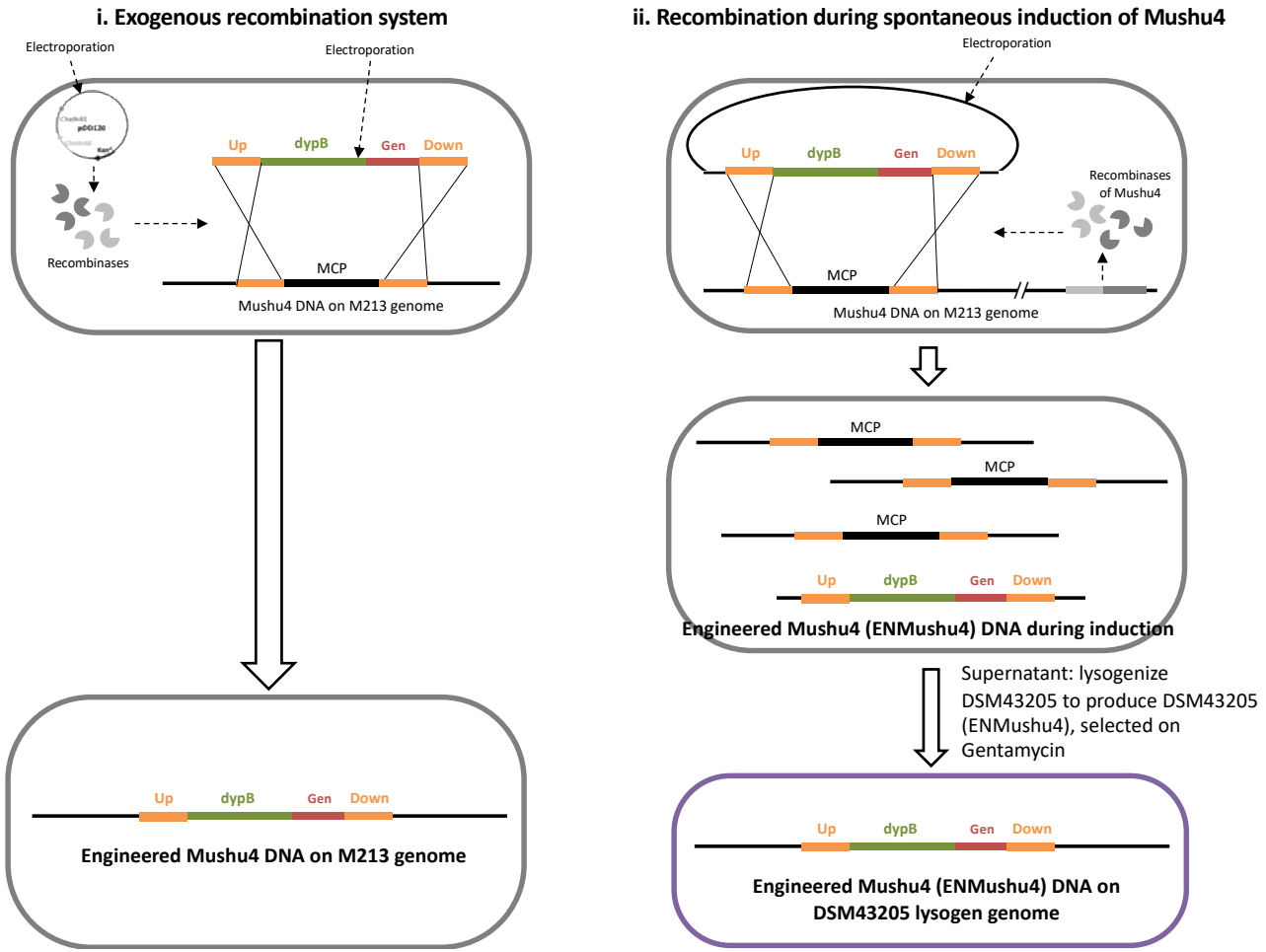

Figure 5.1. Experimental approaches of this study. Recombinases: two different phage recombinases. MCP: major capsid protein gene of Mushu4. Up and Down: upstream and downstream region of MCP. Gen: a gentamicin resistance gene cassette. dypB: a lignin peroxidase gene.

5.3. Materials and Methods

5.3.1. Chemicals, strains, and culture conditions

Imperial™ protein stain, kanamycin, and gentamicin were purchased from Fisher Scientific (Hampton, NH, USA). Reasoner's 2A (R2A) broth was purchased from Teknova (Hollister, CA, USA) and all other mediums such as R2A agar, Luria-Bertani (LB) broth, and LB agar were purchased from VWR (Radnor, PA, USA). All other chemicals used in this study were purchased from Millipore Sigma (Burlington, MA, USA). Strain M213 and *R. jostii* RHA1 (referred as RHA1 hereafter) were kindly provided by Dr. Andrew Ogram, University of Florida (Gainesville, FL) and Dr. Robert Steffan, CB&I (Lawrenceville, NJ), respectively. Strain DSM43205 was purchased from DSMZ, Germany. All *Rhodococcus* strains were cultured aerobically at 200 rpm at 30 °C in R2A broth medium.

5.3.2. Phage Mushu4 DNA preparation, sequencing, genome annotation, and induction

The genomic DNA of phage Mushu4 was previously prepared and sequenced in our previous study (Wang, 2016). For comprehensive genome annotation, genes were predicted using annotation tools (see Appendix A for details). Experiments were conducted to determine the titer of spontaneous induction of phage Mushu4 from strain M213. Briefly, strain M213 was cultured in R2A broth medium at 30 ℃ at 200 rpm up to stationary phase as measured by the optical density (OD_{600}), and the supernatant was separated from the cells by centrifugation at 10,000 g, at 4 ºC for 10 minutes. The

supernatant was filter-sterilized and then used to propagate on DSM43205. The plaque numbers on the DSM43205 plates were determined to confirm the spontaneous induction titers of phage Mushu4. High titers of spontaneous induction of Mushu4 from strain M213 were observed when mitomycin C (MitC) was added in an exponential phase culture of M213. See Appendix B for details.

5.3.3. Plasmid construction

Lignin peroxidase (dypB) for degradation of lignin was derived from RHA1. The information of the gene was summarized in Table 5.1. A gentamicin resistance gene cassette (Gen) was derived from plasmid pBAD24g, which was kindly provided by Dr. Jason J. Gill, Texas A&M University (College Station, TX). All other plasmids used in this study was listed in Table 5.2.

Table 5.1. List of genes used in this study.

Gene	Enzyme	Origin	Size (kB)
dypB	Lignin Peroxidase	*Rhodococcus jostii* RHA1	1.1
Gen	Gentamycin resistance gene cassette	Plasmid pBAD24g	0.6

Table 5.2. List of plasmids used in this study.

Plasmid name	Insert	Backbone	Antibiotic resistance	Length (bp)	Source
pET11a	Empty backbone	pET11a	Ampicillin	5677	Center for Phage Technology (CPT) at Texas A&M University (College Station, TX)
pET11a-Up-dypB	Up, dypB	pET11a	Ampicillin	6919	This study
pET11a-Up-dypB-Gen-Down	Up, dypB, Gen, Down	pET11a	Ampicillin, Gentamycin	8057	This study
pTipQC2	Empty backbone	pTipQC2	Chloramphenicol	8388	AIST Japan (Tokyo, Japan)
pTipQC2-Up-dypB-Gen-Down	Up, dypB, Gen, Down	pTipQC2	Chloramphenicol, Gentamycin	11037	This study
pDD120	Empty backbone	pDD120	Kanamycin	6247	Addgene (Watertown, MA)

(i) Construction of pET11a-Up-dypB-Gen-Down, a plasmid with a desired gene cassette

An integration cassette consisting of lignin peroxidase (*dypB*), gentamicin resistance gene cassette (Gen), and homologous arms (Up and Down) which are 500 bp regions up- and downstream of the MCP gene of Mushu4 were first constructed using Gibson Assembly HiFi 1-Step Kit (SGIDNA, San Diego, CA). RHA1 and M213 were grown in R2A medium at 30 °C for 36 hours and used for DNA extraction. Their genomic DNA were extracted using FastDNA SPIN KIT (MP Biomedicals, Santa Ana, CA). The extracted DNA and pBAD24g were used as templates for PCR amplification of desired gene fragments: dypB, Gen, and homologous arms (Up and Down). Table 5.3 lists the PCR primers used for producing these PCR products.

A 25-μL PCR reaction mixture included 12.5 μL of 2X PCR Master Mix (Promega, Madison, WI), 1 μL of template DNA, 1 μL each of 10 μM forward and reverse

primers, and 9.5 μL of nuclease-free water. PCR reaction was carried out by denaturing at 98 °C for 2 minutes, followed by 35 cycles at 98 °C for 10 seconds, 60 °C for 15 seconds, and 72 °C for 1 minute (*dypB*), 30 seconds (up- and downstream of MCP), or 36 seconds (Gen), with final incubation at 72 °C for 10 minutes for final extension.

Table 5.3. Primer sets used in the cloning work for Gibson Assembly. All primers were designed by primer design tool for Gibson Assembly. Up and Down is up- and downstream of a major capsid protein (MCP) gene of Mushu4. Gen is a gentamicin resistance gene cassette.

Primer name	Sequence (5' -> 3')	Primer length (bp)	Melting temperature (°C)	Expected PCR product size (kb)
Up_FW	AAATAATTTTGTTTAACTTTAAGAAGGAGATATAC ATATGTCAAGAACTGGAGCATCTGA	60	66	0.5
Up_RV	CTTGTGGTGCCAATCTCGCGACTGGGCCTGGCATC CATGGGAGTGTTCCTTTCTTTCAGT	60	78	
dypB_FW	CCATGGATGCCAGGCCCAGT	20	64	1.0
dypB_RV	CAAGAATTCTCATGTTTGACAGCTTATCATCGATA AGCTTGAGCTCTCATTGCGATACTC	60	70	
Gen_FW	GAAAATCGGTGGTCTCAAAGGAGTATCGCAATGA GAGCTCTTAGGTGGCGGTACTTGGGT	60	75	0.6
Gen_RV	TGATCGAACTGGTCCGCGACCAGCACGTACTCAGT CACGACCCGGGTTTGTTTATTTTTC	60	76	
Down_FW	TCGTGACTGAGTACGTGCTG	20	58	0.5
Down_RV	CAAGAATTCTCATGTTTGACAGCTTATCATCGATA AGCTTCGGATCTCGTTGTCGACGGG	60	72	

Four PCR products of Upstream (Up), *dypB*, Downstream (Down), and Gen, were clearly observed as a band of 0.5 kb, 1.0 kb, 0.5 kb, and 0.6 kb, respectively, on the agarose gel (Figure 5.2). The PCR products were then purified by QiAquick Gel Extraction Kit (Qiagen, Hilden, Germany) and used for assembly. The PCR products of Up and *dypB* were firstly assembled into pET11a plasmid between the NdeI-HindIII sites to construct the recombinant plasmid, pET11a-Up-dypB. Each of 10-μL assembly mixture included 3 μL of 50 ng/μL linearized pET11a vector, each 1 μL of purified PCR product (up to 40 ng), and 5 μL of 2X Master Mix. The mixtures were incubated at 50 °C for 1 hour. After ligation, the recombinant plasmids were transformed into competent NEB 5-alpha *Escherichia coli* cells (Product No. C2987H, New England Biolabs, Ipswich, MA, USA), and screened on LB agar with 100 mg/L ampicillin as a selective marker.

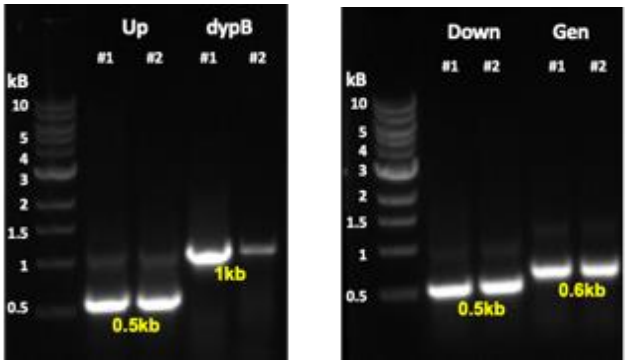

Figure 5.2. PCR products of Up, *dypB*, Gen, and Down fragments on agarose gel. Up and Down: 500 bp of upstream and downstream regions of MCP gene of Mushu4. These two fragments were amplified from M213. *dypB*: lignin peroxidase gene that were amplified from RHA1 genome. Gen: a gentamicin resistance gene cassette that was amplified from plasmid pBAD24g.

The plasmid (pET11a-Up-dypB) DNA (between SacI and HindIII sites) was used for the second cloning work with Gen and Down to construct the target recombinant

plasmid, pET11a-Up-dypB-Gen-Down (Figure 5.3), following the same protocol with the first cloning. The candidate plasmid constructs were extracted using QIAprep Spin Miniprep Kit (Qiagen, Hilden, Germany) and were confirmed by (i) observation of expected fragment sizes of restriction enzymes digested plasmids on the agarose gel and by (ii) verification of plasmid sequence (Eton Bioscience, San Diego, CA, USA).

The observation of expected fragment sizes of restriction enzymes digested plasmids, pET11a-Up-dypB and pET11a-Up-dypB-Gen-Down, on the agarose gel were shown in Figure 5.4a-b.

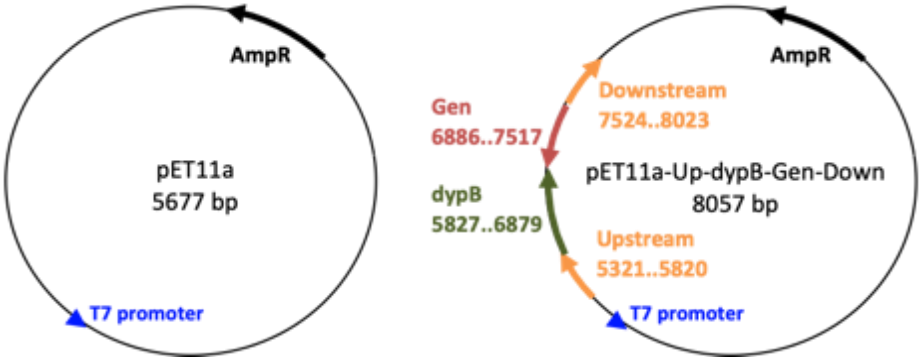

Figure 5.3. Map of the pET11a vector and constructed recombinant plasmid (pET11a-Up-dypB-Gen-Down). Up and Down: 500 bp of upstream and downstream regions of MCP gene of Mushu4. These two fragments were amplified from M213. *dypB*: lignin peroxidase gene that were amplified from RHA1 genome. Gen: a gentamicin resistance gene cassette that was amplified from plasmid pBAD24g.

(a) (b)

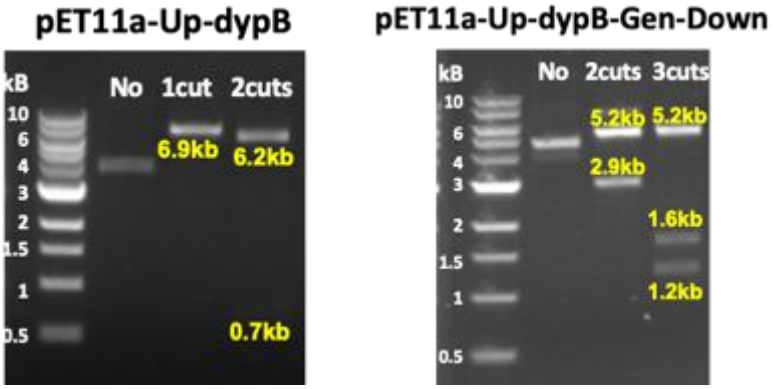

Figure 5.4. Results of restriction enzyme digestion of constructed plasmids. (a) The results of restriction enzymes digested pET11a-Up-dypB. The plasmid (pET11a-Up-dypB) was digested with XhoI (1 cut, expected size: 6.9 kb), BamHI and XhoI (2 cuts, expected sizes: 6.2 and 0.7 kb), or without enzymes (No: no restriction digestion, 4.5 kb). (b) The results of restriction enzymes digested pET11a-Up-dypB-Gen-Down. The plasmid (pET11a-Up-dypB-Gen-Down) was digested with EcoRV (2 cuts, expected size: 5.2 and 2.9 kb), EcoRV and XbaI (3 cuts, expected sizes: 5.2, 1.6 and 1.2 kb), or without enzymes (No: no restriction digestion, 5.0 kb).

(ii) Construction of pTipQC2-Up-dypB-Gen-Down, a plasmid with the integrated gene cassette.

The integration cassette was additionally cloned into *Rhodococcus* shuttle vector pTipQC2 between NdeI-HindIII sites, using In-Fusion® HD Cloning Kit (Clontech, Mountain View, CA) to construct recombinant plasmid, pTipQC2-Up-dypB-Gen-Down (Figure 5.5). The plasmid, pET11a-Up-dypB-Gen-Down, was used for PCR amplification using PCR primers listed in Table 5.4. PCR reaction was conducted as described in section 5.3.3 (i). After that, a 10-μL ligation mixture including 1 μL of linearized pTipQC2 vector, 2 μL of 5X In-Fusion Cloning HD Enzyme Premix, 1 μL of purified PCR product, and 6 μL of deionized water was prepared. The ligation mixtures were incubated at 50 °C for 15 minutes, and the recombinant plasmid was transformed into NEB 5-alpha competent

E. coli, screened on LB agar with 20 mg/L gentamicin as a selective marker and extracted using QIAprep Spin Miniprep Kit. The recombinant plasmid was confirmed by observation of expected sizes of digested PCR products. The expected fragment sizes on the agarose gel were shown in Figure 5.6. The correctness of pTipQC2-Up-dypB-Gen-Down was also confirmed based on its sequence.

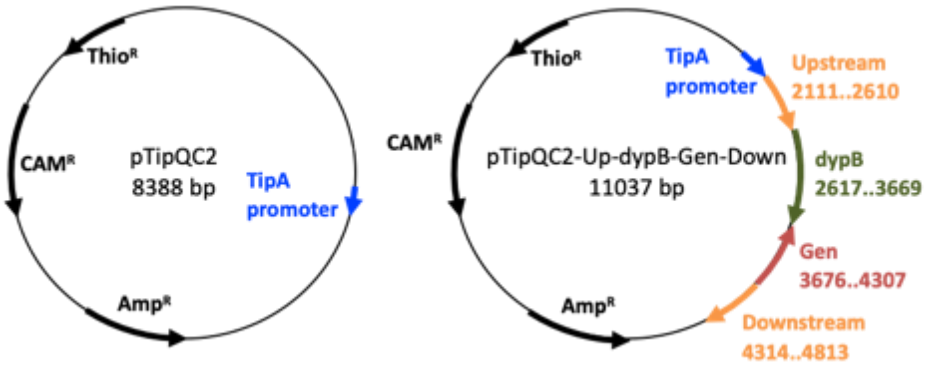

Figure 5.5. Map of the pTipQC2 vector and constructed recombinant plasmid (pTipQC2-Up-dypB-Gen-Down). Up and Down: 500 bp of upstream and downstream regions of MCP gene of Mushu4. These two fragments were amplified from M213. *dypB*: lignin peroxidase gene that were amplified from RHA1 genome. Gen: a gentamicin resistance gene cassette that was amplified from plasmid pBAD24g.

Table 5.4. Primer sets used in the cloning work for In-fusion cloning. All primers were designed by primer design tool for In-fusion cloning. All4 is Up, dypB, Gen, and down for infusion cloning into pTipQC2 vector

Primer name	Sequence (5' -> 3')	Primer length (bp)	Melting temperature (°C)	Expected PCR product size (kb)
All4_FW	CGAGAGATCTAAGCTTTCAAGAACTGGAGCATCTGATGAG	40	66	2.6
All4_RV	AAGGAGATATACATATGCGGATCTCGTTGTCGACGGG	37	68	

Figure 5.6. Results of restriction enzyme digestion of plasmid pTipQC2-Up-dypB-Gen-Down. The plasmid (pTipQC2-Up-dypB-Gen-Down) was digested with HindIII and BamHI (2 cuts, expected size: 8.8 and 2.3 kb), XbaI and XhoI (4 cuts, expected sizes: 5.1, 3.2, 1.6 and 1.1 kb), or without enzymes (No: no restriction digestion, 8.0 kb).

5.3.4. Transformation of constructed plasmids into M213

A commercial plasmid pDD120 containing a pair of bacteriophage recombinase (Che9c60 and Che9c61), pTipQC2 or pTipQC2-Up-dypB-Gen-Down was electroporated into electrocompetent M213 cells as described previously (Gill et al., 2018). (Kalscheuer et al., 1999) Briefly, the electrocompetent cells were mixed with 300 ng of the plasmid and preincubated at 40 °C for 5 minutes. The electroporation was conducted in electrocuvettes (gaps of 2mm) by micropulser (Bio-Rad, Hercules, CA, USA) with the following settings: ec2: 2.5 kV, 600 ohm, and 25 μF. The electroporated cells were recovered in LB media at 30 °C for 4 hours and then spread on LB agar with an appropriate antibiotic: 100 mg/L of kanamycin for pDD120, or 35 mg/L of chloramphenicol for pTipQC2 and pTipQC2-Up-dypB-Gen-Down. The transformants were formed at 30 °C after 3-5 days of incubation and the recombination in the transformants was confirmed by colony PCR as described in section 5.3.7.

5.3.5. Homologous recombination by exogenous recombination system

For recombination with linear fragments as shown in Figure 5.1a, a linear DNA fragment- containing homologous arms, lignin peroxidase, and gentamicin resistance gene cassette- was prepared by PCR amplification using pET11a-Up-dypB-Gen-Down as a template and this primer set, linear DNA_F (5'-TCAAGAACTGGAGCATCTGATGAG-3') and linear DNA_R (5'-CGGATCTCGTTGTCGACGG-3'). Double homologous recombination to replace the MCP gene of Mushu4 was conducted as described previously (DeLorenzo et al., 2018) with some modifications. About 1 μg of linear DNA fragment was transformed into the electrocompetent M213pDD120 (i.e. M213 harboring the plasmid pDD120), recovered in LB media at 30 °C for 6 hours, and then the aliquot was plated on LB agar with 20 mg/L of gentamicin. The electroporation was performed with the same setting in the section 5.3.4. The transformants was formed at 30 °C after 3-5 days and the recombination was confirmed by colony PCR as described in section 5.3.7.

5.3.6. Homologous recombination during spontaneous induction of Mushu4

During the spontaneous induction of Mushu4 from M213, homologous recombination might occur with assistance of the recombinases of Mushu4 if homologous arms are also present in M213 (Figure 5.1b). After transformation, spontaneous induction of Mushu4 was conducted by growing the transformants up to a stationary phase in 50 mL of R2A broth medium aerobically at 200 rpm at 30 °C. The wild type M213 and

M213pTipQC2 (i.e. M213 harboring the plasmid pTipQC2) were used as negative controls. The supernatant of the stationary phase culture of M213, M213pTipQC2, or M213pTipQC2All4 (i.e. M213 harboring the plasmid pTipQC2-Up-dypB-Gen-Down) were collected and filtrated as a lysate. The lysate was propagated on DSM43205 to check for spontaneous induction rate and to lysogenize DSM43205 to produce DSM43205 (ENMushu4). Strain DSM43205 were grown in R2A medium to exponential growth phase (OD_{600} ~0.4), and 4 mL aliquots were transferred to new culture tubes. One mL of each phage lysate was applied to each culture tube. After 24 hours of incubation at 200 rpm at 30 °C, the cell culture was streaked on LB agar with 20 mg/L of gentamicin to isolate lysogen containing the edited Muhsu4 genome. DSM43205 culture without phage lysate was used as a control.

5.3.7. Confirmation of recombination using colony PCR

A colony PCR was conducted to confirm the success of homologous recombination. A 25- μL PCR reaction mixture including 12.5 μL of 2X PCR Master Mix (Promega), 1 μL each of 10 μM forward and reverse primers, and 10.5 μL of nuclease-free water, was used. Each colony was picked and mixed to the PCR reaction mixture. Information of PCR primers was listed in Table 5.5 and the locations of primers on the plasmids were shown in Figure 5.7. The PCR reaction was carried out by denaturing at 98 °C for 2 minutes, followed by 35 cycles at 98 °C for 10 seconds, 53 °C for 1 minutes, and 72 °C for 1 minute per 1 kb of expected PCR fragment size, with a final incubation at 72 °C for 10 minutes for final extension.

Table 5.5. Primer sets used in the colony PCR.

Primer name	Sequence (5' -> 3')	Primer length (bp)	Melting temperature (°C)
M1	GTACGGAAATGTGGAAGCGAAGG	23	60
M2	GTGAACTCGTGGAGAGCGAC	20	58
P1	CAAACTGGTGCTCGGCAAGG	20	60
P2	CGCGACGCAATTCCCTGATC	20	60
P3	TCAGAAGAACTCGTCAAGAAGGC	23	58
P4	GAAAACGCAAGCGCAAAGAGAA	22	59

(a)

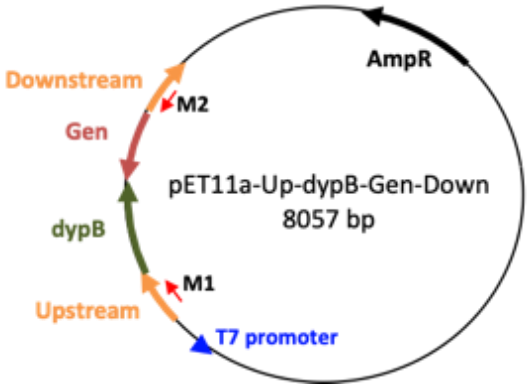

(b)

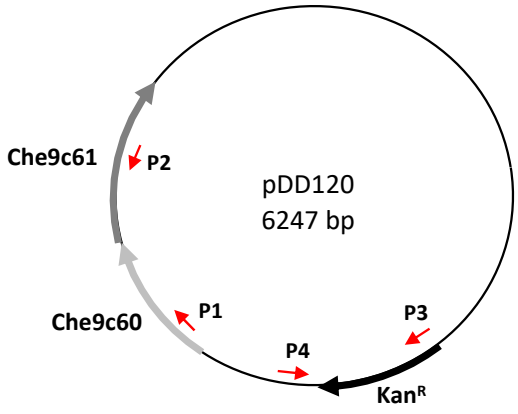

Figure 5.7. Locations of primers (listed in Table 5.5) on the plasmids. (a) Primers of M1 and M2 location on plasmid pET11a-Up-dypB-Gen-Down. (b) Primers of P1, P2, P3, and P4 location on plasmid pDD120.

5.4. Results and discussion

5.4.1. Homologous recombination by an exogenous recombination system

To facilitate the site-directed insertion at the correct location using phage recombinases, a plasmid pDD120 containing a pair of phage recombinases, Che9c60 and Che9c61, was inserted into the strain M213 by electroporation. The transformation efficiency of pDD120 into the strain M213 was $2x10^3$ cfu/mL on LB agar containing 100 mg/L of kanamycin. Colonies formed on the plates were selected, purified, and then used for homologous recombination in M213pDD120. The linear DNA fragment containing the homologous arms of the MCP gene, lignin peroxidase (*dypB*), and Gen was used for homologous recombination as described in Fig 5.1a. However, similar number of colonies were obtained from the negative control plates (without linear DNA fragment) and sample plates (with linear DNA fragment). Three colonies of each of two plates (controls and samples) were selected to check any contamination by colony PCR. Colony PCR results showed that all colonies from the plates had the band for the MCP region of the phage Mushu4, indicating that all strains were M213 (Figure 5.8). However, the results indicated that homologous recombination had not occurred at the correct MCP gene region because the band size was 1.5 kb (expected PCR product size for MCP gene), not 2.2 kb (expected PCR product size for *dypB* and Gen). It is possible that the transformants of M213pDD120 might have developed a resistance to gentamycin like its known ability to develop a resistance toward kanamycin, because kanamycin and gentamycin are same group of aminoglycoside antibiotics (Choi et al., 1980; Sydor et al., 2013).

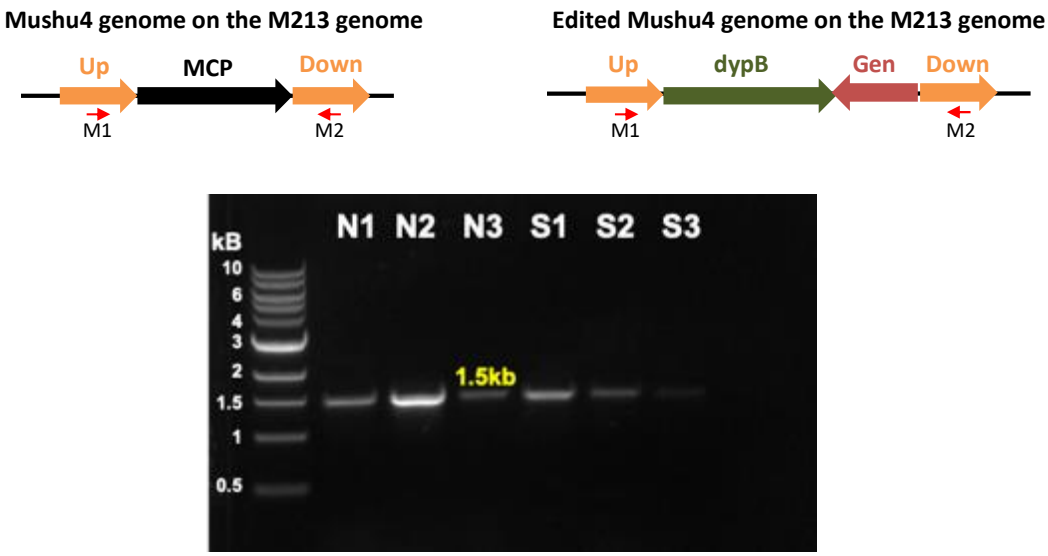

Figure 5.8. Colony PCR results of homologous recombination in M213pDD120. MCP is major capsid protein gene of phage Muhsu4 and the size of MCP is 1kb. The size of *dypB* and Gen is 1.1 kb and 0.6 kb, respectively. N1-N3: negative controls (M213pDD120 without linear DNA fragment). S1-S3: samples of M213pDD120 received linear DNA fragments of Up-dypB-Gen-Down).

Another possible reason of the failure of homologous recombination might be due to the phage recombinases did not work properly in the M213pDD120. To confirm this, colony PCR was performed to detect the presence of the region of Che9c60 and Che9c61 in M213pDD120. The colony PCR results showed that only the region of recombinases presents in the initial transformant M213pDD120, not in the 2nd subculturing of M213pDD120 on LB agar with 100 mg/L of kanamycin (Figure 5.9). However, the bands of Kan^{R} gene and MCP region were still detected, suggesting no change of Mushu4 genome in the bacterial genome of M213 strain (Figure 5.9). This indicated that the failure of homologous recombination might be due to the knock-out of the phage recombinases during purification of M213pDD120.

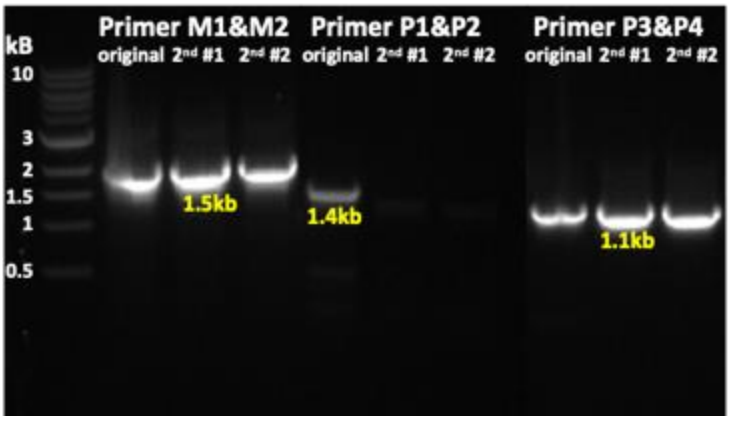

Figure 5.9. Colony PCR results of pDD120 transformation into the strain M213. The expected size of Che9c60 and Che9c61 region using primers P1 and P2 is 1.4 kb. Kan^R region was amplified with primers P3 and P4, resulting an expected size of 1.1 kb. Original: sample of M213 harboring pDD120 right after transformation. 2^{nd}: sample of 2^{nd} subculture of M213 harboring pDD120 on LB agar with 100 mg/L of kanamycin.

5.4.2. Homologous recombination during spontaneous induction of Mushu4

To investigate if homologous recombination at the correct site was facilitated by recombinases of phage Mushu4, spontaneous induction of phage Mushu4 from M213pTipQC2All4 was conducted. Following transformation, only 7 transformants were formed on a LB agar plate with 35 mg/L of chloramphenicol. The purified transformants were then used for spontaneous induction of Mushu4 and the supernatant was applied to DSM43205 culture for 24 hours. However, the incubated DSM43205 cultures with the supernatant of M213pTipQC2All4 did not form any colony on LB agar with 20 mg/L of gentamicin as like DSM43205 only culture, DSM43205 with a supernatant of M213, and DSM43205 with a supernatant of M213pTipQC2. This indicated that homologous recombination had not occurred and the lysogen DSM43205 containing the edited Mushu4 genome was not generated. The possible reason of this failure might be due to a low spontaneous induction rate of phage Mushu4. All supernatants, which prepared from

M213, M213pTipQC2, and M213pTipQC2All4, showed the low titer range of Mushu4 as $10^2 – 10^3$ PFU/ml. The low induction rate may not provide enough DNA copies to allow recovery of recombinants between the inserted plasmid and the genome of Mushu4 during DNA replication because this process relies on the natural recombination rates, which may occur at frequencies of 10^{-4} or less.

5.5. Conclusions

This study explored the possibility of site-directed insertion into the prophage Mushu4 genome to overexpress lignin peroxidase during prophage induction. Two experimental approaches, relying on expression of phage recombinases from a constitutive plasmid (pDD120) or natural function of recombinases of Mushu4 during induction, were applied and explored. The genome annotation of prophage Mushu4 was successfully conducted to identify the major capsid protein gene as a target site. However, the first approach, was unsuccessful due to possible off-target recombination and spontaneous deletion of the recombinase genes, possibly due to their toxicity. The second approach was attempted but not completed due to the low spontaneous induction rate of the phage in M213. Although homologous recombination was not successful in the M213(Mushu4) system, possible failure reasons were identified, and these results provide the groundwork for the development of Mushu4 as an effective tool for lignocellulose pretreatment.

5.6. References

Billion-Ton. 2016. Advancing domestic resources for a thriving bioeconomy, U.S. Department of Energy.

Capecchi, M.R. 1989. Altering the genome by homologous recombination. Science 244, 1288-1292.

Carey, L.B., van Dijk, D., Sloot, P.M., Kaandorp, J.A. and Segal, E. 2013. Promoter sequence determines the relationship between expression level and noise. PLoS Biol 11(4), e1001528.

Carrier, M.J., Nugent, M.E., Tacon, C.A. and Primrose, S.B. 1983. High expression of cloned genes in *E. coli* and its consequences. Trends in Biotechnology 1(4), 109-113.

Casjens, S. 2003. Prophages and bacterial genomics: what have we learned so far? Mol Microbiol 49(2), 277-300.

Chan, J.C., Paice, M. and Zhang, X. 2019. Enzymatic oxidation of lignin: Challenges and barriers toward practical applications. ChemCatChem 12(2), 401-425.

Choi, E.C., Nishimura, T., Tanaka, Y. and Tanaka, N. 1980. *In vivo* and *in vitro* cross-resistance of kanamycin-resistant mutants of *E. coli* to other aminoglycoside antibiotics. The Journal of Antibiotics 33(12), 1527-1531.

Conway, J.F., Cheng, N., Ross, P.D., Hendrix, R.W., Duda, R.L. and Steven, A.C. 2007. A thermally induced phase transition in a viral capsid transforms the hexamers, leaving the pentamers unchanged. J Struct Biol 158(2), 224-232.

DeLorenzo, D.M., Rottinghaus, A.G., Henson, W.R. and Moon, T.S. 2018. Molecular toolkit for gene expression Control and genome modification in *Rhodococcus opacus* PD630. ACS Synthetic Biology 7(2), 727-738.

Desomer, J., Crespi, M. and Van Montagu, M. 1991. Illegitimate integration of non-replicative vectors in the genome of *Rhodococcus fascians* upon electrotransformation as an insertional mutagenesis system. Molecular Microbiology 5(9), 2115-2124.

Doss, J., Culbertson, K., Hahn, D., Camacho, J. and Barekzi, N. 2017. A review of phage therapy against bacterial pathogens of aquatic and terrestrial organisms. Viruses 9(3).

Dunn, J.J. and Studier, F.W. 1983. Complete nucleotide sequence of bacteriophage T7 DNA and the locations of T7 genetic elements. J. Mol. Biol. 166, 477-535.

Fakruddin, M., Mazumdar, R.M., Mannan, K.S.B., Chowdhury, A. and Hossain, M.N. 2013. Critical factors affecting the success of cloning, expression, and mass production of enzymes by recombinant *E. coli*. ISRN Biotechnol 2013, 590587.

Gill, J.J., Wang, B., Sestak, E., Young, R. and Chu, K.H. 2018. Characterization of a novel *tectivirus* phage Toil and its potential as an agent for biolipid extraction. Scientific Reports 8(1), 1062.

Hwangbo, M., Tran, J.L. and Chu, K.H. 2019. Effective one-step saccharification of lignocellulosic biomass using magnetite-biocatalysts containing saccharifying enzymes. Science of the Total Environment 647, 806-813.

Kirchner, O. and Tauch, A. 2003. Tools for genetic engineering in the amino acid-producing bacterium *Corynebacterium glutamicum*. Journal of Biotechnology 104(1-3), 287-299.

Kumar, P., Barrett, D.M., Delwiche, M.J. and Stroeve, P. 2009. Methods for pretreatment of lignocellulosic biomass for efficient hydrolysis and biofuel production. Industrial and Engineering Chemistry Research 48, 3713-3729.

Lambertz, C., Ece, S., Fischer, R. and Commandeur, U. 2016. Progress and obstacles in the production and application of recombinant lignin-degrading peroxidases. Bioengineered 7(3), 145-154.

Liang, Y., Jiao, S., Wang, M., Yu, H. and Shen, Z. 2020. A CRISPR/Cas9-based genome editing system for *Rhodococcus ruber* TH. Metab Eng 57, 13-22.

Miki, Y., Ichinose, H. and Wariishi, H. 2010. Molecular characterization of lignin peroxidase from the white-rot basidiomycete *Trametes cervina*: a novel fungal peroxidase. FEMS Microbiol Lett 304(1), 39-46.

Nlewem, K.C. and Thrash, M.E.J. 2010. Comparison of different pretreatment methods based on residual lignin effect on the enzymatic hydrolysis of switchgrass. Bioresour Technol 101(14), 5426-5430.

Plácido, J. and Capareda, S. 2015. Ligninolytic enzymes: A biotechnological alternative for bioethanol production. Bioresources and Bioprocessing 2(23).

Santos, A., Mendes, S., Brissos, V. and Martins, L.O. 2014. New dye-decolorizing peroxidases from *Bacillus subtilis* and *Pseudomonas putida* MET94: towards biotechnological applications. Appl Microbiol Biotechnol 98(5), 2053-2065.

Sun, S., Sun, S., Cao, X. and Sun, R. 2016. The role of pretreatment in improving the enzymatic hydrolysis of lignocellulosic materials. Bioresource Technology 199, 49-58.

Sydor, T., von Bargen, K., Hsu, F.F., Huth, G., Holst, O., Wohlmann, J., Becken, U., Dykstra, T., Sohl, K., Lindner, B., Prescott, J.F., Schaible, U.E., Utermohlen, O. and Haas, A. 2013. Diversion of phagosome trafficking by pathogenic *Rhodococcus equi* depends on mycolic acid chain length. Cell Microbiol 15(3), 458-473.

van Kessel, J.C. and Hatfull, G.F. 2007. Recombineering in *Mycobacterium tuberculosis*. Nat Methods 4(2), 147-152.

Wang, B. (2016) Producing biolipids from lignocellulose: Cultivation of lipid-accumulating bacteria and bacteriophage-based lipid extraction, Texas A&M University.

Wang, B., Rezenom, Y.H., Cho, K.C., Tran, J.L., Lee, D.G., Russell, D.H., Gill, J.J., Young, R. and Chu, K.H. 2014. Cultivation of lipid-producing bacteria with lignocellulosic biomass: effects of inhibitory compounds of lignocellulosic hydrolysates. Bioresour Technol 161, 162-170.

Young, R., Wang, I.N. and Roof, W.D. 2000. Phages will out: Strategies of host cell lysis. Trends in Microbiology 8(3), 120-128.

6. SUMMARY, CONCLUSIONS, AND FUTURE RESEARCH

6.1. Summary and conclusions

Lipid-based biofuel, manufactured from starting materials biolipids, is an ideal replacement for petroleum-based biofuel, as biolipids can be produced by living microorganisms including lipid-producing bacteria using renewable resources, lignocellulose. However, the overall production cost of lipid-based biofuel is still not competitive because of several challenges including inefficient pretreatment steps of lignocellulose, sterilization of culture medium for cultivating biolipid-accumulating microorganisms, and costly lipid harvesting and extraction process from biolipid-filled microorganisms.

To address overcome the challenges described above, the overall goal of this study was to develop phage-based technologies to enable economical non-sterile biolipid production from lignocellulose. To reach this goal, three technical objectives were proposed and conducted. A brief summary of results obtained from these technical objectives is described as follows:

(i) Objective 1: Develop an effective one-step saccharification of lignocellulosic biomass using reusable saccharifying enzymes (SEs) that are active under similar optimal pH and temperature.

Summary (for Chapter 3): This study verified production of crude lignocellulose-saccharifying enzymes (SEs) in large quantity from engineered *E. coli*., and successfully applied these five produced crude SEs to saccharify lignocellulosic biomass under the

optimal conditions (pH 6.0 and temperature 50 °C). There is no a tedious purification step for the produced enzymes and the saccharification process is simply. Furthermore, the reusability of immobilized SEs by magnetite-biocatalysts (M-SE-CLEAs) was demonstrated.

(ii) Objective 2: Develop a salt-tolerant *Rhodococcus opacus* PD631 with phage lytic cassette for non-sterile biolipid production and extraction.

Summary (for Chapter 4): Production and release of TAGs from non-sterile growth medium was successfully demonstrated by using a newly developed salt-tolerant *R. opacus* PD631 harboring the inducible phage lytic cassette plasmid. The newly developed strain enabled cell lysis to release TAGs into liquid medium, suggesting itself as a promising candidate to address the two major challenges – high costs associated with sterilization cultivation and TAGs extraction – of current biolipid-based biofuel production.

(iii) Objective 3: Engineer prophage DNA in *Rhodococcus* strains to express high levels of lignin peroxidase for effective depolymerization of lignin.

Summary: Research efforts were placed on editing of prophage Mushu4 DNA that is present in the genome of *Rhodococcus* to overexpress lignin peroxidase for effective depolymerization of lignin. Two homologous recombination approaches, one relying on inserted phage recombinases and the other one relying on own recombinases of prophage Mushu 4, were applied and explored to develop desired engineered prophage. For this, genome annotation of prophage Mushu4 was successfully conducted. However, illegitimate insertion frequently occurred, and the inserted phage recombinases was

knock-out during purification. Also, homologous recombination relied on own recombinases of Mushu4 during DNA replication was not successfully occurred due to the low spontaneous induction rate of M213.

Overall, biolipids can be produced from non-sterile growth medium and then released by engineered salt-tolerant lipid-producing bacteria with a plasmid containing phage lytic cassette, using pretreated lignocellulose, prepared by an efficient one-step saccharification. Although two homologous recombination approaches not succeeded in the prophage genome of *Rhodococcus*, possible failure reasons were already found, and it might be overcome in the future study. The results might provide the groundwork for the development of *Rhodococcus* as an efficient tool to produce lignin peroxidase for reducing the overall costs of biofuel production from lignocellulose

6.2. Future research

This study provided the novel phage-based approaches to reduce the overall costs of lipid-based biofuel production from lignocellulosic biomass. The engineered salt-tolerant lipid-producing bacteria was also introduced and discussed for biolipid production and release from non-sterilized growth medium. However, the phage genome editing via homologous recombination to overexpress lignin peroxidase for lignin depolymerization was not successful in this study. The results of this study have partially addressed the challenges associated with biolipid production and release from lignocellulose biomass. In the meantime, more interesting questions have been raised that should be investigated in future studies. Below are recommended future studies.

1) Reuse of saccharifying enzymes is an efficient way to reduce the cost of enzyme hydrolysis that is needed to release sugars from pretreated lignocellulosic biomass. In this study, the reusability of magnetite cross-linked saccharifying enzyme aggregates for enzyme hydrolysis of pretreated lignocellulose was low. Using find particles of pretreated lignocellulose and making magnetic nanoparticles to locate inside of immobilized enzymes will be useful to increase the reusability of aggregates sacchrifying enzymes.

2) The engineered salt-tolerant lipid-producing bacteria (PD631SpAHB) showed the ability of non-sterile TAGs production and extraction by the induction of phage lytic gene cassette. However, the extraction efficiency in non-sterile growth medium was not high and the optimal condition of phage lytic gene expression was not investigated in this study. The change of Shine Dalgarno (SD) sequence for *LysB* and *Holin* gene with the strong SD sequence of pTipQC2 might be helpful to increase the gene expression levels, leading to more effective cell lysis and biolipids extraction efficiency. Also, further research is required to find an optimal condition for expression of phage lytic genes.

3) The exogenous recombination system using a pair of phage recombinases in this study was not effective to edit the prophage genome inside *Rhodococcus*

strain because of the knock-out of phage recombinases. This might be due to the toxicity of phage recombinases to *Rhodococcus* strain. A leaky transcription of inducible promoter might be useful to provide phage recombinases as a low expression levels for the exogenous recombination. The plasmid pTipQC2 having the thiostrepton inducible promoter, pTipA, which was already confirmed the availability for *Rhodococcus*, can be used for this. Further research is required to maintain the phage recombinases for the exogenous recombination system in *Rhodococcus*.

4) To increase success rate of the natural selection of homologous recombination between inserted plasmid and Mushu4 genome, the spontaneous induction rate of Mushu4 from M213 would need to be increased. The normal spontaneous induction rate of Mushu4 was not high as $10^2 – 10^3$ PFU/ml. As DSM43205 (Mushu4) lysogen showed the high spontaneous induction rate of Mushu4 as $10^6 – 10^8$ PFU/ml (Wang, 2016), a much higher possibility of successful homologous recombination based on the recombinases of Mushu4 during its DNA replication might be achieved if DSM43205 (Mushu4) is used. Further research is required to explore this aspect.

6.3. References

Wang, B. (2016) Producing biolipids from lignocellulose: Cultivation of lipid-accumulating bacteria and bacteriophage-based lipid extraction, Texas A&M University.

APPENDIX A

CHARACTERIZATION AND GENOME ANNOTATION OF PHAGE MUSHU4

For genome annotation of phage Mushu4, genes were predicted using Glimmer3 (Delcher et al., 1999) or MetaGeneAnnotator (Noguchi et al., 2008) and functionally annotated by InterProScan (Jones et al., 2014) and BLAST (Camacho et al., 2009) against to NCBI nr, SwissProt, and TrEMBL databases (Consortium, 2018). All annotation tools are available on the Galaxy (https://cpt.tamu.edu/galaxy/) of Center for Phage Technology (CPT) at Texas A&M University (College Station, TX).

Mushu4 as a prophage, was isolated from a stationary phase culture of M213, showing titer range of Mushu4 in the supernatant of M213 as 10^2 – 10^3 PFU/ml. Compared to spontaneous induction rate of Mushu4, the maximal titer of plate lysate was 5×10^9 PFU/ml (Wang, 2016). Interestingly, large amounts of Mushu4 DNA exist in extracted DNA of Mushu2, as a virulent phage which infects M213, which indicates that prophage Mushu4 is induced from Mushu2-infected M213 (Wang, 2016). However, the spontaneous induction rate of Mushu4 from Mushu2-infected M213 was not increased, showing the titer was 3×10^2 PFU/ml.

Based on Blast-N results, the genome of Mushu4 was found on the contigs 173 (AJYC01000153.1, as an accession number of GenBank databases) and 245 (AJYC01000218.1) of M213 genome assembly (ASM26474v1). Mushu4 has a 46.3 kb genome with 66 coding regions, 38 have a predicted function, and the G+C content of 65.2%. Also, Mushu4 is a novel phage because it only shares 14.12% nucleotide sequence

identity with *Gordonia* phage Cynthia (accession no. MN586055.1), Savage (accession no. MK279912.1), Sproutie (accession no. MK279911.1), and Haley23 (accession no. MK875797.1), and shows 22 similar proteins out of 66 with *Gordonia* phages by BLASTp. In the genome of Mushu4 (Figure A.1), genes encoding proteins related to phage morphogenesis were identified including portal protein, capsid maturation protease (CMP), scaffold protein, major capsid protein (MCP), head stabilizing protein (HSP), minor capsid protein, tail tube protein, tail assembly chaperone, tape measure protein, minor tail protein, and tail fiber protein. Terminase large subunit, head-to-tail connector protein, and terminase small subunit proteins were detected, which are associated with gDNA packaging (Garneau et al., 2017). Proteins for DNA replication and DNA biosynthesis genes were identified. Also, Mushu4 contains integrase protein and holiday junction resolvase (HJR), which are usually related to lysogeny formation (Casjens, 2003). The lysis genes, endolysin (lysA), and holin was identified, and the holin is a class II holin with two transmembrane domains. Mushu4 also has an esterase (lysB) which can degrade the mycolic acids layer outside the cell wall (Payne et al., 2009).

Mushu4 lysogenized DSM43205 to make DSM43205 (Mushu4), showing a high spontaneous induction rate of Mushu4 from DSM43205 (Mushu4) as 10^6 – 10^8 PFU/ml (Wang, 2016). Based on Blast-N results of Mushu4 DNA sequence to the genome of DSM43205 (NZ_LRRG01000000), the attachment site (att) of Mushu4 was determined as a 44 bp of 5'- GTGCCCCCGGCAGGATTCGAACCTGCGACCAAGAGA(G/T)T (C/A)G(C/A)AGG -3'. The attP site is right downstream of integrase (gp31 in Figure 5.8), covering a perfect 10 bp inverted repeat. The attB site was found on the contig 47 of

DSM43205 genome (NZ_LRRG01000047), which is in an tRNA-Arg gene (anticodon: TCT). The tRNA is a popular phage integration site because it is conserved and has a stem-loop structure (Campbell, 2003), and mycobacteriophages generally use tRNAs as the attB site (Hatfull, 2018).

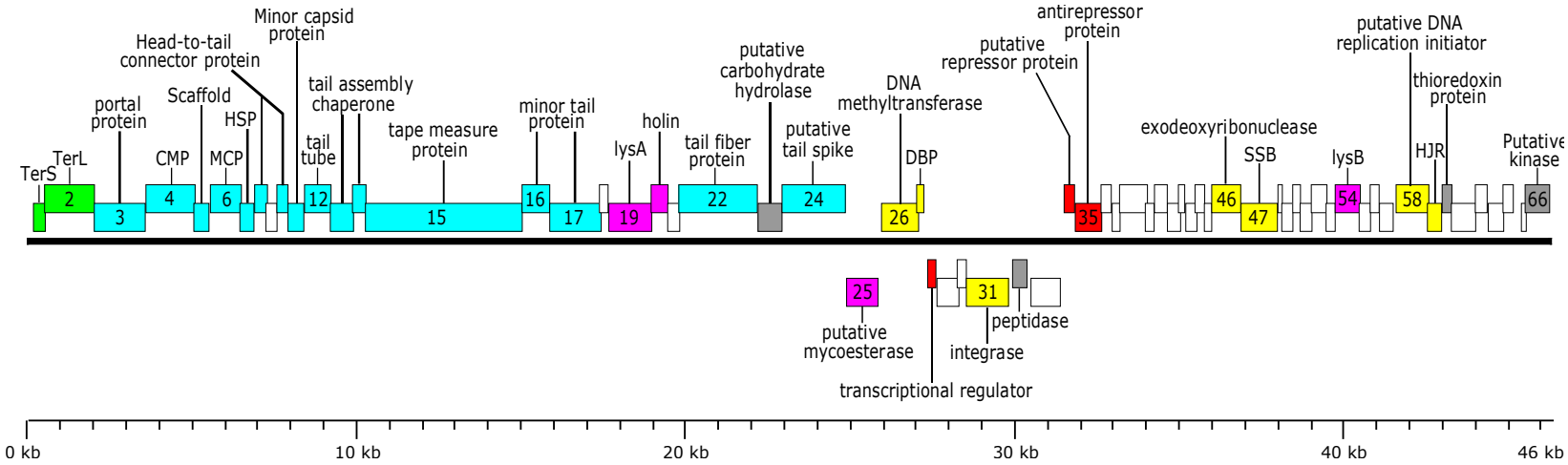

Figure A.1. Genome map of phage Mushu4. Gene names or ORFs numbers are indicated for genes with the annotated function. The ORFs are color-coded based on their functional category: green for DNA packaging, blue for morphogenesis, pink for lysis, yellow for DNA replication and recombination, red for regulation, and grey for other enzymes. Predicted functions of genes are annotated: Terminase small subunit (TerS), terminase large subunit (TerL), capsid maturation protease (CMP), major capsid protein (MCP), head stabilizing protein (HSP), predicted endolysin (lysA), DNA binding protein (DBP), single strand binding protein (SSB), predicted esterase (lysB), and holliday junction resolvase (HJR).

APPENDIX B

PHAGE MUSHU4 INDUCTION BY MITOMYCIN C

Phage Mushu4 was spontaneously induced from a stationary phase culture (OD_{600} ~1.3 – 1.5) of M213 in R2A medium (Wang, 2016). The normal titer range of Mushu4 in the supernatant of the stationary phase culture of M213 is $10^2 – 10^3$ PFU/ml. To obtain high titers of phage Mushu4 from strain M213, mitomycin C (MitC) was applied to an exponential phase culture of M213. An aliquot of the overnight culture of M213 was added to 50 mL of R2A medium, resulting an initial OD600 ~0.01. When reaching exponential growth phase (OD_{600} ~0.5 - 0.7), a different final concentration of MitC were applied; 0 mg/L as a control, 0.5 mg/L, 1 mg/L and 2 mg/L. After 24 hours, OD_{600} of the cell suspension was monitored and supernatant was used to confirm the induction rate of phage Mushu4 by MitC.

An exponentially growing culture of M213 was exposed to a different concentration of mitomycin C (MitC) to experimentally increase the ability of lysogenic to lytic conversion of prophage Mushu4. M213 culture without MitC was used as a negative control. As shown in Figure B.1a, after 24 hours of adding MitC, all conditions were not strongly inhibited the growth. However, increasing the concentration of MitC from 0.5 mg/L to 2 mg/L resulted in more growth inhibition (i.e., the final optical density was from 1.09 to 0.86). Interestingly, the supernatant of M213 with 0.5 mg/L of MitC showed the highest titer as $3.3x10^4$ PFU/ml, which is 10 times higher than other conditions

(Figure B.1b). The results suggested that adding an optimal concentration of MitC would increase the induction rate of Mushu4 from the stationary phase culture of M213.

(a)

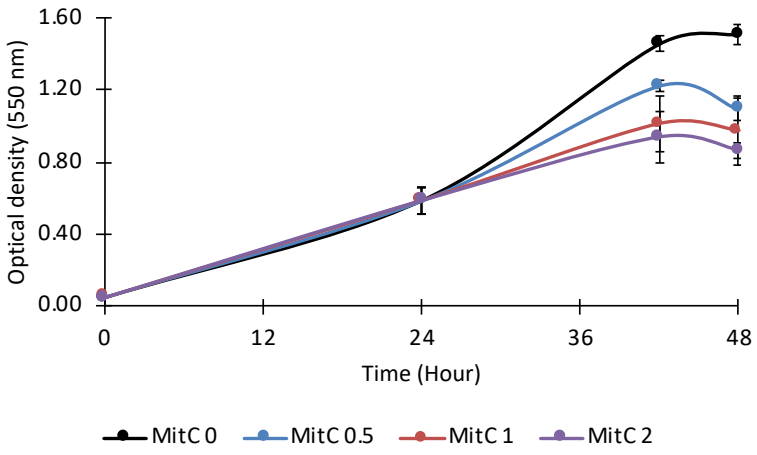

(b)

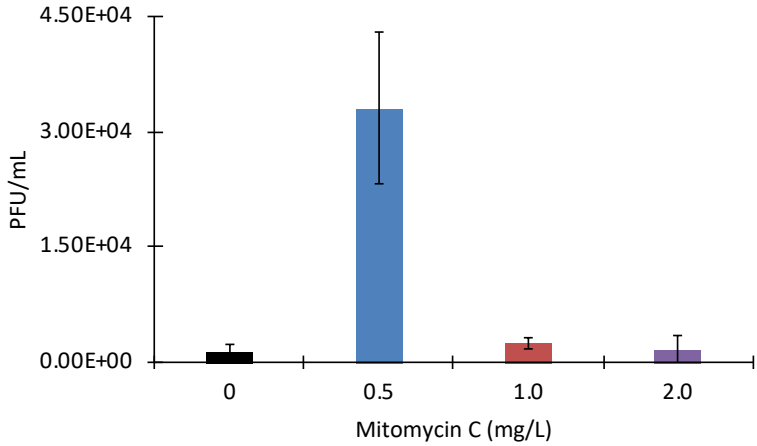

Figure B.1. (a) Cell growth curves of M213 grown in the different mitomycin C (MitC) conditions. The arrow indicates the addition point of different concentration of MitC. (b) Prophage Mushu4 release from M213 with different concentration of MitC. All experiments were conducted in duplicate.

References

Camacho, C., Coulouris, G., Avagyan, V., Ma, N., Papadopoulos, J., Bealer, K. and Madden, T.L. 2009. BLAST+: architecture and applications. BMC Bioinformatics 10, 421.

Campbell, A. 2003. Prophage insertion sites. Research in Microbiology 154(4), 277-282.

Casjens, S. 2003. Prophages and bacterial genomics: what have we learned so far? Mol Microbiol 49(2), 277-300.

Consortium, U. 2018. UniProt: the universal protein knowledgebase. Nucleic Acids Res 46(5), 2699.

Delcher, A.L., Harmon, D., Kasif, S., White, O. and Salzberg, S.L. 1999. Improved microbial gene identification with GLIMMER. Nucleic Acids Res 27(23), 4636-4641.

Garneau, J.R., Depardieu, F., Fortier, L.C., Bikard, D. and Monot, M. 2017. PhageTerm: a tool for fast and accurate determination of phage termini and packaging mechanism using next-generation sequencing data. Sci Rep 7(1), 8292.

Hatfull, G.F. 2018. Mycobacteriophages. Microbiol Spectr 6(5).

Jones, P., Binns, D., Chang, H.Y., Fraser, M., Li, W., McAnulla, C., McWilliam, H., Maslen, J., Mitchell, A., Nuka, G., Pesseat, S., Quinn, A.F., Sangrador-Vegas, A., Scheremetjew, M., Yong, S.Y., Lopez, R. and Hunter, S. 2014. InterProScan 5: genome-scale protein function classification. Bioinformatics 30(9), 1236-1240.

Noguchi, H., Taniguchi, T. and Itoh, T. 2008. MetaGeneAnnotator: detecting species-specific patterns of ribosomal binding site for precise gene prediction in anonymous prokaryotic and phage genomes. DNA Res 15(6), 387-396.

Payne, K., Sun, Q., Sacchettini, J. and Hatfull, G.F. 2009. Mycobacteriophage Lysin B is a novel mycolylarabinogalactan esterase. Molecular Microbiology 73(3), 367-381.

Wang, B. (2016) Producing biolipids from lignocellulose: Cultivation of lipid-accumulating bacteria and bacteriophage-based lipid extraction, Texas A&M University.